PEOPLE'S DEMOCRATIC REPUBLIC OF ALGERIA

**MINISTRY OF HIGHER EDUCATION AND SCIENTIFIC RESEARCH**

**ECHAHID CHEIKH LARBI TEBESSI UNIVERSITY**




Faculty of Exact Sciences and Natural and Life Sciences

Department of Mathematics and Computer Science

**Doctoral Thesis of The Third Cycle**

Field: **Computer Science**

Option: **Artificial Intelligence**

Presented by

**Selma MAMMERI**

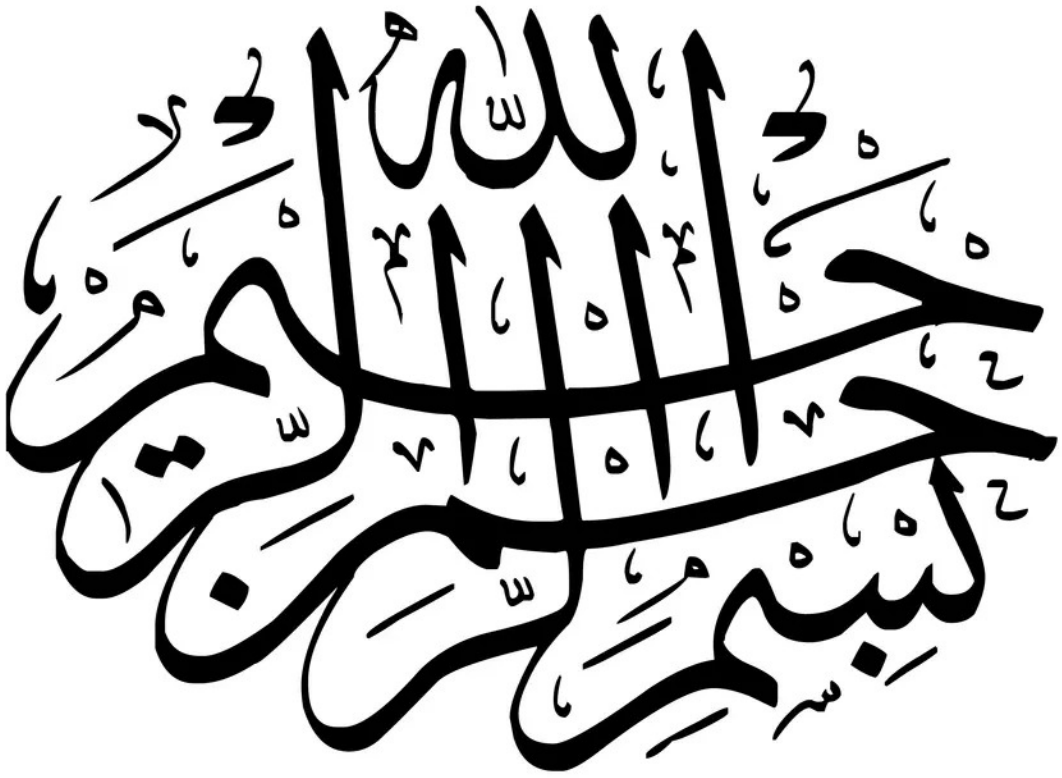
Theme

# An intelligent approach for lung cancer detection and classification

Jury:

| | | | |
|---|---|---|---|
| President | Djeddi Chawki | Professor | Echahid Cheikh Larbi Tebessi university |
| Examiner | Gasmi Mohamed | MCA | Echahid Cheikh Larbi Tebessi university |
| Examiner | Ahmim Ahmed | Professor | Mohamed Cherif Messaadia University |
| Director | Amroune Mohamed | Professor | National School of Nanoscience and Nanotechnology |
| Co-Director | Haouam Mohamed-Yassine | MCA | Echahid Cheikh Larbi Tebessi university |

*2025*


بسم الله الرحمن الرحيم

# Acknowledgments

Praise be to Almighty ALLAH, whose boundless grace has granted me the faith, courage, and patience to undertake and complete this work. Without His divine guidance, none of this would have been possible.

I would like to express my profound gratitude to my supervisor, **Pr. Amroune Mohamed**, from the National School of Nanoscience and Nanotechnology, whose guidance, mentorship, and unwavering support have been invaluable throughout this journey. Your profound expertise, insightful feedback, and dedication to my development have shaped not only this thesis but also the way I approach research and problem-solving. Your encouragement, even in moments of doubt, has taught me the importance of perseverance, and your ability to challenge me while fostering my growth has been a source of inspiration. The countless hours you spent reviewing my work, offering advice, and discussing ideas have made a lasting impact on both my academic and personal growth. I am incredibly fortunate to have had the privilege of working under your supervision. Your belief in my potential, coupled with the intellectual freedom you granted me, allowed me to push boundaries and grow as a researcher. The lessons you've imparted, both academic and life, will resonate with me throughout my career and beyond. For your patience, generosity, and wisdom, I am forever grateful, and this achievement would not have been possible without your guidance. Thank you professor.

I wish to express my profound gratitude to my co-supervisor, **Dr. Haouam Mohamed-Yassine**, MCA at Echahid Cheikh Larbi Tebessi University, for their invaluable assistance, insightful advice, and thorough reviews throughout the course of this thesis. Your expertise and thoughtful suggestions have significantly enhanced the quality and clarity of my work. You were always available to answer my questions and provide support during challenging times, which made a tremendous difference in my progress. Your attention to detail and dedication in offering constructive feedback helped elevate this thesis, and I am deeply grateful

for your contributions. Thank you for your commitment, constant encouragement, and for sharing your knowledge so generously. Your support has been instrumental in the completion of this work.

I would like to sincerely thank **Dr. Bendib Issam**, MCA at Echahid Cheikh Larbi Tebessi University for your support and unwavering encouragement throughout my research journey. Your time and patient explanations have been invaluable in deepening my understanding of complex concepts. Your insightful feedback and constructive criticism greatly refined my ideas and improved the quality of my work. I truly appreciate the countless hours you dedicated to our discussions, which allowed me to explore new perspectives. Your mentorship has contributed to the rigor of my work and inspired me to approach future challenges with confidence and a drive for excellence. Your encouragement motivated me to persevere and strive for excellence. Your contributions have significantly impacted my growth as a researcher, and I am deeply grateful for your role in the successful completion of this thesis.

Thanks to **Pr. Aristofanes Correa Silva** from Federal University of Maranhão - Brazil for invaluable help and domain expertise, which have been essential in helping us understand our work. His extensive experience and profound knowledge have greatly enriched our research, allowing us to gain a clearer and more precise perspective on our subject.

I am profoundly grateful to **Pr: Benjenna Hakim** from Echahid Cheikh Larbi Tebessi University, the director of LAMIS laboratory, for his exemplary leadership throughout our research project. His guidance and availability have greatly facilitated our work.

I also extend my gratitude to the jury members, **Pr. Djeddi Chawki** from Echahid Cheikh Larbi Tebessi University, **Dr. Gasmi Mohamed** MCA at Echahid Cheikh Larbi Tebessi University and **Pr. Ahmim Ahmed** MCA at Mohamed Cherif Messaadia University, for taking the time to evaluate my work carefully. Your insightful comments and suggestions have been crucial in refining my research and improving the quality of my work.

Lastly, I extend my heartfelt thanks to everyone who has contributed, in any capacity, to the completion of this work.

# Dedication

I dedicate this work to :

My amazing mother, whose boundless love, support, patience, and encouragement have been the foundation of my strength. Her sacrifices and belief in me have been crucial throughout this journey, and I owe so much to her.

My father for his support, which has contributed to my progress in its own way.

To my husband, whose love, understanding, and constant support have been invaluable throughout this journey. Thanks for always being by my side, believing in me and encouraging me to continue moving forward. I could not have done this without you.

To my beloved children (Mohamed Iyad, Maram and Reem), who inspire me every day. Your laughter and joy have been my motivation to achieve my dreams. I hope this work inspires you to pursue your own passions.

To all my family and friends who have helped me directly or indirectly, and to those who shared with me the emotional moments during the achievement of this work.

Thanks!

*Selma*

# ملخص

يُعتبر سرطان الرئة أحد أبرز الأسباب المؤدية للوفيات المرتبطة بالسرطان على مستوى العالم، ويرجع ذلك أساساً إلى تشخيصه غالباً في مراحل متقدمة، حيث تقل فعالية خيارات العلاج. في معظم الحالات، لا تظهر أعراض سرطان الرئة في مراحله المبكرة، مما يعني أن المرضى لا يشعرون بأية علامات واضحة حتى يتقدم المرض. يؤدي هذا التأخير في ظهور الأعراض إلى زيادة احتمالية اكتشاف المرض في مراحل متأخرة، حيث قد تكون الأورام قد انتشرت خارج الرئتين، مما يقلل بشكل كبير من فعالية العلاجات المتاحة مثل الجراحة، الإشعاع، والعلاج الكيميائي. بالإضافة إلى ذلك، فإن صغر حجم العقيدات الرئوية في مراحلها المبكرة وخصائصها الدقيقة تجعل من الصعب اكتشافها في التصوير الطبي، حيث يمكن بسهولة تفويتها أو تفسيرها بشكلٍ خاطئ من قبل أطباء الأشعة. لذلك، يعد تطوير أساليب الكشف المبكر أمراً حاسماً لتحسين معدلات البقاء على قيد الحياة، حيث يتيح التشخيص في المراحل المبكرة التدخل في الوقت المناسب، وتقديم علاجات قد تكون شافية، وتحقيق نتائج أفضل للمرضى.

تبحث هذه الدراسة في منهجيات متطورة للكشف المبكر وتصنيف سرطان الرئة، مستفيدة من أحدث تقنيات اكتشاف الأجسام والتعلم العميق. تُعتبر العقيدات الرئوية، التي تمثل غالباً أحد أقدم المؤشرات على الإصابة بسرطان الرئة، عاملاً جوهرياً يجب تحديده بدقة لتحسين فرص التشخيص المبكر وتحسين النتائج العلاجية للمرضى. لمعالجة هذا التحدي، نعتمد على بنية ىصشص٧ التي تتميز بسرعتها ودقتها العالية في اكتشاف العقيدات الرئوية من الصور الطبية، مع التركيز بشكل خاص على تحديد العقيدات الصغيرة والدقيقة التي يصعب اكتشافها باستخدام تقنيات التصوير التقليدية.

بعد مرحلة الكشف، نعتمد على التعلم المنتقل باستخدام النموذج المدرب مسبقاً ط٦١ لتصنيف العقيدات المكتشفة. يتيح لنا التعلم بالنقل الاستفادة من قدرة ط٦١ العالية على استخراج الميزات العميقة، مع تحسين النموذج ليصبح أكثر حساسية للخصائص الدقيقة للعقيدات الرئوية. تسهم هذه التقنيات معاً في تعزيز دقة وسرعة وموثوقية عملية اكتشاف وتصنيف العقيدات، مما يعالج التحدي الكبير في تشخيص سرطان الرئة في مراحله المبكرة. من خلال دمج هذه النماذج المتقدمة، لا يساهم نهجنا فقط في تحسين دقة التشخيص، بل يُعد أيضاً أداة قيمة لأطباء الأشعة، مما يساعدهم في اتخاذ قرارات أكثر دقة وفعالية في رعاية المرضى.

**كلمات مفتاحية:** سرطان الرئة، الذكاء الاصطناعي، التعلم العميق، التصنيف، الكشف

# Abstract

Lung cancer remains one of the leading causes of cancer-related deaths worldwide, primarily because it is often diagnosed at an advanced stage when treatment options are less effective. In many cases, early-stage lung cancer is asymptomatic, meaning that patients do not experience noticeable symptoms until the disease has progressed. This delay in symptom onset leads to a higher likelihood of late detection, by which point tumors may have spread beyond the lungs, significantly reducing the effectiveness of available treatments like surgery, radiation, and chemotherapy. Moreover, the subtle and small size of early-stage lung nodules makes them difficult to detect in medical imaging, as they can easily be missed or misinterpreted by radiologists. Therefore, improving early detection methods is critical for increasing survival rates, as early-stage diagnosis allows for more timely intervention, potentially curative treatments, and better overall patient outcomes.

This work investigates advanced methodologies for the early detection and classification of lung cancer, leveraging cutting-edge object detection and deep learning techniques. Lung nodules, often considered one of the earliest indicators of lung cancer, are critical to identify accurately to enhance early diagnosis and improve patient outcomes. To address this, we employ the YOLOv7 architecture, renowned for its speed and precision, to detect lung nodules in medical images, with a particular focus on identifying small, subtle nodules that are often challenging to detect using standard imaging techniques.

Following the detection phase, we utilize transfer learning with the pre-trained VGG16 model for the classification of the detected nodules. Transfer learning allows us to harness the power of VGG16's deep feature extraction while fine-tuning the model to be highly sensitive to lung nodule characteristics. Together, these techniques enhance the accuracy, reliability, and speed of nodule detection and classification, addressing the significant challenge of early-stage lung cancer identification. By integrating these models, our approach not only improves diagnostic precision but also serves as a valuable tool for radiologists, aiding them in making more informed, data-driven decisions in clinical practice.

***Key words:*** *Lung cancer, Artificial Intelligence, Detection, Classification, Deep learning.*

# Résumé

Le cancer du poumon reste l'une des principales causes de décès liés au cancer dans le monde, principalement parce qu'il est souvent diagnostiqué à un stade avancé, lorsque les options de traitement sont moins efficaces. Dans de nombreux cas, le cancer du poumon à un stade précoce est asymptomatique, ce qui signifie que les patients ne ressentent pas de symptômes visibles tant que la maladie n'a pas progressé. Ce retard dans l'apparition des symptômes conduit à une probabilité accrue de détection tardive, à laquelle les tumeurs peuvent s'être propagées au-delà des poumons, réduisant considérablement l'efficacité des traitements disponibles, tels que la chirurgie, la radiothérapie et la chimiothérapie. De plus, la petite taille et la subtilité des nodules pulmonaires à un stade précoce les rendent difficiles à détecter en imagerie médicale, car ils peuvent facilement être manqués ou mal interprétés par les radiologues. Par conséquent, améliorer les méthodes de détection précoce est crucial pour augmenter les taux de survie, car un diagnostic précoce permet une intervention plus rapide, des traitements potentiellement curatifs, et de meilleurs résultats pour les patients.

Ce travail explore des méthodologies avancées pour la détection précoce et la classification du cancer du poumons, en exploitant des techniques de détection d'objets et d'apprentissage profond à la pointe de la technologie. Les nodules pulmonaires, souvent considérés comme l'un des premiers indicateurs du cancer du poumon, sont essentiels à identifier avec précision afin d'améliorer le diagnostic précoce et d'optimiser les résultats pour les patients. Pour ce faire, nous utilisons l'architecture YOLOv7, réputée pour sa rapidité et sa précision, pour détecter les nodules pulmonaires dans les images médicales, avec un accent particulier sur l'identification des nodules petits et subtils, souvent difficiles à détecter à l'aide des techniques d'imagerie conventionnelles.

Après la phase de détection, nous utilisons l'apprentissage par transfert avec le modèle pré-entraîné VGG16 pour la classification des nodules détectés. L'apprentissage par transfert nous permet d'exploiter la puissance de l'extraction de caractéristiques profondes de VGG16 tout en ajustant le modèle pour qu'il soit très sensible aux caractéristiques des nodules pulmonaires. Ensemble, ces techniques améliorent la précision, la fiabilité et la rapidité de la détection et de la classification des nodules, répondant ainsi au défi majeur de l'identification du cancer du poumon à un stade précoce. En intégrant ces modèles, notre approche améliore non seulement la précision diagnostique, mais fournit également aux radiologues un outil précieux pour prendre des décisions plus informées et basées sur les données dans la pratique clinique.

***Mots clés :*** *Le cancer du poumons, Intelligence artificielle, Detection, Classification, Apprentissage profond.*

# Contents

**List of Figures** **3**

**List of Tables** **5**

**List of Abbreviations** **7**

**General introduction** **9**

Problematic . . . 9
Objectives . . . 11
Methodology . . . 12
Thesis outline . . . 13

**1 Lung Cancer From a Medical Perspective** **15**

1.1 Introduction . . . 16
1.2 Respiratory system . . . 17
1.3 Lung cancer . . . 19
1.3.1 Lung cancer types . . . 20
1.3.2 Stages of lung cancer . . . 22
1.4 Epidemiology of lung cancer . . . 25
1.5 Lung cancer factors, diagnosis and treatment . . . 30
1.6 Current Challenges in Lung Cancer Diagnosis . . . 38
1.7 Conclusion . . . 39

**2 AI for the Detection and Classification of Lung Cancer** **41**

2.1 Introduction . . . 42
2.2 AI in lung cancer diagnosis . . . 42
2.3 Key Concepts in AI . . . 44
2.3.1 Artificial Intelligence . . . 44

2.3.2 Machine learning . . . 45
2.3.3 Deep learning . . . 48
2.4 Computer-Aided Detection and Diagnosis (CAD) system for lung cancer . . . 55
2.4.1 Available datasets for lung cancer . . . 56
2.4.2 Computer-Aided Detection (CADe) systems for lung cancer . . . 60
2.4.3 Computer Aided Diagnosis (CADx) system for lung cancer . . . 72
2.5 Conclusion . . . 74

**3 A new approach based on deep learning for the detection and classification of lung cancer 76**
3.1 Introduction . . . 77
3.2 Related works . . . 77
3.3 Proposed Method . . . 82
3.3.1 Data preparation . . . 83
3.3.2 Lung nodule detection using transfer learning of YOLOv7 . . . 91
3.3.3 Lung nodule classification with transfer learning of vgg16 . . . 95
3.4 Conclusion . . . 100

**4 Results and Discussion 101**
4.1 Introduction . . . 102
4.2 Software and Hardware . . . 102
4.3 Results . . . 102
4.3.1 Lung nodules detection . . . 104
4.3.2 Lung nodules classification . . . 110
4.4 Dicsussion . . . 112
4.5 Perspective . . . 119
4.6 Conclusion . . . 119

**General Conclusion 120**

**Scientific Production 122**

**Bibliography 123**

# List of Figures


1.1 Respiratory system [13] . . . 17
1.2 Lung Cancer [17] . . . 20
1.3 Types of Non Small Cell Lung cancer [19] . . . 21
1.4 Stage of Non Small Cell Lung Cancer [22] . . . 23
1.5 Stage of Small Cell Lung Cancer [22] . . . 25
1.6 Different type of lung nodule [28] . . . 31
1.7 Representation of juxtapleural lung nodules in CT scan images . . . 32
1.8 Lung cancer risk factor . . . 33

2.1 Machine learning algorithms . . . 46
2.2 Machine learning Vs. Deep learning [79] . . . 49
2.3 Neuron in Artificial Neural Network [80] . . . 50
2.4 The most common loss functions . . . 51
2.5 Feedforward neural network composed of three layers [81] . . . 52
2.7 Activation functions: (a): basic non-linear functions, (b): advanced non-linear function [83] . . . 53
2.6 The structure of a CNN [82] . . . 53
2.8 The scheme of RNN with one hidden layer [86] . . . 55
2.9 CAD system for lung cancer . . . 56
2.10 Timeline of YOLO variants [104] . . . 64
2.11 RCNN architecture [86] . . . 65
2.12 U-net architecture [128] . . . 71

3.1 The overall architecture of the proposed approach [158] . . . 83
3.2 Example of a CT scan image in DICOM format [159]. . . . 84
3.3 The Hounsfield scale of CT numbers [160] . . . 85
3.4 The outcome after each step of lung segmentation process. . . . 90

3.5 Schematic plot for (a) one-stage detector and (b) two-stage detector [163] . . 91
3.6 Training YOLO process . . . . . 92
3.7 First approach architecture . . . . . 98
3.8 Second approach architecture . . . . . 99
3.9 Third approach architecture . . . . . 100

4.1 Box loss, mAP, Precision and Recall curves of the first senario using whole images [158] . . . . . 105
4.2 Box loss, mAP, Precision and Recall curve using preprocessed images with median filter [158] . . . . . 106
4.3 Box loss, mAP, Precision and Recall curve using preprocessed images with adaptive median filter [158] . . . . . 107
4.4 Box loss, mAP, Precision and Recall curves using segmented images [158] . . 109
4.5 Some samples of lung nodule detection using three different inputs (result 1: for whole image, result 2: for preprocessed images, result 3: for lung segmented images [158]) . . . . . 110
4.6 Confusion matrix of the first model [158] . . . . . 111
4.7 Confusion matrix of the second model [158] . . . . . 111
4.8 Confusion matrix of the third model . . . . . 112
4.9 mAP metric of different presented models . . . . . 113
4.10 Comparison of three different models . . . . . 113
4.11 Some samples that show the ability of the model to detect lung nodules when using whole images as input in training. . . . . 115
4.12 The model's ability to detect small nodules . . . . . 116

# List of Tables

1.2 New Cases and Deaths for 10 types of cancers in 2020 worldwide [24] . . . . 27
1.1 New Cases and Deaths for 10 types of cancers in 2018 worldwide [25] . . . . 27
1.3 New Cases and Deaths for 10 types of cancers in 2022 worldwide [2] . . . . . 28
1.4 New Cases for 10 types of cancers in Algeria, 2022 [26] . . . . . 29
1.5 Cancer-related deaths for 10 cancer categories in Algeria, 2022 [26] . . . . . 29
1.6 5-year prevalence of 10 type of cancer in Algeria, 2022 [26] . . . . . 30

2.1 Available databases . . . . . 58
2.2 Thresholding types . . . . . 67

4.1 Results of fine-tuned YOLOv7 for lung nodule detection [158] . . . . . 104
4.2 Comparison results between the proposed method and some lung nodule detection methods. . . . . 118

# List of Abbreviations

| | |
|---|---|
| **pH**: | potentiel Hydrogène |
| **NCSLS**: | Non-Small Cell Lung Cancer |
| **SCLC**: | Small Cell Lung Cancer |
| **WHO**: | World Health Organization |
| **IARC**: | International Agency for Research on Cancer |
| **HRCT**: | high-resolution CT |
| **MDCT**: | multidetector CT |
| **CDSS**: | Clinical Decision Support Systems |
| **AI**: | Artificial Intelligence |
| **CT**: | Computed Tomography |
| **MRI**: | Magnetic Resonance Imaging |
| **PET**: | Positron Emission Tomography |
| **EBUS**: | Endobronchial Ultrasound |
| **CAD**: | Computer-Aided Detection and Diagnosis |
| **CADe**: | Computer-Aided Detection |
| **CADx**: | Computer-Aided Diagnosis |
| **ML**: | Machine Learning |
| **DL**: | Deep Learning |
| **PCA**: | principal component analysis |
| **t-SNE**: | t-distributed Stochastic Neighbor Embedding |
| **SGD**: | Stochastic Gradient Descent |
| **FNN**: | Feedforward Neural Networks |
| **RNN**: | Recurrent Neural Networks |
| **CNN**: | Convolutional Neural Network |
| **RGB**: | Red,Green and Blue |
| **Tanh**: | Hyperbolic Tangent |
| **ReLU**: | Rectified Linear Unit |
| **DICOM**: | Digital Imaging and Communications in Medicine) |

| | |
|---|---|
| **HU**: | Hounsfield units |
| **LIDC-IDRI**: | Lung Image Database Consortium and Image Database Resource Initiative |
| **AAPM**: | American Association of Physicists in Medicine |
| **NCA**: | National Cancer Institute |
| **NLST**: | National Lung Screening Trial |
| **LDCT**: | Low-Dose Computed Tomography |
| **ISBI**: | International Symposium on Biomedical Imaging |
| **LUNA16**: | LUng Nodule Analysis 2016 |
| **ACRIN**: | American College of Radiology Imaging Network |
| **ROI**: | Region Of Interest |
| **FCM**: | Fuzzy C-Means clustering |
| **YOLO**: | You Only Look Once |
| **SSD**: | Single Shot MultiBox Detector |
| **FPN**: | Feature Pyramid Networks |
| **SPP**: | Spatial Pyramid Pooling |
| **E-ELAN**: | Extended Efficient Layer Aggregation Network |
| **R-CNN**: | Region-based Convolutional Neural Network |
| **RPN**: | Region Proposal Networks |
| **SVM**: | Support Vector Machines |
| **KNN**: | K-Nearest Neighbors |
| **GAN**: | Generative Adversarial Networks |
| **mAP**: | mean Average Precision |
| **AP**: | Average Precision |
| **IoU**: | Intersection over Union |
| **MD**: | Malignancy Degree |
| **FP**: | False Positive |
| **FN**: | False Negative |
| **TP**: | True Positive |
| **TN**: | True Negative |

# General introduction

Cancer is a group of diseases characterized by the uncontrolled growth and spread of abnormal cells. If left unchecked, this can lead to death. It can develop almost anywhere in the body and is classified based on the organ or type of cell where it begins. The development of cancer is a multi-step process, often taking years or even decades to manifest symptoms. It typically starts with genetic changes in cells, leading to the formation of a tumor, which can be benign (non-cancerous) or malignant (cancerous). Malignant tumors have the ability to invade nearby tissues and spread to other parts of the body through the bloodstream and lymphatic system, a process known as metastasis. Among the various types of cancer, lung cancer is particularly notorious due to its high mortality rate and aggressive nature [1], accounting more than 1.8 million deaths globally in 2022 [2], making it the leading cause of cancer-related mortality worldwide .

Lung cancer originates in the tissues of the lungs, usually in the cells lining the air passages. It is often diagnosed at a late stage because its early symptoms are easily mistaken for common respiratory ailments. This late diagnosis contributes to its high fatality rate. Lung cancer remains one of the most critical areas of oncology, demanding ongoing research and advances in detection, treatment, and prevention. Despite the use of advanced diagnostic tools like X-rays, Computed Tomography (CT) scans, Magnetic Resonance Imaging (MRI), and Positron Emission Tomography (PET) scans, each method presents challenges such as high costs, radiation exposure, and the risk of false positives. Biopsies, while definitive, are invasive and time-consuming [3]. These issues highlight the need for more efficient, cost-effective, accurate and intelligent approache for early detection, especially in high-risk cancers like lung cancer [4, 5].

## Problematic

The central problem addressed in our work can be divided into three main areas: the limitations in lung cancer diagnosis, the challenges associated with accurately classifying lung

cancer and the availability of dataset.

1. **Limitations in lung cancer diagnosis**

    - Dependence on radiologist expertise: The primary imaging tools used for lung cancer detection are CT scans and X-rays. While these technologies are valuable for visualizing lung structures and identifying abnormalities, their effectiveness largely depends on the skills and judgment of the radiologists who interpret them. Radiologists must analyze complex images and detect subtle differences in lung tissues, which can be subjective and prone to human error. The variability in expertise among radiologists means that interpretations can differ, sometimes leading to inconsistencies in diagnoses. This reliance on human analysis underscores the need for adjunct tools that can assist in enhancing the precision and reliability of image interpretation [6].
    - Impact of late-stage detection on survival rates: Lung cancer is often not detected until it has progressed to an advanced stage [6], which substantially impacts patient prognosis. Once lung cancer reaches later stages, it is more likely to have metastasized, spreading to other parts of the body and making it far more difficult to treat effectively. Treatments such as surgery, chemotherapy, and radiation are less successful when the disease has progressed, leading to lower survival rates. Early-stage detection is critical as it increases the chances of successful treatment and improved outcomes, emphasizing the urgent need for improved early diagnostic methods.
    - Detection challenges in early-stage lung nodules: Detecting small nodules is particularly challenging because these nodules may be tiny, faint, or obscured by other lung structures on imaging. The subtle nature of these early lesions can cause them to be overlooked during routine image analysis. Additionally, small nodules may not exhibit distinctive features that set them apart from benign formations, complicating the detection process. This difficulty highlights the limitations of current imaging technologies and the need for advanced detection tools capable of identifying these subtle signs of early disease more reliably [7].

2. **Challenges in lung cancer classification**

    - Challenges in differentiating benign and malignant nodules: One of the most significant challenges in lung cancer diagnostics is differentiating between benign

and malignant nodules. Both types of nodules can share similar characteristics in terms of size, shape, and density, making them difficult to classify based on visual cues alone [8]. This ambiguity can lead to diagnostic errors such as false positives, where benign nodules are mistakenly classified as malignant, resulting in unnecessary invasive procedures and patient anxiety. Conversely, false negatives, where malignant nodules are misclassified as benign, can delay critical treatment, allowing the cancer to progress undetected. Adding to this complexity, the presence of nodules with indeterminate features that do not clearly align with either benign or malignant characteristics. These nodules occupy a critical diagnostic middle ground, creating uncertainty in diagnosis and treatment planning and emphasizing the need for advanced methods to refine classification.

3. **Dataset availability**:

    - One of the major challenges in lung cancer diagnosis using artificial intelligence (AI) is the lack of standardized and structured datasets. Many existing datasets do not have a format that is directly compatible with AI algorithms, which limits their utility for training and evaluation. The absence of proper image annotations and inconsistent classification of nodules, often make it difficult to utilize these datasets effectively. This lack of structure necessitates significant preprocessing to create a dataset that can support various AI approaches, ensuring reliable and accurate model development.

# Objectives

The objectives of this thesis are as follows:

- **Develop an intelligent approach for lung cancer diagnosis:** Create an intelligent approach that integrates advanced artificial intelligence technologies to assist radiologists in the accurate detection and diagnosis of lung cancer. This approach should minimize human error and improve efficiency in analyzing medical imaging.
- **Prepare a dataset:** Collect and prepare a comprehensive lung cancer dataset from existing sources, ensuring that it is structured to be compatible with AI algorithms. This includes ensuring the dataset has standardized formats for image annotations and nodule classification. This structured dataset will serve as a reliable foundation for training and evaluating various AI models for lung cancer detection.

- **Focus on early detection of lung cancer:** The system should prioritize the early identification of lung cancer, leveraging the fact that early detection significantly improves patient outcomes. By identifying subtle signs of cancer in its early stages, the system can prompt timely medical intervention.
- **Detect small nodules:** Early-stage lung cancer often presents as small nodules that may be challenging to detect. The system must be fine-tuned to detect nodules within the 3-30 mm range, ensuring that even the smallest, most elusive nodules are identified.
- **Classification of lung cancer:** Once nodules are detected, the system should be capable of distinguishing between benign and malignant lesions. By providing a reliable classification, it supports radiologists in making more accurate diagnoses and helps reduce the likelihood of misdiagnosis.

# Methodology

Artificial intelligence holds immense potential to transform lung cancer diagnostics by addressing challenges that traditional methods often fail to overcome. Among these AI-driven strategies, object detection has proven particularly effective in identifying early-stage lung nodules, enhancing precision in abnormality detection. This capability serves as a foundation for advanced classification techniques, enabling comprehensive diagnostic solutions.

Building on this foundation, we propose an intelligent approach that integrates object detection with transfer learning. This method excels in detecting small nodules, even within the complex and heterogeneous structures of the lungs. Once detected, transfer learning classifies them, offering a reliable system to support radiologists in early diagnosis and treatment planning.

- **Object Detection for Lung Cancer Nodule Identification:** We emphasize the critical role of object detection techniques in lung cancer diagnostics, particularly in identifying nodules as small as 3 mm and up to 30 mm in size. The early detection of such nodules is paramount, as it significantly impacts the timely diagnosis and treatment of lung cancer. However, this task is challenging due to the heterogeneous nature of lung structures. The lungs are composed of varying tissue densities and complex anatomical features, including airways, blood vessels, bronchi, and alveoli. These diverse structures contribute to an intricate visual environment in CT scans, where nodules can be easily obscured or confused with normal anatomical components.

Adding to the complexity, lung nodules can present in different morphological forms. Each form has distinct imaging characteristics, complicating the detection process. Furthermore, non-nodular structures, such as blood vessels or parts of the bronchi, can mimic nodular appearances. This similarity increases the likelihood of false positives, where benign lesions or normal structures are mistaken for nodules, or false negatives, where actual nodules are missed altogether. Despite these challenges, object detection techniques have proven effective in navigating this complexity, offering a reliable method for identifying abnormalities within the lungs. These techniques lay the foundation for early diagnosis, which is critical for improving patient outcomes.

- **Nodule Classification via Transfer Learning:** Building upon the capabilities of object detection, we employed transfer learning to classify the detected nodules. Transfer learning leverages pre-trained models, which have been fine-tuned using our specific dataset, to enhance classification accuracy. This approach is particularly beneficial in medical imaging, where labeled data is often limited. By utilizing the features learned from large-scale datasets, transfer learning accelerates model training and improves its ability to differentiate subtle patterns within lung nodules.

  Our aim was to design a high-performance system capable of assisting radiologists in the early detection and classification of lung cancer. This intelligent approach not only enhances diagnostic accuracy but also reduces the workload of radiologists, enabling them to focus on complex cases requiring their expertise. The integration of object detection and transfer learning demonstrates the potential of advanced AI techniques in addressing the intricacies of lung cancer diagnosis, ultimately contributing to better patient care and outcomes.

## Thesis outline

This thesis is composed of four chapters which are:

- **Chapter 1: Lung Cancer from a Medical Perspective**- This chapter explores lung cancer from a medical standpoint.

- **Chapter 2: Artificial Intelligence for the Detection and Classification of Lung Cancer**- Defines the application of artificial intelligence (AI) in the detection

and classification of lung cancer.

- **Chapter 3: A New Approach Based on Deep Learning Techniques for the Detection and Classification of Lung Cancer**- Describes an overview of the related work, as well as our proposed method to detect and classify lung cancer.

- **Chapter 4: Results and discussion**- Dedicated to experimentation and analysis of the results obtained, followed by a comparative study to validate the proposed work.

This thesis concludes with a general summary and future perspectives, offering a synthesis of the proposed work and insights into potential advancements.

# Chapter 1

# Lung Cancer From a Medical Perspective

## 1.1 Introduction

The respiratory system is vital for numerous physiological functions, playing a crucial role in maintaining homeostasis and supporting life. It regulates gas exchange, supports cellular functions, maintains potentiel hydrogène (pH) balance, and protects against pathogens. The lungs, as key components of this system, facilitate gas exchange between the body and the external environment, delivering oxygen to tissues, and removing carbon dioxide [9].

Among the most perilous diseases affecting the lungs is lung cancer, which poses a significant public health threat due to its high mortality rates and challenges in early detection. As one of the deadliest cancers, it often remains asymptomatic in its initial stages, leading to delayed diagnoses and limited treatment options [10]. The risk increases due to its potential to metastasize, spreading beyond the lungs and complicating effective treatment. Therefore, early diagnosis is critical for improving outcomes. However, the lack of distinctive symptoms in the early stages complicates this effort. To combat the significant threat posed by lung cancer, raising awareness, promoting regular screenings for high-risk individuals, and investing in innovative diagnostic research are essential. Timely detection can markedly enhance treatment success rates and improve prognoses for affected individuals.

In addressing the challenges of lung cancer detection, Artificial Intelligence (AI) has rapidly transformed the medical landscape, revolutionizing disease detection, diagnosis, and treatment. With its capacity to process vast amounts of data and identify patterns that may elude human observers, AI technologies significantly enhance diagnostic accuracy and efficiency [11]. For instance, in medical imaging, they demonstrate remarkable effectiveness in interpreting complex radiological scans, such as X-rays, CT scans, and MRIs, with high precision. These advancements enable clinicians to identify abnormalities earlier.

In the realm of lung cancer, AI assumes a particularly critical role in addressing the diagnostic challenges outlined earlier. By harnessing AI tools, the early detection of small lung nodules, classification of tumor types, and prediction of malignancy become more precise, leading to improved treatment planning and outcomes [12]. AI's ability to analyze subtle variations in imaging or tissue samples significantly reduces the risk of missed diagnoses and enhances the detection of cancer in its nascent stages. As AI continues to evolve, its integration into clinical practice holds the promise of transforming cancer care, offering new hope for early intervention and personalized treatment strategies.

In this chapter, we will explore lung cancer from a medical standpoint. We begin with an overview of the respiratory system, followed by an in-depth examination of lung cancer, including its epidemiology, risk factors, diagnostic methods, and treatment options. Lastly,

we will address the various challenges faced in managing this disease.

## 1.2 Respiratory system

The respiratory system is a complex biological system responsible for exchanging gases, particularly oxygen and carbon dioxide, between the body and the external environment. It includes various organs and structures that work together to facilitate the process of breathing and ensure that the body receives an adequate supply of oxygen while expelling carbon dioxide [13].

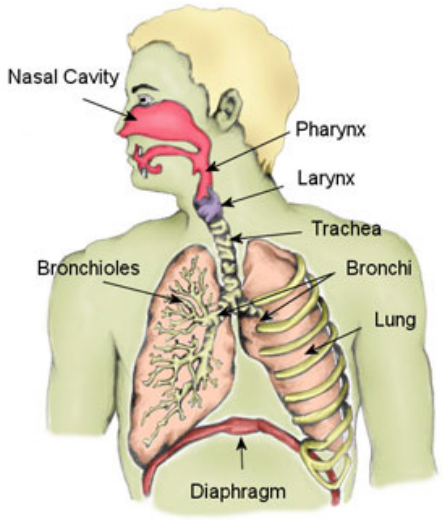



figure 1.1: Respiratory system [13]

Figure1.1 presents the key components of the respiratory system include the following [14]:

- *Nose and Nasal Cavity:* The nose and nasal cavity filter, humidity and warm the incoming air before it reaches the lungs.
- *Pharynx (throat):* The pharynx is a passage that connects the nose and mouth to the larynx. It serves both the respiratory and digestive systems.
- *Larynx (Voice Box):* The larynx contains the vocal cords and is involved in producing sound for speech.
- *Trachea (Windpipe):* The trachea is a tube that carries air from the larynx to the lungs. It is reinforced with cartilage to prevent collapsing.

- *Bronchi and Bronchioles:* The trachea branches into two bronchi, each leading to a lung. These bronchi divide into smaller bronchioles, forming the respiratory tree.
- *Lungs:* The lungs are the main organs of respiration. They are soft, spongy organs that house the bronchial tree and facilitate the exchange of gases in tiny air sacs called alveoli.
- *Alveoli:* Alveoli are small, thin-walled sacs in the lungs where the exchange of oxygen and carbon dioxide occurs in the bloodstream.
- *Diaphragm:* The diaphragm is a muscular partition that separates the chest (thoracic) cavity from the abdominal cavity. It plays a crucial role in breathing by contracting and relaxing, causing changes in thoracic pressure.

The respiratory system facilitates breathing through two processes: inhalation and exhalation. Inhalation involves taking in air through the nose or mouth, which travels down the trachea, bronchi, and bronchioles to reach the alveoli in the lungs. Oxygen from the air diffuses through the alveolar walls into the bloodstream, where it binds to red blood cells and is delivered to the body's cells to support their function.
Exhalation is the process of expelling air from the body. Carbon dioxide, a waste product of cellular activity, moves from the cells into the bloodstream, travels to the alveoli, and is expelled during breathing out.
Gas exchange between the lungs and the bloodstream occurs due to a concentration gradient: oxygen moves from the alveoli into the blood, while carbon dioxide moves from the blood into the alveoli to be exhaled [15].

The mechanics of breathing involve:

- Inhalation (Inspiration): The diaphragm contracts and moves downward, while the intercostal muscles between the ribs contract, expanding the chest cavity and decreasing pressure to draw air into the lungs.
- Exhalation (Expiration): The diaphragm relaxes and moves upward, while the intercostal muscles relax, reducing chest cavity size and increasing pressure to expel air.

The lungs are part of the respiratory system, the group of organs and tissues necessary for breathing. There are two lungs, and they take up almost all the space inside the chest. Each lung is divided into lobes (sections), where the right lung has three lobes and is slightly wider than the left lung, and the left lung has two lobes. The heart rests on the cardiac

incisura, which is a hollow in the lower lobe. The main functions of the lungs are to transfer oxygen from the air into the blood and to release carbon dioxide from the blood into the air. Air enters through the mouth or nose and travels down the trachea, bronchi, and bronchioles to the alveoli. The exchange between oxygen and carbon dioxide takes place in the alveoli. The alveoli absorb oxygen from the air before sending it into the blood, which circulates it throughout the body.
Carbon dioxide, which is a waste product from body cells, passes from the blood to the alveoli before being exhaled [16]. The lungs produce a mixture of fat and protein called lung surfactant. The surfactant coats the surface of the alveoli, making it easier for them to expand and contract with each inhale/exhale. They also help protect the body from harmful substances in the air, such as smoke, pollution, bacteria, and viruses. These substances can pass through the nose and become trapped in the lungs. The lungs produce a thick viscous fluid called mucus that can trap and partially destroy these substances from the air. The cilia move quickly to push mucus into the bronchi, where it is evacuated when the person coughs or swallows.

## 1.3 Lung cancer

Cancer is a broad group of diseases characterized by the uncontrolled growth and spread of abnormal cells in the body. Normally, human cells grow, divide, and die in an orderly manner. However, in cancer, the genetic material (DNA) of a cell becomes damaged or altered, leading to mutations that disrupt normal cell function. These changes cause the cells to grow and divide uncontrollably, forming a mass of tissue called a tumor. Some cancers, like leukemia, don't form tumors but instead affect the blood or bone marrow.
Cancer can be benign or malignant:

- Benign tumors: Non-cancerous growths that do not spread to other parts of the body.
- Malignant tumors: Cancerous growths that invade nearby tissues and can spread to other parts of the body (a process called metastasis).

It is classified based on the origin of the affected cells or tissue, as well as the specific organ or body part where it begins. For example, cancer that starts in the lungs is called lung cancer, while cancer originating in the breast tissue is known as breast cancer, and cancer that begins in the liver is termed liver cancer.

Lung cancer, one of the most aggressive forms of cancer, originates in the cells of the lungs, typically within the airways (bronchi) or the alveoli, where oxygen exchange takes place. It develops when lung cells undergo abnormal changes, leading to uncontrolled growth and the formation of a tumor, as shown in Figure 1.2. It is the leading cause of cancer-related deaths worldwide, largely due to its strong link to smoking, as well as other environmental risk factors. Its aggressive nature and tendency to be diagnosed at advanced stages contribute to its high mortality rate.

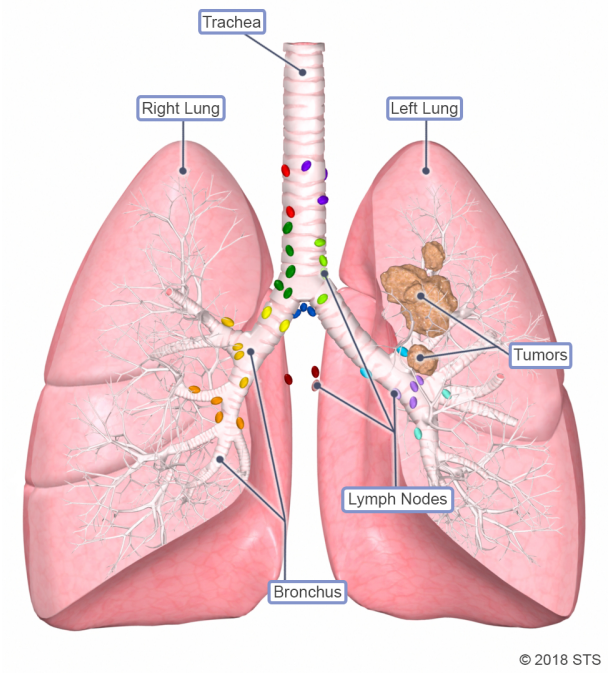



figure 1.2: Lung Cancer [17]

### 1.3.1 Lung cancer types

There are two main types of lung cancer, classified based on the appearance of the cancer cells under a microscope. Non-small cell lung cancer (NSCLC) is the most common type, accounts for almost 85% of all lung cancers and can develop from various types of cells within lung tissue. On the other hand, SCLC (Small Cell Lung Cancer) is less common, accounting for almost 15% of lung cancers, and arises from cells that line the bronchi [18].

- Non-Small Cell Lung Cancer (NSCLC) tends to grow and spread more slowly than SCLC, it can develop from various types of cells within the lung tissue, including squamous cells, glandular cells, and cells that line the bronchi, and often starts in the outer regions of the lungs and may be present for a longer period before symptoms

become noticeable. The NSCLC is divided into three main subtypes, each one has distinct characteristics and may respond differently to treatment that depends on the stage of cancer, but can include surgery, radiation therapy, chemotherapy, targeted therapy, and immunotherapy. Figure1.3 presents the the different subtypes of NSCLC [19], which are:

- Adenocarcinoma: Usually begins in mucus-producing cells and is more common in non-smokers.
- Squamous cell carcinoma: Originates in the flat cells lining the airways, often associated with smoking.
- Large cell carcinoma: A less common, fast-growing type that can appear in any part of the lung.

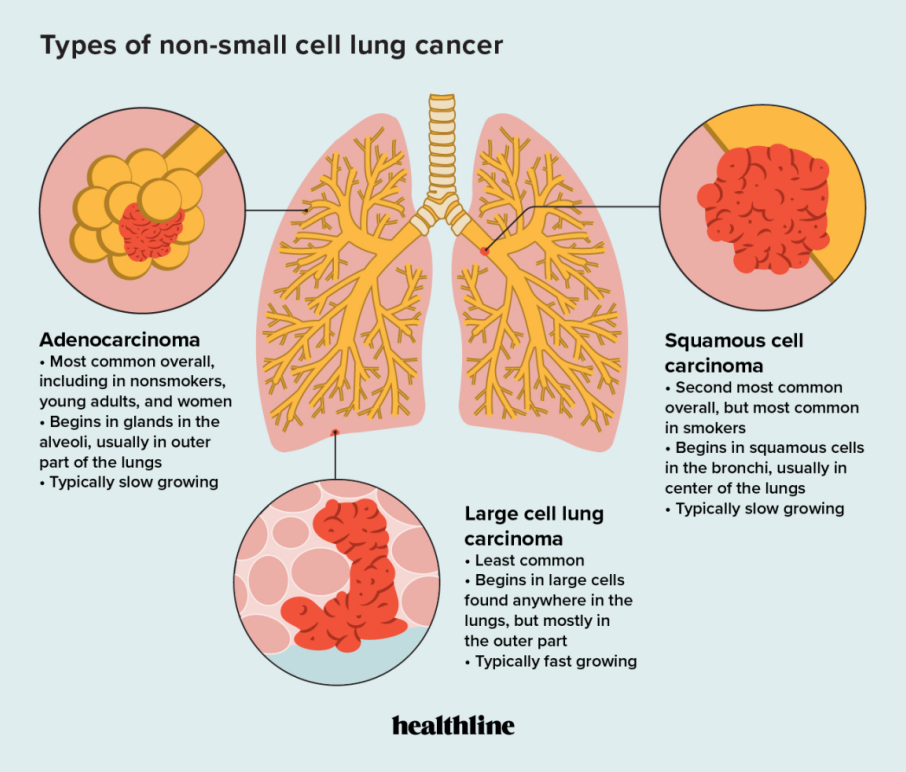



figure 1.3: Types of Non Small Cell Lung cancer [19]

- Small Cell Lung Cancer (SCLC) is often associated with heavy smoking and characterized by its rapid growth and early spread to other parts of the body, including distant organs. It is considered more aggressive than NSCLC.
  SCLC is divided into two stages: the limited stage, where cancer is confined to one

lung and nearby lymph nodes, and the extensive stage, where cancer has spread beyond the lung. It is typically treated with chemotherapy, radiation therapy is also commonly used, especially for limited-stage of SCLC but surgery is generally not a primary treatment option due to the aggressive nature and early spread of SCLC.

Lung cancer symptoms can vary and may not appear in the early stages of the disease. As the cancer progresses, symptoms may become more noticeable, some of them combine breathing problems and a change in the patient's general condition such as:

- The onset of a cough or an increase in chronic bronchitis cough.
- Bloody sputum (hemoptysis).
- Appearance or worsening of difficulty breathing (dyspnea or shortness of breath) in the absence of proven heart problems.
- Recurrent lung infections (bronchitis or pneumonia).
- Severe acute or chronic pain (such as a side stitch suggesting a muscle tear or shoulder pain suggesting rheumatism).
- Unusual and persistent fatigue.
- Loss of appetite.
- Weight loss.

Patients with lung cancer may experience less common symptoms caused by nerve or organ compression within the respiratory system. These include voice changes (dysphonia), difficulty swallowing (dysphagia), wheezing due to airway compression, and chest pain from conditions like pleurisy or pericarditis.

### 1.3.2 Stages of lung cancer

Lung cancer staging is critical for determining treatment options and prognosis. It describes the size of the tumor, its spread within the lungs, and whether it has metastasized (spread) to other parts of the body [20, 21]. The most commonly used staging system for lung cancer is the TNM classification:

- T (Tumor): Describes the size and extent of the main tumor.

- N (Nodes): Indicates whether the cancer has spread to nearby lymph nodes.
- M (Metastasis): Refers to whether the cancer has spread to other parts of the body.

Based on these factors, NSCLC is classified into stages ranging from Stage 0 to Stage IV as presented in Figure1.4 based on the extent of the disease as follow:

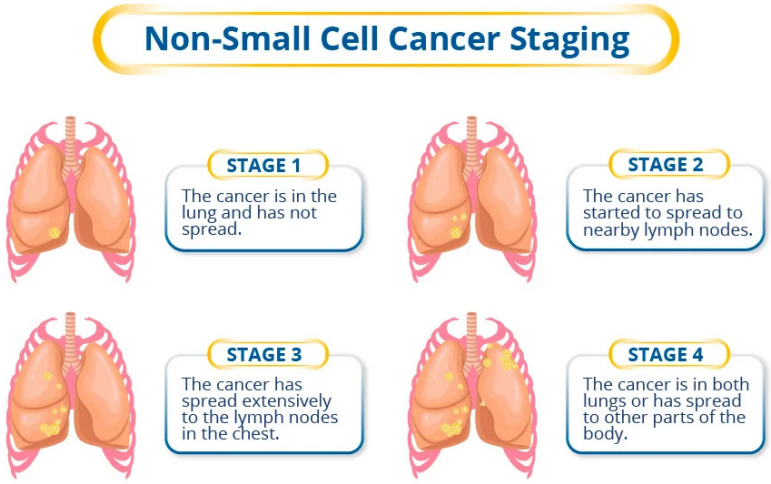



figure 1.4: Stage of Non Small Cell Lung Cancer [22]

- Stage 0 (Carcinoma in Situ): Is characterized by the presence of abnormal cells confined to the lining of the airways, without invasion into deeper lung tissues or lymph nodes. This stage is often asymptomatic, making it typically detectable only through screening. The prognosis for Stage 0 is favorable, with a high likelihood of successful treatment, usually achieved through surgical removal of the affected tissue if identified early.
- Stage 1: Localized Cancer is characterized by tumors confined to the lungs, with no spread to lymph nodes or other areas. In Stage 1A, the tumor is 3 cm or smaller and remains restricted to lung tissue, while Stage 1B involves tumors between 3 and 4 cm that may have invaded nearby tissues, such as the bronchus, but still without lymph node involvement or metastasis. Patients in this stage are often asymptomatic or present with nonspecific symptoms, like a persistent cough, making early detection challenging. It is frequently identified incidentally during imaging for other issues. The prognosis for Stage 1 lung cancer is generally favorable, with high treatment success rates, particularly through surgical resection, which can potentially lead to a cure if detected early.

- Stage 2: Larger Tumor or Lymph Node Involvement is characterized by tumors that may be larger in size and the potential for early spread to nearby lymph nodes, although there is no metastasis to distant body parts. In Stage 2A, the tumor ranges from 4 to 5 cm and may involve nearby lymph nodes, possibly extending into the main bronchus or visceral pleura. In Stage 2B, the tumor may exceed 5 cm, with limited lymph node involvement, or it could be smaller but more invasive, affecting surrounding structures like the chest wall. Patients in this stage may begin to experience symptoms such as shortness of breath, wheezing, chest pain, or frequent respiratory infections; however, these symptoms can still be quite vague. The prognosis for Stage 2 lung cancer remains relatively favorable, as it is still considered localized, and treatment options such as surgery combined with chemotherapy or radiation therapy can often lead to long-term remission, though the risk of recurrence is higher compared to Stage 1.

- Stage 3: Locally Advanced Disease is characterized by the spread of cancer to nearby lymph nodes and potential invasion of nearby structures such as the chest wall, diaphragm, or mediastinum (the space between the lungs). It is subdivided into two categories: Stage 3A, where the cancer has spread to lymph nodes on the same side of the chest as the primary tumor and may involve structures like the chest wall, pericardium (lining of the heart), or diaphragm, and Stage 3B, where the cancer has spread to lymph nodes on the opposite side of the chest or above the collarbone, potentially involving major structures such as the heart, trachea, or esophagus. Symptoms become more pronounced in Stage 3, including persistent coughing, coughing up blood (hemoptysis), chest pain, difficulty breathing, hoarseness, and fatigue. Systemic symptoms like weight loss and night sweats may also arise due to the spread to lymph nodes. Treating Stage 3 lung cancer is challenging, requiring a combination of surgery, chemotherapy, and radiation therapy, but long-term remission is still possible, especially with newer treatments like immunotherapy.

- Stage 4: Metastatic Disease is the most advanced stage of lung cancer, where the cancer has spread (metastasized) to distant organs such as the brain, liver, bones, or other parts of the lungs. In Stage 4A, the cancer may have spread to the other lung, pleural fluid (causing malignant pleural effusion), or to limited distant sites, such as a single organ. In Stage 4B, the cancer has widely metastasized to multiple organs or areas throughout the body. Symptoms vary depending on the affected organs—brain metastases may cause headaches, seizures, or cognitive changes, while bone metastases can lead to bone pain or fractures. General symptoms of advanced cancer include

fatigue, loss of appetite, weight loss, and severe respiratory difficulties. The prognosis for Stage 4 lung cancer is generally poor, with treatment primarily focused on palliative care to manage symptoms and improve quality of life.

On the other hand, the Small Cell Lung Cancer (SCLC) is classified into two stages [20]: limited stage and extensive stage as indicated in the Figure1.5.

- Limited stage: The cancer is confined to one lung and may or may not have spread to nearby lymph nodes in the mediastinum (the area between the lungs). This stage is generally considered more treatable and localized, often managed with a combination of chemotherapy and radiation therapy.
- Extensive stage: Occurs when the cancer has spread beyond the originally affected lung to the opposite lung, pleura, or distant organs such as the liver, bones, or brain. This stage is more challenging to treat and requires systemic therapies like chemotherapy, with a focus on controlling symptoms and extending survival.

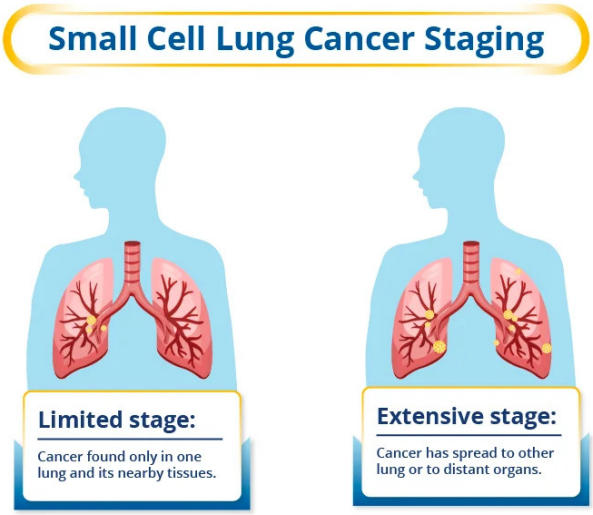



figure 1.5: Stage of Small Cell Lung Cancer [22]

## 1.4 Epidemiology of lung cancer

Lung cancer stands as a pervasive and formidable health challenge, its prevalence having a profound impact on global public health. As one of the most prevalent cancers worldwide,

its sheer incidence places an enormous burden on healthcare systems. The World Health Organization (WHO) reports millions of new cases annually, emphasizing the urgent need for effective prevention, early detection, and treatment strategies. In particular, lung cancer exhibits gender disparities, historically affecting more men, although an increasing incidence in women is evident. Geographical variations further contribute to its prevalence, with regional differences reflecting diverse smoking patterns, environmental exposures, and healthcare infrastructure [23]. Linked predominantly to age, the majority of lung cancer cases manifest in individuals over 65, underscoring the aging demographic as a significant factor.
The strong association with cigarette smoking remains a primary contributor to the disease's prevalence, emphasizing the crucial role of tobacco control in mitigating its impact. The economic ramifications are substantial and encompass the costs of diagnosis, treatment, and the broader social toll through productivity losses. Recognizing the prevalence of lung cancer emphasizes the imperative for concerted efforts in research, public health initiatives, and policy interventions to reduce its incidence, enhance early detection, and ultimately alleviate the considerable burden it places on individuals and healthcare systems globally.

When analyzing data from the tables (Table1.1 , Table1.2 , and Table 1.3), which represent the number of new cancer cases between 2018 and 2022, we have found that lung cancer has become the most prevalent type of cancer that ranked first in terms of new cases detected in 2018, and it held the top position in the number of new cancer deaths in both 2018 and 2020 [24, 25], By 2022, lung cancer helds the number one spot for both new cases and deaths [2]. This alarming increase indicates that lung cancer is rapidly spreading and poses a significant threat to the population. It is noteworthy that lung cancer was previously thought to be limited to men, but recent statistics show that it is now affecting a group of women as well. These findings suggest that there is a pressing need for greater awareness and preventative measures to combat this deadly disease [26].

| Cancer | Number of new cases | Number of depths with cancer |
|---|---|---|
| Female breast | **2261419 (11.7)** | 684996 (6.9) |
| Lung | 2206771 (11.4) | **1796144 (18.0)** |
| Prostate | 1414259 (7.3) | 375304 (3.8) |
| Nonmelanoma of skin | 1198073 (6.2) | 63731 (0.6) |
| Colon | 1148515 (6.0) | 576858 (5.8) |
| Stomach | 1089103 (5.6) | 768793 (7.7) |
| Liver | 905677 (4.7) | 830180 (8.3) |
| Rectum | 732210 (3.8) | 339022 (3.4) |
| Cervix uteri | 604127 (3.1) | 341831 (3.4) |
| Esophagus | 604100 (3.1) | 544076 (5.5) |

Table 1.2: New Cases and Deaths for 10 types of cancers in 2020 worldwide [24]

| Cancer | Number of new cases | Number of dephts with cancer |
|---|---|---|
| Lung | **2093876 (11.6)** | **1761007 (18.4)** |
| Breast | 2088849 (11.6) | 626679 (6.6) |
| Prostate | 1276106 (7.1) | 358989 (3.8) |
| Colon | 1096601 (6.1) | 551269 (5.8) |
| Nonmelanoma of skin | 1042056 (5.8) | 65155 (0.7) |
| Stomach | 1033701 (5.7) | 782685 (8.2) |
| Liver | 841080 (4.7) | 781631 (8.2) |
| Rectum | 704376 (3.9) | 310394 (3.2) |
| Esophagus | 572034 (3.2) | 508585 (5.3) |
| Cervix uteri | 569847 (3.2) | 311365 (3.3) |

Table 1.1: New Cases and Deaths for 10 types of cancers in 2018 worldwide [25]

In Algeria, lung cancer ranks third among the most common cancers in Algeria, with 5040 new cases, representing 7.8% of all cancer diagnoses reported in 2022 as presented in Table 1.4. Despite this relatively lower incidence compared to breast and colorectal cancers, it is one of the most fatal, responsible for 4599 deaths, accounting for 12.9% of cancer-related mortality (Table 1.5). Additionally, the five-year prevalence of lung cancer stands at 6725 cases, with a proportional rate of 14.8 per 100000 people (Table 1.6), reflecting its substantial burden on the healthcare system. This disparity between incidence and mortality underscores the

| **Cancer** | **Number of new cases** | **Number of dephts with cancer** |
|---|---|---|
| Lung | **2480301 (12.4)** | **1817172 (18.7)** |
| Breast | 2308897 (11.6) | 665684 (6.9) |
| Colon | 1926118 (9.6) | 903859 (9.3) |
| Prostate | 1466680 (7.3) | 396792 (4.1) |
| Nonmelanoma of skin | 331647 (1.7) | 58645 (0.6) |
| Stomach | 968350 (4.9) | 659853 (6.8) |
| Liver | 865269 (4.3) | 757948 (7.8) |
| Thyroid | 821173 (4.1) | 47485 (0.5) |
| Cervix uteri | 661021 (3.3) | 348189 (3.6) |
| Bladder | 613791 (3.1) | 220349 (2.3) |
| Non-Hodgkin lymphoma | 553010 (2.8) | 250475 (2.6) |

Table 1.3: New Cases and Deaths for 10 types of cancers in 2022 worldwide [2]

aggressive nature of lung cancer and highlights the challenges in early detection and effective treatment, emphasizing the urgent need for targeted public health initiatives focused on prevention, early screening, and innovative therapies.

Given the strong association with smoking and other environmental factors which will be explained in the next section, lung cancer remains a pressing public health issue not only in Algeria but around the world. Comprehensive prevention efforts, such as smoking cessation programs and early detection, are critical to reducing the disease's impact.

| **Cancer** | **Number of new cases** | **% of new cases** |
|---|---|---|
| Breast | 14601 | 22.6 |
| Colorectum | 7747 | 12 |
| Lung | 5040 | 7.8 |
| Prostate | 3514 | 5.4 |
| Bladder | 3240 | 5 |
| Stomach | 2785 | 4.3 |
| Thyroid | 2519 | 3.9 |
| NHL | 2226 | 3.4 |
| Brain CNS | 2038 | 3.1 |
| Cervix uteri | 1799 | 2.8 |

Table 1.4: New Cases for 10 types of cancers in Algeria, 2022 [26]

| **Cancer** | **Number of Deaths** | **% of new cases** |
|---|---|---|
| Breast | 4893 | 13.7 |
| Colorectum | 4380 | 12.2 |
| Lung | 4599 | 12.9 |
| Prostate | 1333 | 3.7 |
| Bladder | 1818 | 5.1 |
| Stomach | 2250 | 6.3 |
| Thyroid | 358 | 1.0 |
| NHL | 1187 | 3.3 |
| Brain CNS | 1575 | 4.4 |
| Cervix uteri | 1013 | 2.8 |

Table 1.5: Cancer-related deaths for 10 cancer categories in Algeria, 2022 [26]

| **Cancer** | **Number** | **Prop. (per 100000)** |
|---|---|---|
| Breast | 47259 | 210.6 |
| Colorectum | 22192 | 42.9 |
| Lung | 6725 | 14.8 |
| Prostate | 8124 | 35.5 |
| Bladder | 9863 | 21.8 |
| Stomach | 4330 | 9.6 |
| Thyroid | 8599 | 19.0 |
| NHL | 7118 | 15.7 |
| Brain CNS | 7675 | 16.9 |
| Cervix uteri | 5442 | 24.3 |

Table 1.6: 5-year prevalence of 10 type of cancer in Algeria, 2022 [26]

## 1.5 Lung cancer factors, diagnosis and treatment

Before examining the factors associated with lung cancer, it is essential to understand lung nodules, as they can serve as important indicators of potential risk for the disease. The presence of lung nodules may suggest the possibility of malignancy, particularly when they exhibit certain characteristics such as irregular shape, size greater than 1 cm, or noticeable growth over time. This is especially significant for individuals with a history of smoking, exposure to carcinogens, or a family history of lung cancer. In these cases, the detection of a lung nodule heightens the suspicion of cancer and necessitates further diagnostic evaluation.

In the context of lung cancer screening, lung nodules can be categorized into two main types: solid, and sub-solid nodules [27] as presented in the Figure 1.6, each of which carries varying degrees of clinical significance.

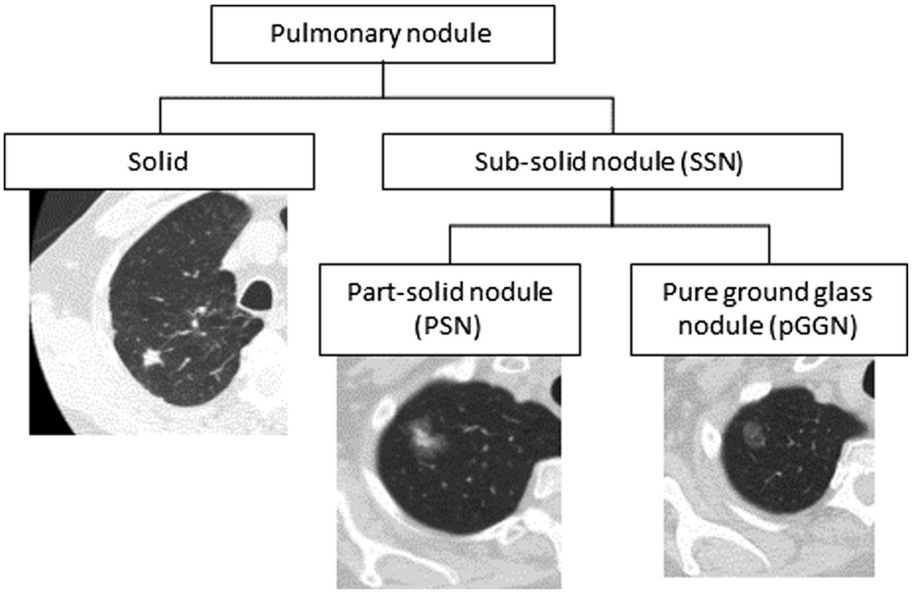



figure 1.6: Different type of lung nodule [28]

- A solid nodule: Is a dense area that completely obscures the underlying lung structures on imaging, such as a CT scan. These nodules may be benign, such as scars or granulomas, but they also raise concern for malignancies like lung cancer.
- Subsolid nodules: Are less dense than solid nodules and are further categorized into two types: part-solid nodules and ground-glass nodules (GGNs).
  - A part-solid nodule: Contains both a solid component and a less-dense ground-glass area. The presence of both components makes part-solid nodules more suspicious for cancer, particularly invasive adenocarcinoma, and they often require closer follow-up.
  - Ground-glass nodules (GGNs): Appear as hazy areas on scans, through which the underlying lung tissue remains visible. GGNs are less dense than solid nodules and are often associated with early-stage lung adenocarcinoma. Although they can also arise from benign causes like inflammation or infection, persistent GGNs, particularly those that develop a solid component, are more concerning and typically warrant long-term monitoring.

If nodules are located adjacent to the pleura, they are referred to as juxtapleural nodules, as shown in Figure1.7. These nodules can arise from various conditions, including benign processes like infections or inflammation, as well as malignant conditions such as lung cancer. When juxtapleural nodules are detected in high-risk individuals, their proximity to the pleura

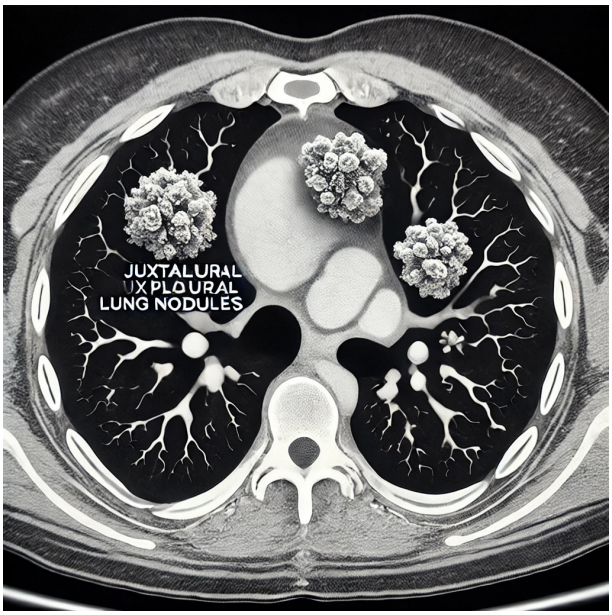



figure 1.7: Representation of juxtapleural lung nodules in CT scan images

makes them critical in assessing lung cancer risk. Nodules that exhibit irregular characteristics or show growth over time are particularly concerning, which leads medical guidelines to recommend close monitoring and evaluation.

While not all nodules are cancerous, their detection is a crucial signal for increased scrutiny and appropriate follow-up, especially in high-risk populations. On the other hand, micro-nodules, typically measuring less than 10 mm, are often benign and usually do not pose significant health risks. These smaller nodules can arise from various factors, including infections, inflammation, or other non-cancerous conditions. However, as nodules increase in size—particularly those exceeding 30 mm in diameter or those within the 10 mm to 30 mm range—the likelihood of abnormalities [29], including malignancy, becomes greater. Thus, while larger nodules may still be benign, their potential association with lung cancer necessitates careful evaluation.

Lung cancer is rarely caused by a single factor, but typically develops from a combination of multiple risk elements. These factors include environmental exposures, occupational hazards, and lifestyle choices, all of which contribute to the risk of developing the disease as present in the Figure1.8.

Active smoking is the leading contributor responsible for 9 out of 10 cancers in men (87%) and 7 out of 10 cancers in women (70%) [30]. In addition to smoking, exposure to harmful substances in both everyday and professional environments further heightens the risk. The lungs, being directly exposed to inhaled toxins, are particularly vulnerable, with smoking

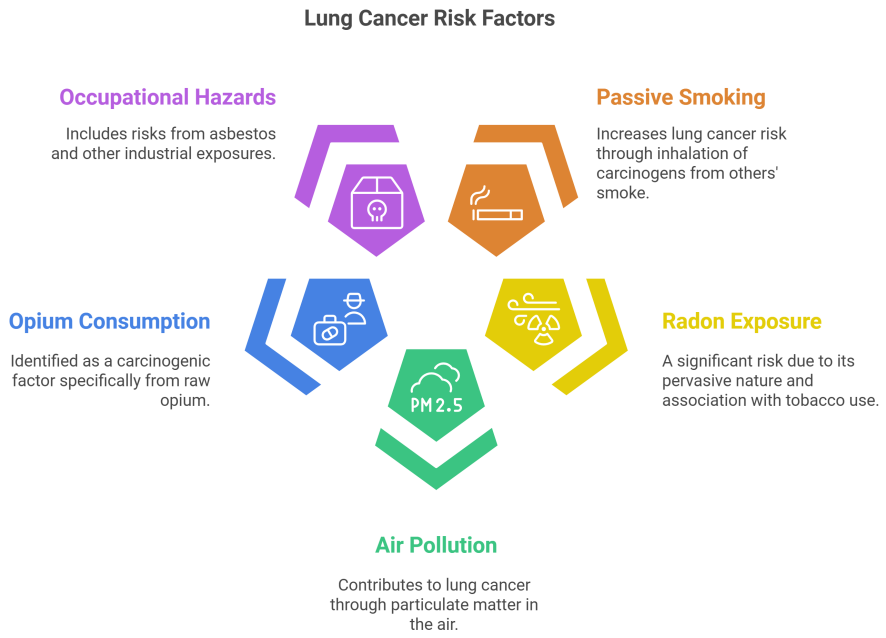



figure 1.8: Lung cancer risk factor

dramatically increasing the likelihood of lung cancer. Each of these factors, especially the impact of smoking, will be explored in detail.

1. **Environmental factors**

   - Passive smoking or second-hand smoke: exposure to passive smoking in living spaces, whether at home or in the workplace, increases the risk of lung cancer by 20-30% in non-smoking adults [31, 32]. In a non-smoking person continuously exposed to the smoke of others, the risk of cancer increases by 26%. Non-smokers exposed to secondhand smoke inhale many of the same carcinogens and toxic substances as smokers. Even short-term exposure to secondhand smoke can cause cellular damage that initiates the cancer process. Similarly to direct smoking, the risk of lung cancer increases with the duration and intensity of exposure to second-hand smoke.
   - Radon: originating from the decay of uranium-238, pervades indoor and outdoor environments and poses a significant lung cancer risk to both smokers and nonsmokers. Found in underground mines and penetrating buildings through soil, water, and construction materials, this inert gas has been extensively documented, through studies on miners and animal research, to cause lung cancer. Therefore, radon is recognized as an essential risk factor for lung cancer among the general

population, attributed to its widespread nature and extensive exposure in indoor environments [33].

Radon stands as the second leading cause of lung cancer [34], and it is classified as a definitive carcinogen by the World Health Organization (WHO) in 1987. Its danger, particularly when combined with tobacco use, is notable, the risk of developing lung cancer from exposure to radon is twenty times greater in smokers than in nonsmokers, this underscores the compounded risk factors for radon and tobacco, highlighting the critical need for awareness and preventative measures against radon exposure.

- Outdoor air pollution: Air pollution, particularly PM2.5, was estimated to be responsible, in 2015, for 4% of all newly diagnosed cases of lung cancer as mentioned in the research conducted by D. F. Xing et al. [35], where they explained the relation between outdoor air pollution and lung cancer.
- Opium consumption: In september 2020, the International Agency for Research on Cancer (IARC) identified as a confirmed carcinogenic factor for lung cancer. This classification applies specifically to the consumption of raw opium, and derived from opium waste [36]. As an environmental exposure, opium consumption highlights how certain substances in the environment, particularly those encountered in specific cultural or geographic contexts, can contribute to the development of lung cancer. However, this classification does not extend to other opiates such as heroin, morphine, or codeine, nor does it include synthetic opioids like fentanyl used in medical settings. This underscores the broader impact of environmental exposures, beyond tobacco, in contributing to lung cancer risk.

2. **Professional exhibitions:**

   - Approximately 10 to 15% of lung cancers are attributable to occupational exposure to asbestos. It is the most common occupational exposure associated with bronchial cancer. According to the National Institute for Research and Safety, around 15% of all lung cancers are caused by professional exposure [37, 38].

3. **Suspected risk factors:** Other risk factors for lung cancer, identified as group 2A by the International Agency for Research on Cancer (IARC) [39], are considered probable human carcinogens. These include exposure to:

   - Cobalt metal in the presence of tungsten carbide

- Dichloromethane
- A-chlorinated toluenes
- Epichlorohydrin

### Lung cancer diagnosis

Lung cancer often presents in advanced stages, which is why early diagnosis is crucial to improve outcomes and increase survival rates. Due to the lack of noticeable symptoms in the early stages and the rapid progression of the disease, lung cancer is frequently diagnosed after it has already spread to other parts of the body. However, with advances in screening programs and increased awareness of risk factors, early detection efforts are becoming more effective.

Screening programs, such as computed tomography (CT) scans for individuals at high risk, can help detect lung cancer at earlier, more treatable stages before symptoms develop. Identifying lung cancer in its early stages allows for more effective treatment options, including surgical resection, targeted therapy, immunotherapy, and radiation therapy. In addition, early diagnosis provides patients with the opportunity to participate in clinical trials and access novel therapies that can improve outcomes and prolong survival. Diagnosis methods for lung cancer typically involve a combination of imaging studies, laboratory tests, and tissue sampling. Below are several prevalent diagnostic techniques used to identify and confirm lung cancer:

1. **Medical imaging**: Is interesting in the diagnosis and management of lung cancer. Various imaging modalities are utilized to detect, characterize, and stage lung tumors, among the common imaging techniques employed in lung cancer diagnosis we cite:

    - **X-rays (Chest Radiography):** Are utilized to examine the chest, providing an image that reveals the density of structures within the thoracic cavity. Chest X-rays serve as the primary imaging tool in the initial evaluation of individuals suspected of having lung cancer [40], enabling the detection of abnormalities like lung nodules, masses, consolidations, or pleural effusions. However, they have limited sensitivity to identify small or early stage tumors and may not provide detailed anatomical information. Furthermore, distinguishing between benign and malignant lesions may prove challenging with chest X-rays alone.
    - **Computed Tomography (CT) scans:** It is widely used in the evaluation of lung cancer, it utilizes X-rays to generate detailed cross-sectional images of the

lungs and surrounding structures, which aids in the detection and characterization of tumors. CT scans offer exceptional sensitivity to detect small nodules, assess tumor size and location, delineate invasion into nearby structures such as the chest wall or mediastinum, and identify metastases to distant organs or lymph nodes [40].

- **Positron Emission Tomography (PET) Scan:** Utilizes a radioactive tracer, usually fluorodeoxyglucose, to detect regions of increased metabolic activity within the body. When combined with CT imaging (PET/CT), PET scans offer comprehensive anatomical and functional information. They play a crucial role in staging lung cancer, identifying distant metastases, evaluating treatment efficacy, and tracking disease advancement. However, PET scans can produce false positive findings in areas of inflammation or infection and have inferior spatial resolution compared to CT scans. Furthermore, PET scans involve exposure to ionizing radiation, which is an important consideration in clinical decision-making.
- **Magnetic Resonance Imaging (MRI):** Employs magnetic fields and radio waves to generate highly detailed images of the chest, offering superior soft tissue contrast and intricate anatomical details. Although it's less frequently utilized compared to CT scans for lung cancer diagnosis, MRI holds particular value in specific scenarios, such as examining tumors that may have invaded adjacent structures like the mediastinum or chest wall. It's especially useful for assessing vascular involvement, evaluating mediastinal masses, or providing further characterization of lesions initially identified through other imaging techniques, leveraging its exceptional capability to distinguish between different types of tissues.

2. Laboratory Tests These tests involve analyzing various samples from the body, such as blood, sputum, or other bodily fluids, to detect specific markers or abnormalities associated with the disease. There exist more kinds of laboratory tests like [41]:

   - *Blood test:* While blood tests alone do not diagnose lung cancer, they offer valuable insight into the general health of a patient and the functioning of various organs in the body.
   - *Sputum Cytology:* analyzing mucus expelled from the lungs to identify cancer cells, this diagnostic method can detect lung cancer cells, particularly for cancers originating in the major airways of the lung, such as squamous cell lung cancers.

3. **Biopsy and Tissue Sampling**

- *A lung biopsy:* Is a critical diagnostic tool for identifying various lung diseases, including tumors, infections, and other lung conditions. The procedure involves collecting lung tissue samples and requires a collaborative, interdisciplinary team approach for optimal execution and patient care. This process not only helps in diagnosing the condition but also in planning the best treatment strategy, emphasizing the importance of preparation, technique, and post-procedure management to minimize complications and improve patient outcomes [42].
- *Bronchoscopy*: Is a procedure that uses a flexible tube called a bronchoscope to directly observe the lungs and airways, it is enhanced by Endobronchial Ultrasound (EBUS) technology, which integrates ultrasound imaging. This combination allows for the visualization of structures beyond the airway walls, such as nearby lymph nodes, making EBUS-guided biopsies invaluable for sampling suspicious lesions within the lungs and mediastinum for both diagnostic and staging purposes. The minimally invasive nature of EBUS, along with its ability to offer real-time guidance during biopsy procedures, significantly reduces the necessity for more invasive surgical interventions, making it a key technique in the management of lung cancer [43].

**Lung cancer treatment**

The treatment and prognosis of lung cancer are influenced by several factors, including the specific type of cancer, the disease's stage at diagnosis, and the patient's medical history. Generally, early-stage lung cancer offers better recovery prospects compared to advanced stages, making early detection crucial for enhancing the quality of life for patients and their families, which can lead to improved treatment outcomes. First-line treatments for lung cancer typically include three main approaches:

- Surgery: Often utilized in the early stages when the tumor is localized and has not spread to other parts of the body.
- Radiotherapy: This method uses radiation to target and shrink tumors.
- Drug Treatments, which encompass:
  - Chemotherapy: Aimed at reducing tumor size and killing cancer cells.
  - Targeted Therapies: These focus on specific genetic markers or pathways involved in cancer growth.

– Immunotherapies: These enhance the body's immune response against cancer.

Multidisciplinary teams of specialists collaborate to provide comprehensive treatment and care for lung cancer patients. Additionally, supportive care plays a vital role in managing symptoms, and offering emotional support to improve the overall well-being of those affected by lung cancer.

## 1.6 Current Challenges in Lung Cancer Diagnosis

Challenges persist in the diagnosis of lung cancer, particularly in terms of subjectivity and variability between observers. These hurdles are prominently observed in the interpretation of imaging studies and histopathological specimens. Radiologists and pathologists often exhibit variations in their assessments and interpretations of lung cancer-related findings, leading to inconsistencies in diagnostic accuracy and treatment decisions. Such disparities can arise from differences in expertise, experience, and subjective interpretation of imaging features or histological characteristics. For example, subtle changes in the appearance of lung nodules or infiltrates in imaging studies can elicit varying interpretations, affecting the diagnosis of malignancy. Similarly, histopathological evaluations can involve subjective judgments on the presence of tumor cells, tissue architecture, or the degree of cellular atypia, contributing to interobserver variability among pathologists. Addressing these challenges requires standardized diagnostic criteria, robust quality assurance protocols, and the integration of advanced technologies like artificial intelligence to provide objective and reproducible diagnostic assessments in lung cancer diagnosis and management.

Traditional lung cancer diagnostic methods suffer from several limitations that can affect their effectiveness and reliability. Firstly, many of these methods, such as bronchoscopy, biopsy are invasive procedures that carry risks of complications and discomfort for patients. While bronchoscopy is a valuable tool for diagnosing lung cancer by visualizing the airways and collecting tissue samples, it can be uncomfortable for patients and carries risks such as bleeding, infection, or bronchospasm. It may not always reach peripheral lung lesions, which limits its diagnostic utility. Furthermore, biopsy-based methods can produce samples that do not fully capture the heterogeneity of lung tumors, which can consist of multiple subtypes with varying genetic mutations and histological features. Consequently, biopsy samples may not accurately represent the entire molecular profile of the tumor, potentially leading to misdiagnosis or suboptimal treatment selection.

Furthermore, certain imaging modalities like chest X-rays that are widely used for initial screening and detection of lung abnormalities may have limited sensitivity and specificity to detect small or early-stage lung tumors, resulting in missed diagnoses or delayed detection. In addition, they may not provide sufficient anatomical detail or differentiation between benign and malignant lesions, leading to false-negative or inconclusive results.

In addition, the interpretation of CT imaging and histopathological specimens by radiologists and pathologists can be subjective, leading to variability in diagnostic precision and discrepancies between observers. The classification of lung cancer based on tumor size and extent is crucial for determining treatment options, but the interpretation of malignancy degree and tumor characteristics can vary, causing inconsistencies in diagnosis. Cost and accessibility are also significant challenges, as some diagnostic tests may be expensive and inaccessible to all patients. Furthermore, false positives and overdiagnosis can result in unnecessary follow-up tests, interventions, and psychological distress for patients. Addressing these limitations requires advances in noninvasive biomarkers, improved imaging techniques, and AI-based approaches to enhance diagnostic accuracy and efficiency, while minimizing patient discomfort and risks. Accurately assessing the malignancy degree of lung tumors using more objective diagnostic tools is essential for improving outcomes, allowing for a better understanding of the tumor's aggressiveness and guiding more effective treatment decisions.

## 1.7 Conclusion

In conclusion, lung cancer poses a significant health challenge due to its high mortality rates and the complexities involved in its diagnosis and treatment. Its tendency to progress undetected until advanced stages limits effective treatment options. The importance of early detection is paramount, as it greatly improves the chances of successful treatment outcomes and improves the prognosis of the patient. Regular screenings are crucial for early identification, particularly for high-risk individuals.
Early intervention enables the use of diverse treatment approaches, such as surgery, chemotherapy, radiation, and innovative therapies like targeted therapy and immunotherapy.

This chapter has provided an overview of the respiratory system, detailed lung cancer epidemiology, risk factors, diagnostic methods, treatment options, and highlighted the current challenges in diagnosing lung cancer, emphasizing the limitations of each method and the need for continued research and improved diagnostic technologies.
Through increased public awareness and advances in medical research, the focus on employing

intelligent approaches for early detection remains central to improving survival rates and quality of life for those affected by lung cancer.

# Chapter 2

# AI for the Detection and Classification of Lung Cancer

## 2.1 Introduction

Artificial Intelligence (AI) has emerged as a transformative force in modern medicine [44], offering unprecedented capabilities in data analysis, pattern recognition, and decision-making. In the context of lung cancer, AI has shown immense potential [45] in enhancing diagnostic accuracy and efficiency, particularly through the development of Computer-Aided Detection and Diagnosis (CAD) systems. These technologies are designed to assist radiologists and clinicians by automating the detection and classification of lung abnormalities, such as nodules, from medical images like CT scans, X-rays, and PET scans.

Lung cancer remains one of the most lethal cancers globally, partly due to challenges in early detection. Traditional diagnostic methods, while effective, are often limited by the complexity of medical images and the potential for human error. AI-driven CAD systems address these limitations by leveraging machine learning and deep learning algorithms to analyze vast amounts of imaging data, detect subtle patterns, and differentiate between benign and malignant lesions with high precision.

By integrating AI and CAD into the diagnostic process, clinicians are better equipped to identify lung cancer at earlier stages, potentially improving patient outcomes. Moreover, AI-based tools continue to evolve, learning from large datasets to refine their predictive capabilities, ultimately playing a crucial role in personalized medicine and tailored treatment strategies [46].

This chapter explores the application of artificial intelligence (AI) in the detection and classification of lung cancer. It begins by highlighting the importance of AI in healthcare care and its potential to revolutionize medical diagnosis and treatment. Next, it delves into the fundamental concepts of artificial intelligence, focusing on machine learning and deep learning techniques. Finally, the chapter provides a comprehensive overview of the development process of computer-aided detection and diagnosis (CAD) systems specifically designed for lung cancer detection, outlining the methodology and key considerations involved in creating these innovative tools.

## 2.2 AI in lung cancer diagnosis

Advanced technologies like artificial intelligence (AI) are essential for addressing the limitations of traditional diagnostic methods for lung cancer [47]. AI excels at analyzing large volumes of medical imaging data with high precision, significantly reducing the likelihood of false-negative or false-positive results. By automating image analysis, AI enhances the

diagnostic process, enabling healthcare professionals to focus on more complex cases. Additionally, AI-powered screening tools facilitate the early detection of subtle abnormalities indicative of early-stage lung cancer, leading to timely interventions and improved patient outcomes [48].

AI also plays a crucial role in personalized medicine by integrating imaging features, and clinical data to customize treatment strategies for individual patients, optimizing therapeutic effectiveness while minimizing adverse effects. Moreover, AI contributes to risk stratification, prognostication, and treatment planning through multimodal data integration and predictive modeling, helping healthcare providers make informed decisions and enhance patient management.

Overall, the integration of AI in lung cancer diagnosis and management holds great potential for transforming patient care and improving health outcomes.

AI has widespread applications in healthcare, including:

- Medical Imaging and Diagnostics: AI algorithms analyze imaging modalities like X-rays, CT scans, and MRIs to assist radiologists and pathologists in identifying abnormalities, facilitating timely interventions [49–51].

- Personalized Medicine: AI supports precision medicine by analyzing genetic data to tailor prevention and treatment plans to individual patient characteristics, thereby enhancing care [52, 53].

- Computer-Aided Detection and Diagnosis (CAD) Systems: These systems aim to improve the accuracy and efficiency of medical exams [54, 55]. While adoption is limited due to reliability and integration challenges, AI-enhanced CAD systems promote personalized care and collaboration in radiology [54, 55] due to the use of AI algorithms to highlight suspicious findings in medical images, improving the sensitivity and accuracy of disease detection in different medical fields, including lung cancer [56], breast cancer [57], and neurological conditions [58].

- Clinical Decision Support Systems (CDSS): AI-based CDSS analyze patient data to provide evidence-based recommendations, aiding healthcare providers in making informed decisions [59].

- Drug Discovery and Development: AI accelerates drug discovery by predicting interactions, identifying candidates, and optimizing designs, ultimately streamlining the development process.

## 2.3 Key Concepts in AI

### 2.3.1 Artificial Intelligence

Artificial intelligence has evolved over several decades, and various definitions have been proposed by researchers and experts in the field. The first definition of AI provided by McCarthy in a proposal for the Dartmouth Conference in 1956 [60], laid the foundation for the field of AI and its subsequent development, who defined AI as :

"Artificial intelligence is the science and engineering of making intelligent machines, especially intelligent computer programs. It is related to the similar task of using computers to understand human intelligence, but AI does not have to confine itself to biologically observable methods."

Another widely accepted definition of artificial intelligence, as provided by Russell and Norvig in their book, "Artificial Intelligence: A Modern Approach" [61], states that: "Artificial Intelligence (AI) refers to the development of computer systems that can perform tasks that typically require human intelligence. These tasks include learning, reasoning, problem-solving, perception, understanding natural language, and interacting with the environment. AI systems are designed to emulate human cognitive functions and adapt to new situations by learning from data patterns and experiences. AI encompasses various subfields, including machine learning, natural language processing, computer vision, robotics, and expert systems. AI aims to create intelligent machines capable of autonomously solving complex problems and making decisions without human intervention."

The first definition, attributed to John McCarthy and proposed in the Dartmouth Conference proposal in 1956 [60], focuses on AI as the science and engineering of making intelligent machines, particularly intelligent computer programs. This definition emphasizes the scientific and engineering aspects of AI, with a focus on creating machines that can imitate human intelligence and perform tasks traditionally associated with human cognition. It also highlights the interdisciplinary nature of AI, which draws from fields such as computer science, mathematics, psychology, and philosophy. However, the second definition emphasizes the development of computer systems that can perform tasks that require human intelligence, such as learning from data, reasoning, problem solving, and interacting with the environment. This definition provides a broad overview of AI and its various subfields, including machine learning, natural language processing, computer vision, robotics, and expert systems.

Highlights the goal of AI of creating intelligent machines capable of autonomous decision making based on algorithms and data patterns. Although both definitions share common

themes, such as emulation of human intelligence and the development of intelligent machines, they differ in their level of detail, scope, and historical context.
Among the different technologies of AI, we can cite machine learning and deep learning as two of the most prominent and widely used approaches, particularly in the medical field.

### 2.3.2 Machine learning

Machine learning is a subset of artificial intelligence and a scientific discipline that focuses on the development of algorithms that allow computers to learn from and make predictions or decisions based on data [62]. Its significance lies in its capacity to derive insights from vast and complex datasets, automating decision-making processes and enhancing the efficiency of tasks traditionally performed by humans. It finds application in a broad spectrum of fields, including security services, where it is used for tasks such as face detection [63], while in finance it detects fraud, manages risks, and optimizes customer experiences [64].
In industry, retail benefits from recommendation systems and demand forecasting, while manufacturing relies on predictive maintenance and quality control [65]. Transportation sectors employ machine learning [66] for route optimization and autonomous vehicles, while natural language processing and enables sentiment analysis. Recently, it has been used in different domains of healthcare [67,68] and biotechnology [69], by helping in medical imaging analysis, disease diagnosis, and personalized treatment recommendations. In these domains, machine learning drives innovation, improves decision-making, and propels organizations toward data-driven excellence.
Machine learning algorithms are computational techniques that empower computers to glean insights from data and formulate predictions or decisions autonomously, without requiring explicit programming. Figure 2.1 illustrates that machine learning algorithms come in various types, each designed for particular learning tasks. This diversity allows them to be flexible and adaptable, effectively tackling a wide range of data challenges. These types include:

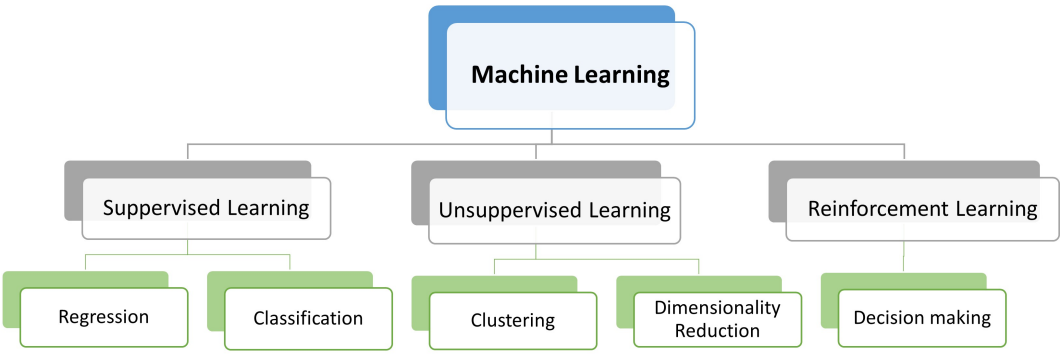



figure 2.1: Machine learning algorithms

- **Supervised Learning** :

  Supervised learning is a branch of machine learning in which machines are trained using labeled data to predict output based on input. Labeled data refer to input data already associated with the correct output [70]. The training data provided serves as a guide for machines to accurately predict output [71]. In supervised learning, algorithms attempt to model a target output using input data. They are supplied with a training database containing labeled examples. Utilizing this dataset, the algorithm learns rules, enabling it to predict labels for new observations. Essentially, supervised learning algorithms analyze historical data to identify relationships with the highest predictive accuracy.

  Supervised learning can be subdivided into two types of problem: Regression and classification.

  – *Regression*: Regression analysis is used to discern the relationship between one variable and one or more others. In machine learning, the objective of regression is to predict a numerical output value based on a set of input features. It is used to forecast continuous values [71]. The process entails fitting a mathematical model to observed data points, facilitating the estimation of relationships between input variables and a continuous target variable [72] , put differently, how one variable influences the other. Regression algorithms aim to identify the optimal line,

curve, or surface that represents the association between input features and the target variable, allowing the prediction of numerical results. These algorithms find widespread application as predicting stock prices, estimating house prices, and forecasting sales. Among popular regression algorithms: linear regression, ridge regression, and polynomial regression [70, 73].

- *Classification*: Refers to the systematic process of recognizing, comprehending, and organizing objects and concepts into predefined categories, with machine learning programs using pre-categorized training datasets and various algorithms to achieve accurate categorization. The prediction task is classified as a type of classification when the target variable is discrete [74]. In this process, the model aims to anticipate the accurate label of a provided input data set, undergoing a thorough training and evaluation before being deployed to make predictions on new unseen data [75]. There are several algorithms used in classification process, some of the most commonly used ones include Logistic regression, decision trees, random forest, Support Vector Machines (SVM), K-Nearest Neighbors (KNN).

- **Unsupervised Learning Algorithms**: The idea of unsupervised learning revolves around the ability of algorithms to autonomously identify patterns or structures within data without being explicitly told what to look for. In contrast to supervised learning, where the algorithm is trained on labeled data with known outcomes, unsupervised learning operates on unlabeled data [76].

  Imagine that we have a large dataset containing various data points, but without any labels or categories attached to them. Unsupervised learning algorithms are designed to analyze these data and discover inherent patterns, relationships, or clusters within them. These algorithms explore the data, searching for similarities or differences between data points and grouping them accordingly. The main applications of unsupervised learning are:

  - *Clustering*: A cluster refers to a collection of data points that demonstrate similarity to one another in relation to neighboring data points. The clustering technique is used to group data points into clusters based on their similarities. This aims to partition the data into groups, or clusters, where data points within the same cluster are more similar than those in other clusters.

  - *Dimensionality Reduction*: Used for reducing the number of features or variables in the dataset while preserving its essential information. Examples include principal component analysis (PCA) and t-distributed stochastic neighbor embedding (t-SNE).

- **Reinforcement Learning Algorithms**:

  Used for training agents to take actions in an environment to maximize cumulative rewards. Examples include Q-learning, deep Q-networks (DQN), policy gradient methods, and actor-critic methods.

### 2.3.3 Deep learning

Deep learning, a specialized branch of machine learning, utilizes sophisticated multi-layered neural networks, known as deep neural networks, as its foundational technology to mimic the complex decision-making processes characteristic of the human brain [77]. Figure 2.2 illustrates how deep learning methods autonomously learn hierarchical features at multiple levels of abstraction, enabling them to directly address complex tasks from raw data, functioning as efficient hierarchical feature extractors, particularly at high levels of semantic abstraction. In contrast, traditional machine learning involves manual feature extraction from input data, such as images or signals, followed by classification within predefined categories using an Artificial Intelligence (AI) model. Typically, experts design mathematical operations, known as descriptors or feature extractors, based on domain knowledge to facilitate feature extraction in traditional machine learning approaches [78]. In this subsection, we present the main findings necessary for understand how deep learning models work.

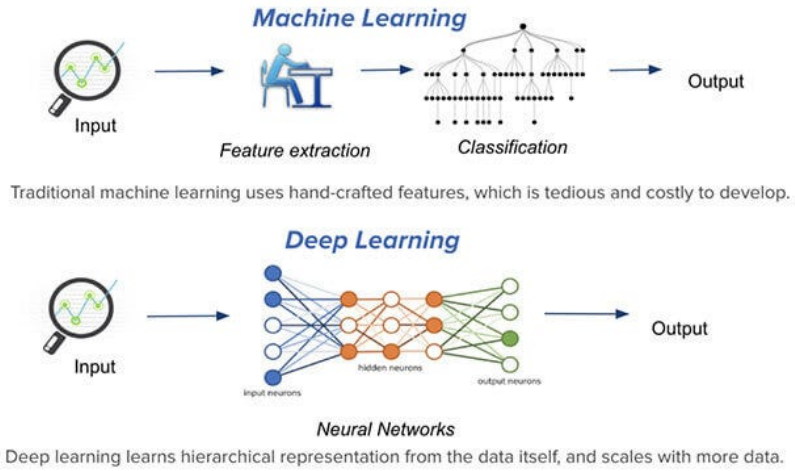



figure 2.2: Machine learning Vs. Deep learning [79]

The components of Neural Networks comprise neurons, or nodes as presented in the Figure2.3, which are the fundamental processing elements receiving input signals, applying transformations through an activation function, and generating an output signal. These neurons are structured into layers, including the input layer that takes in the data, hidden layers which are intermediary phases that extract features from the data, and the output layer that delivers the network's final prediction or classification. The connections between these neurons are defined by weights, dictating the connection's strength, and biases, These additional parameters enable the network to capture more complex patterns. Another essential component of neural network, which is, the activation function, that is applied by each neuron to its weighted input sum to incorporate non-linearity into the model, with ReLU (Rectified Linear Unit), sigmoid, and Tanh being among the commonly used functions. This layered arrangement and the interplay of these components allow neural networks to perform intricate computations and pattern recognitions, simulating aspects of human cognitive functions.

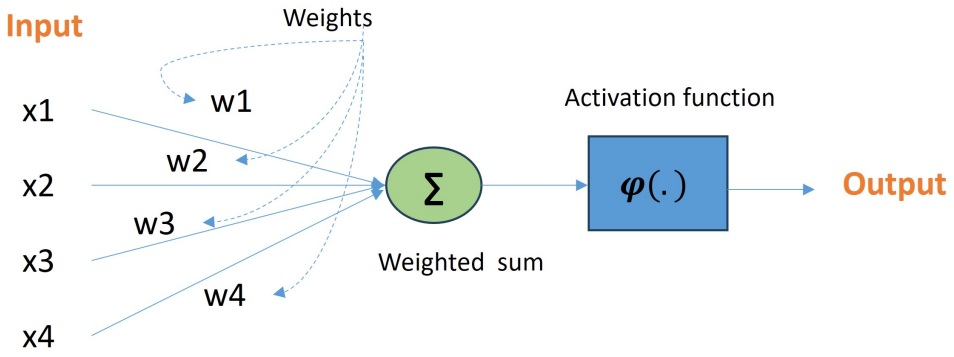



figure 2.3: Neuron in Artificial Neural Network [80]

### Training neural network

Training neural networks is a multistep process that involves several key components, each contributing to the network's ability to learn from data and improve its performance over time:

- **Forward Propagation**: Training a neural network starts with forward propagation, where input data is passed through each layer of the network to generate predictions. At every layer, calculations are performed using learned parameters (weights and biases), which transform the input into meaningful representations. This process can be mathematically described by computing the activation $a^l$ at each layer $l$ using the input data $x$, Weights $W^l$, biases $b^l$, and activation functions $g^l$ such as presented in the equation (2.1, 2.2)

$$Z^l = W^l \times a^{(l-1)} + b^l \tag{2.1}$$

$$a^l = g^l \times z^{(l)} \tag{2.2}$$

  Here $Z^l$ represents the input to layer $l$ obtained by applying the weights $W^l$ to the activations $a^{l-1}$ from the previous layer and adding biases $b^l$. The resulting $Z^l$ is then passed through the activation function $g^l$ to compute the activations $a^l$ for that layer. This process is repeated for each layer until the final output layer is reached, producing the network's predictions. Forward propagation enables neural networks to transform input data into meaningful output predictions through a series of computational steps.

- **Loss Function Evaluation**: After the network processes the input data and generates predictions, these predictions are compared to the true labels using a loss function.

The loss function $L$ quantifies the difference between the predicted outputs $\hat{y}$ and the actual ground truth labels $y$. A lower loss value signifies better model accuracy. This evaluation step is critical because it provides feedback that drives the optimization process, helping to adjust the network's parameters to minimize errors. Through continuous learning and parameter updates, the neural network gradually improves its performance, reducing the prediction error over time. The specific form of the loss function varies depending on the task, such as indicated in the Figure 2.4.

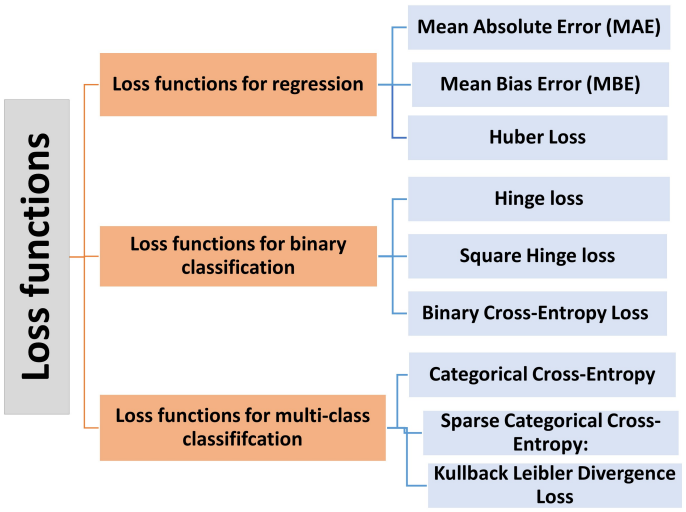



figure 2.4: The most common loss functions

- **Backpropagation**: The process of training neural networks involves backpropagation, where the algorithm adjusts weights and biases to minimize the error between predicted and actual outputs. After computing the loss (discrepancy between predictions and ground truth), the algorithm calculates the gradients of the loss function with respect to each parameter by applying the chain rule of calculus, starting from the output layer and moving backward. These gradients indicate how much each parameter influences the error and help determine the necessary adjustments.
  Optimization algorithms like Stochastic Gradient Descent (SGD) then update the weights and biases iteratively, moving in the direction that minimizes the loss. The process continues until the model converges to an acceptable performance. Common optimization techniques include Gradient Descent, SGD, and Mini-Batch Gradient Descent, with the choice depending on the specific task and model performance on validation data.

**Different types of neural network**

- **Feedforward Neural Networks (FNNs)**: is the simplest type of neural network, where information flows in one direction, from input nodes through hidden nodes to output nodes without forming any cycles or loops, as illustrated in the Figure 2.5. These networks are characterized by their simple architecture, with data passing sequentially through the layers, and there are no connections that loop back to previous layers. Each neuron in a feedforward neural network receives input from the neurons in the previous layer, processes this input using a set of weights and biases, applies an activation function, and then passes the transformed output to the neurons in the next layer. FNNs are widely used for tasks such as classification, regression, and pattern recognition. In addition they serve as the foundation for more complex neural network architectures.

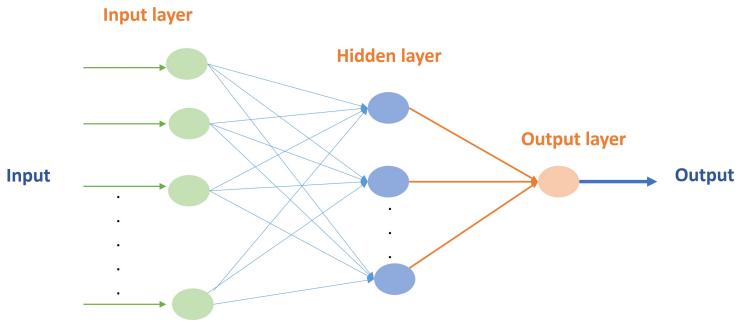



figure 2.5: Feedforward neural network composed of three layers [81]

- **Convolutional Neural Networks (CNNs)**: A Convolutional Neural Network (CNN) is a specialized neural network designed for processing grid-like data, such as images. It utilizes convolutional layers to detect spatial hierarchies of features, with deeper layers recognizing more complex patterns. CNNs comprise multiple layers, including convolutional, pooling, and fully connected layers, as illustrated in Figure 2.6

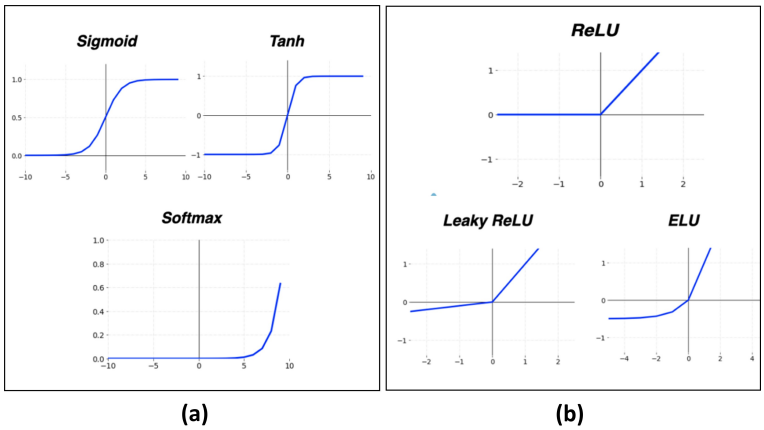



figure 2.7: Activation functions: (a): basic non-linear functions, (b): advanced non-linear function [83]

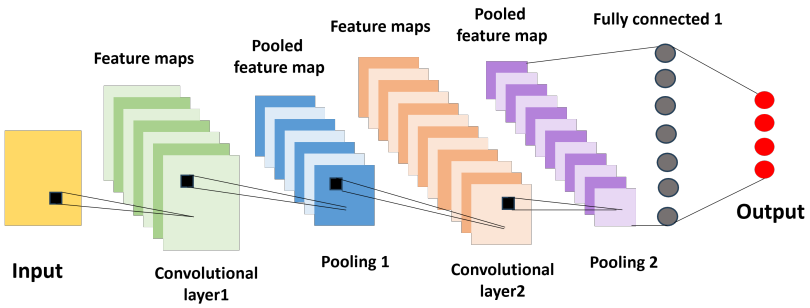



figure 2.6: The structure of a CNN [82]

– Convolutional Layers extract features such as edges and are typically followed by activation functions that are generally non-linear. Figure2.7 presents the key activation functions, which includes:

  * Softmax: Used in multi-class classification tasks, it outputs a probability distribution across various classes.
  * Rectified Linear Units (ReLU): Widely used for its computational simplicity and efficiency, this function outputs the input directly if positive; otherwise, it outputs zero, facilitating faster convergence.
  * Leaky ReLU: A variation of ReLU that allows a small, non-zero gradient for negative inputs, helping maintain the updating process during training and avoiding "dying neurons".
  * ELU (Exponential Linear Unit): Provides non-zero gradients for negative inputs, helping to mitigate the vanishing gradient problem for positive inputs.

  - Pooling Layers reduce the size of feature maps, simplifying computations.
  - Fully Connected Layers aggregate features for classification. Additional techniques, such as batch normalization and dropout, enhance training stability and prevent overfitting.

  This hierarchical structure and the interconnectedness of layers enable CNNs to automatically learn discriminative features from input data, making them highly effective for a variety of computer vision tasks, including image classification, object detection, and segmentation. The output layer produces the desired prediction, such as the classification label for the input image [84, 85].

- **Recurrent Neural Networks (RNNs)**: are designed to handle sequential data with temporal dependencies, making them ideal for tasks such as language modeling and time series forecasting. Unlike traditional neural networks, RNNs can maintain memory across sequences by incorporating outputs from previous steps as inputs for subsequent ones. This capability allows the network to leverage historical information essential for understanding context.
  At the core of an RNN is the Recurrent Unit, which preserves a hidden state to effectively capture sequential dependencies. To tackle the challenges of long-term dependencies, enhancements like Long Short-Term Memory (LSTM) units and Gated Recurrent Units (GRU) have been developed, enabling the network to retain relevant information over extended sequences.
  An RNN's architecture typically consists of layers that process input sequences and propagate their outputs to subsequent timesteps within the same layer, allowing the network to maintain a memory of past inputs—an essential feature for processing sequential data effectively.

  The scheme presented in Figure 2.8 provides an overview of a recurrent neural network (RNN), emphasizing its compact structure on the left side with a recurrent loop. On the right side, the temporal unfolding of this loop and the hidden layer illustrates network structures at different time points, including $t-1$ , $t$, and $t+1$. Each connection between input and output sequence points highlights distinct representations corresponding to these time points. The recurrent loop, depicted by the black square with $C$, establishes connections between nodes $h_{t-1}$, $h_t$, ...$h_{t+1}$, enabling communication between adjacent time steps. Dots on the right side indicate remaining unfolded connections, representing final sequence calculations for $Xt$, $H_t$, and $Y_t$.

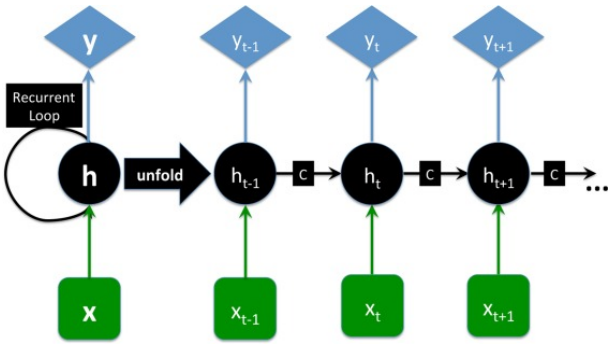



figure 2.8: The scheme of RNN with one hidden layer [86]

Building upon the advancements in machine learning and deep learning, these technologies have found extensive applications in the development of Computer-Aided Detection and Diagnosis (CAD) systems. Where they leverage the predictive capabilities of AI to assist clinicians in detecting, diagnosing, and monitoring diseases with greater accuracy and efficiency.

## 2.4 Computer-Aided Detection and Diagnosis (CAD) system for lung cancer

A Computer-Aided Detection and Diagnosis (CAD) system for lung cancer is a computerized tool designed to help radiologists and clinicians detect, diagnose and characterization of lung cancer from medical imaging data, such as chest radiographs, computed tomography (CT), or magnetic resonance imaging (MRI) scans of the lungs. These CAD systems use advanced algorithms from artificial intelligence technologies to analyze medical images and identify suspicious areas or lesions that can indicate the presence of lung cancer, in order to assist radiologists by providing additional information and highlighting areas of concern. They serve as decision support tools, helping early detection, accurate diagnosis, and treatment planning for patients with lung cancer, As highlighted in [56], the paper offers a comprehensive overview of state-of-the-art techniques currently utilized to implement each stage of the CAD system.

As depicted in Figure 2.9, Computer Aided Detection and Diagnosis (CAD) system is divided into two subsystems, Computer-Aided Detection (CADe) and Computer-Aided Diagnosis (CADx) [87]. This aims to involve separating the tasks of detecting abnormalities or lesions from the process of diagnosing and characterizing them. Before detailed these two subsystems, let's talking about the available datasets for lung cancer.

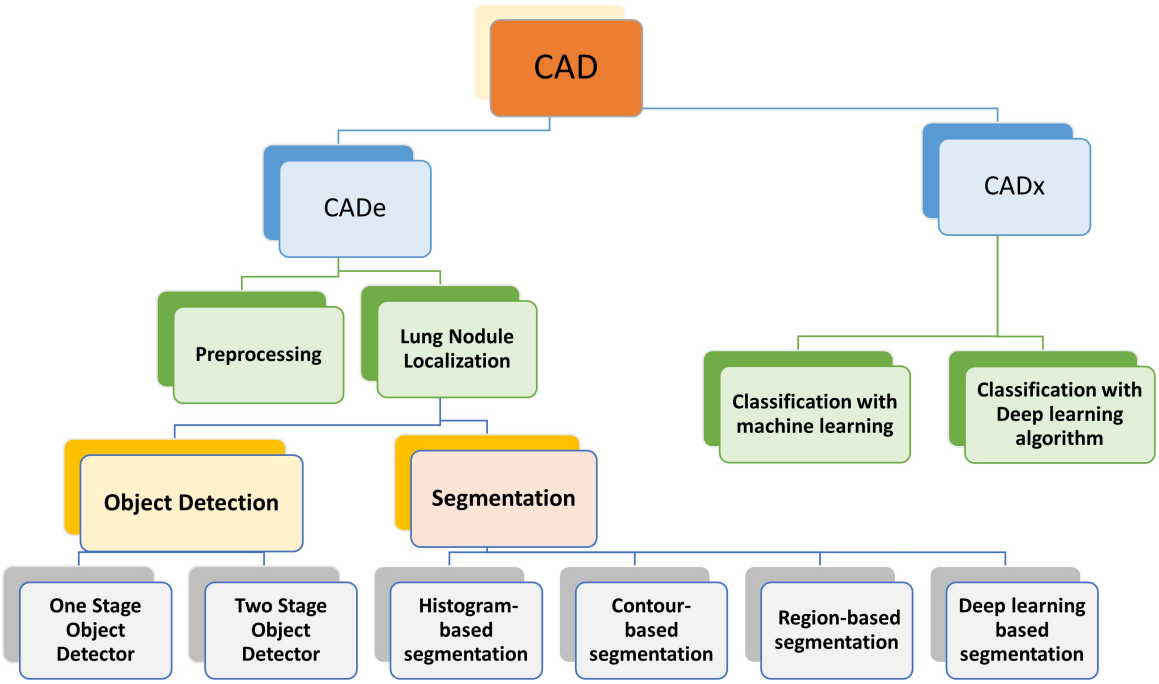



figure 2.9: CAD system for lung cancer

### 2.4.1 Available datasets for lung cancer

To develop an artificial intelligence model, the first step is to select an appropriate dataset. This involves analyzing the dataset's structure, including the number of cases it contains and the types of images included. It is also essential to provide an overview of images and their various types, as this foundational understanding informs subsequent model development.

Images are fundamental representations of visual data that serve as crucial tools in fields ranging from art and entertainment to science and medicine. At their core, images consist of collections of pixels organized in two-dimensional grids, where each pixel encodes color, intensity, and spatial position. These images come in various types, including grayscale, color, and binary images [88], each offering different levels of visual information.
Medical imaging is essential for diagnosing and treating diseases by providing detailed views of anatomical structures and physiological processes. Common modalities include X-rays, computed tomography (CT), magnetic resonance imaging (MRI), ultrasound, and positron emission tomography (PET). In lung cancer, CT scans are typically stored in the DICOM (Digital Imaging and Communications in Medicine) format, which includes both image data and critical metadata, such as patient identifiers and imaging parameters.

Understanding the role of Hounsfield units (HU) in assessing tissue density is crucial, as these measurements are derived from the detailed medical images stored in the DICOM

format, which provides essential data for diagnosing and treating diseases like lung cancer. Hounsfield units (HU), represented using 12 bits, measure the attenuation of X-rays by different tissues, with values ranging from -1024 (air) to 3071 (dense tissues like bone). HU is calculated using DICOM properties, specifically rescale slope and rescale intercept [89]. HU value is calculated using two DICOM properties: rescal slope (slope) and rescal intercept (intercept), by applying the following linear transformation presented in the equation 2.3:

$$HU = pixelValue * slope + intercept \tag{2.3}$$

In addition to slope and intercept parameters, the DICOM file contains other important properties [90] such as :

- SOP Instance UID: Used for distinguishing uniquely each DCM slice.
- Instance Number: Used to indicate the serial number of a group of slices, this property can be used to sort the slices directly.
- The image position: Indicates the x, y, and z coordinates of the upper left corner of the image in the space coordinate system, in millimeters.
- Slice Location: Is the relative position of the slice z-axis, in millimeters, it is mostly the same as z in Image Position
- Pixel Spacing: indicates the physical spacing between the centers of the pixels.
- Rescale Intercept and Rescale Slope: Used to transform a pixel value into Hounsfield unit or other units.
- Slice Thickness: Used to indicate the thickness of the slice in the z-direction in millimeters.

In the development of CAD systems for lung cancer, various datasets are utilized, as shown in Table 2.1, which includes:

| Database | Access | Number of cases | Number of images | Size | first version | last update |
|---|---|---|---|---|---|---|
| LIDC-IDRI | public | 1018 | 244527 | 125GB | 2011 | 2020 |
| SPIE-AAPM Lung CT Challenge | public | 70 | 22489 | 12.1GB | 2014 | 2016 |
| ISBI 2018 lung cancer dataset challenge | private | 100 | .. | * | 2018 | - |
| Luna16 | public | 888 | 1186 | 66.7GB | 2016 | * |
| Lung TIME dataset (TIME1) | public | 148 | 2462 | 11.7GB | 2009 | - |
| Lung TIME dataset (TIME2) | public | 9 | 638 | 0.2GB | 2010 | - |
| NSCLC (Non Small Cell Lung Cancer) | public | 211 | 286754 | 97.6GB | 2015 | 2021 |
| National Lung Screening Trial (NLST) | public | 26254 | 21082502 | 11.3TB | 2013 | 2021 |
| The IQ-OTHNCCD lung cancer dataset | public | 110 | 1190 | 149MB | 2020 | 2023 |

Table 2.1: Available databases

- **Lung Image Database Consortium and Image Database Resource Initiative (LIDC-IDRI)** [91]: is a publicly accessible repository of medical images and associated data focused specifically on lung cancer imaging. Established through a collaborative effort between the National Cancer Institute (NCI) and several academic and medical institutions, this database comprises 1018 cases. Each case consists of clinical thoracic

computed tomography (CT) scan images along with an accompanying XML file documenting the outcomes of a two-phase image annotation process conducted by four experienced thoracic radiologists. This XML file provides comprehensive annotations and metadata related to CT scans and identified nodules for each patient, including details such as Patient Information, Scan Information, Nodule Annotations, Radiologist Annotations, and Image Metadata.

- **LUNGx SPIE-AAPM-NSI lung CT challenge** [92]: This dataset was created as part of the 2015 SPIE Medical Imaging Conference, supported by the American Association of Physicists in Medicine (AAPM) and the National Cancer Institute (NCI) during a "Grand Challenge" focused on quantitative image analysis methods for distinguishing between malignant and benign lung nodules. The dataset includes 70 subjects, divided into 10 for training and 60 for testing, encompassing a total of 22,489 images. The patient IDs for the training set start with "CT-Training," while those for the test set start with "LUNGx." The SPIE-AAPM Lung CT Challenge database also includes two excel files: CalibrationSetNoduleData and TestSetNoduleData, which contain detailed nodule data for the calibration and test sets, respectively:

  - CalibrationSetNoduleData: This file contains information for each subject in the training set. It includes the (x, y) location of nodules within the CT scans, the corresponding slice number where the nodule is located, and the diagnosis for each nodule (malignant or benign).
  - TestSetNoduleData: Contains the same type of information of test set, this file is used to evaluate the performance of algorithms developed during the challenge for detecting and diagnosing lung nodules.

  These Excel files provide essential annotations and metadata for lung nodules present in CT scans of the Lungx database.

- **International Symposium on Biomedical Imaging (ISBI) 2018 lung cancer dataset challenge**: Is a competition organized as part of the ISBI conference, it includes images of the lungs and annotations indicating the presence, location, and characteristics of lung nodules, which are potential indicators of lung cancer. Based on Sequential CT Scans, they use a set of 100 patients with sequential Low-Dose Computed Tomography (LDCT) (total of 200 scans), including an equal number of cancer and non-cancer cases.

The training dataset contain 60 LDCT scans (30 subjects) that include scans from two sequential time intervals and the test database contain 140 LDCT scans (70 subjects) that include scans from two sequential time intervals.

- **LUng Nodule Analysis 2016 (LUNA16)** [93]: Is specifically created for research in lung nodule detection and analysis. It is a subset of the LIDC/IDRI database that contains 888 CT scan with 1186 nodules annotated by at least three radiologists.
- **Lung TIME dataset** [94]: Is a publicly available database that contains 157 subjects with 394 nodules divided into two parts (TIME 1 and Time 2), where TIME 1 data is obtained from adolescents with 148 subjects and TIME 2 data from adult patients with 9 subjects. This data set also contains an XML file that includes annotations such as the XML file compatible with LIDC annotations [95].
- **NSCLC Non-Small Cell Lung Cancer** [96]: It comprises computed tomography (CT) and PET/CT images, alongside semantic annotations of tumors observed in medical images using a controlled vocabulary. Additionally, segmentation maps of tumors in the CT scans are provided. It contains 211 cases of non-small cell lung cancer (NSCLC), totaling 286754 images.
- **National Lung Screening Trial (NLST)** [97]: Is a lung cancer screening trial funded by the National Cancer Institute (NCI) and administered jointly by the American College of Radiology Imaging Network (ACRIN) and the Lung Screening Study group. It is the largest among the databases cited with 11.3TB, which contains 26254 subjects with 21082502 images.
- **The IQ-OTHNCCD lung cancer dataset** [98]: Was collected in The Iraq-Oncology Teaching Hospital/National Center for Cancer Diseases (IQ-OTH/NCCD), it contains 1190 images of 110 cases divided into (15 cases as malignant, 55 cases as benign, and 55 cases classified as normal cases.)

### 2.4.2 Computer-Aided Detection (CADe) systems for lung cancer

CADe systems are designed to locate lung nodules in medical imaging by analyzing images to automatically identify suspicious regions or lesions that may indicate the presence of lung cancer. These systems play a crucial role in assisting radiologists by highlighting potentially concerning areas, facilitating the interpretation of medical images, and potentially enabling earlier detection and diagnosis of lung cancer.

CADe systems typically involve two main steps: preprocessing, which enhances image quality by reducing noise and improving contrast, and lung nodule localization. The primary goal of these systems is to detect and localize potential abnormalities within medical images. Localization can be accomplished through object detection methods, which identify nodules and their locations using bounding boxes, or through segmentation processes, which delineate the precise boundaries of the nodules. Both approaches aide radiologists in identifying regions of interest and improving diagnostic accuracy.

### Preprocessing

Noise in medical images, such as CT, MRI, or X-rays, poses challenges to accurate diagnosis. It can result from sensor noise, patient motion, or scanner imperfections, distorting important anatomical details. Noise, which correlates with detected photons, often makes images appear marbled or granular, degrading image quality and risking misdiagnosis.
To mitigate these challenges, preprocessing steps are used to enhance image quality, reduce noise, and improve contrast, helping to highlight critical areas for more accurate diagnosis and treatment planning.

Various methods are widely used in this step such as:

- **Filtering methods**: Filtering methods are crucial in medical imaging processing, significantly enhancing image quality by reducing noise, removing artifacts, and extracting vital diagnostic information. These techniques address various challenges in medical imaging, such as noise suppression, edge sharpening, and anatomical structure highlighting, making them essential tools for improving clarity and diagnostic accuracy. They not only improve contrast and feature extraction, but also prepare images for further analysis for accurate diagnoses and optimal patient care.

  Among the diverse techniques used for preprocessing lung cancer databases, the median filtering , non-linear filter, widely utilized in digital image processing [99,100], effectively reduces salt-and-pepper noise while maintaining the integrity of image edges, as shown by Nadkarni N. S. and Borkar S [101]. The main idea of this method is to replace each pixel with the median value of its neighborhood, making it particularly effective at removing outliers and preserving edges in images. This makes it useful for tasks as noise reduction, edge preservation, and image enhancement in various applications, including medical imaging, photography, and signal processing [102].

  The adaptive median filter is widely used in medical imaging, particularly for preprocessing CT scans. A study by S. Indira Priyadharsini et al. [99] found that this filter

outperformed others by dynamically adjusting its window size for each pixel, enabling it to preserve image details while effectively removing non-impulsive noise. Unlike the standard median filter, which struggles with high levels of impulsive noise [102], the adaptive version effectively smooths noise without blurring, making it ideal for enhancing image quality in medical applications.

- **Histogram equalization**: A widely used technique in medical imaging [100] is contrast enhancement through intensity adjustment, which redistributes pixel intensities to expand the most common values across a wider range. This improves overall image contrast, particularly in areas with lower local contrast, allowing for better visualization of subtle structures. However, it may reduce contrast in regions with less frequent pixel values.

### Lung nodule localization

Lung nodule localization is a critical step in the detection and diagnosis of lung cancer, as it focuses on identifying the precise location of abnormalities within medical images. This process helps radiologists efficiently pinpoint regions of interest that may require further analysis or intervention.
Lung nodule localization can be achieved through two main approaches which are: object detection and segmentation

1. **Object Detection**: This method identifies the presence of nodules and their approximate location within medical images, typically represented by bounding boxes. It includes one-stage detectors and two-stage detectors. These methods enable precise localization of lung nodules, a critical step for accurate diagnosis and effective treatment planning.

   The success of these techniques lies in their ability to handle the complex and heterogeneous nature of lung structures. In the context of lung cancer detection, both one-stage and two-stage object detectors are widely utilized. One-stage detectors, like YOLO and Single Shot MultiBox Detector (SSD), offer rapid processing, making them suitable for real-time applications. Two-stage detectors, like Faster R-CNN and Mask R-CNN, excel in delivering higher accuracy by leveraging a more detailed analysis of candidate regions.

   These algorithms achieve remarkable performance in detecting lung nodules by utilizing deep learning frameworks trained on large datasets. This allows them to effectively dis-

tinguish nodules from surrounding tissues and other anatomical structures, significantly improving the reliability of lung cancer detection systems.

- One-Stage Object Detectors: such as YOLO (You Only Look Once) and SSD (Single Shot MultiBox Detector), are known for their speed and efficiency. They directly predict bounding boxes and class probabilities for objects in a single pass through the neural network. In the context of lung nodule detection, one-stage detectors can quickly identify potential nodules within CT scan images without the need for multiple stages or extensive post-processing. However, they may struggle with accurately localizing small nodules or distinguishing between nodules and other structures due to their single-pass nature.
  The use of the You Only Look Once (YOLO) object detection algorithm introduced by Joseph Redmon, Santosh Divvala, Ross Girshick, and Ali Farhadi in their famous research paper "You Only Look Once: Unified, Real-Time Object Detection [103]" in 2015 has garnered significant attention in the medical field for its efficacy in automating various tasks, including medical image analysis and object detection. YOLO's single-stage architecture, capable of rapid and accurate detection of objects in real-time, makes it particularly suitable for medical applications where timely diagnosis and treatment are critical.
  In medical imaging, YOLO has been employed for tasks such as lesion detection, tumor localization and segmentation. Its ability to process large volumes of medical images quickly and accurately has paved the way for advancements in CAD systems, aiding healthcare professionals in early disease detection, treatment planning, and patient management. Furthermore, YOLO's versatility and scalability make it adaptable to different imaging modalities and medical specialties, demonstrating its potential to revolutionize various aspects of healthcare delivery and patient care [103].
  Various YOLO variants are depicted in the timeline presented in the Figure 2.10.

  - YOLOv2 (2016): Used Darknet-19 backbone, anchor boxes, batch normalization, and multi-scale training for improved accuracy and stability [105].
  - YOLOv3 (2018): Upgraded to Darknet-53, added feature pyramid networks (FPN) and multi-scale anchor boxes for better object detection [106].
  - YOLOv4 (2020): Introduced Cross Stage Partial Network (CSPNet) and GHM loss to enhance performance, especially on imbalanced datasets [107].

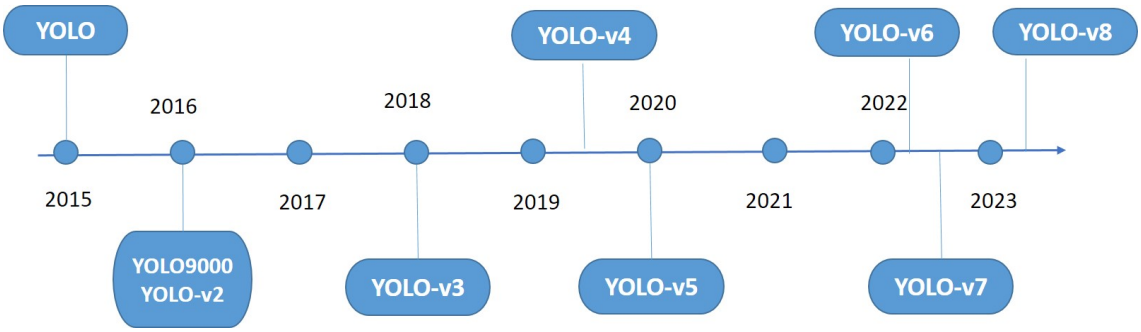



figure 2.10: Timeline of YOLO variants [104]

  - YOLOv5: Shifted to EfficientDet architecture, used spatial pyramid pooling (SPP) and CIoU loss for better detection and generalization [108].
  - YOLOv6 (2022): Adopted EfficientNet-L2 with multi-scale feature fusion and regularization techniques to improve efficiency and accuracy [109].
  - YOLOv7: Introduced Extended Efficient Layer Aggregation Network (E-ELAN) for optimized training and better performance across detection and segmentation tasks [110].

- Two-Stage Object Detectors: such as Faster R-CNN (Region-based Convolutional Neural Network), follow a two-step process. First, they propose regions of interest (ROIs) within the image using techniques such as selective search or region proposal networks (RPN). Then, they refine and classify these proposed ROIs to generate final detection results.

  Figure 2.11 presents the Region-based Convolutional Neural Network (R-CNN) architecture [111] that revolutionized object detection by cleverly integrating selective search to generate potential object regions in an image, then using a convolutional neural network (CNN) to extract features from each region. These features were subsequently classified using class-specific linear Support Vector Machines (SVMs) to determine the presence of objects. Additionally, R-CNN employed a bounding box regressor to refine the positions of detected objects, significantly improving detection accuracy. Despite its groundbreaking results, R-CNN's reliance on processing each region proposal independently led to high computational costs and slow analysis speeds, paving the way for the development of more efficient successors like Fast R-CNN and Faster R-CNN that were used in different studies of lung cancer detection as presented by Ying Su et al. [112] and Mmhammad omid.K et al. [113]. These two algorithms optimized the feature extraction and

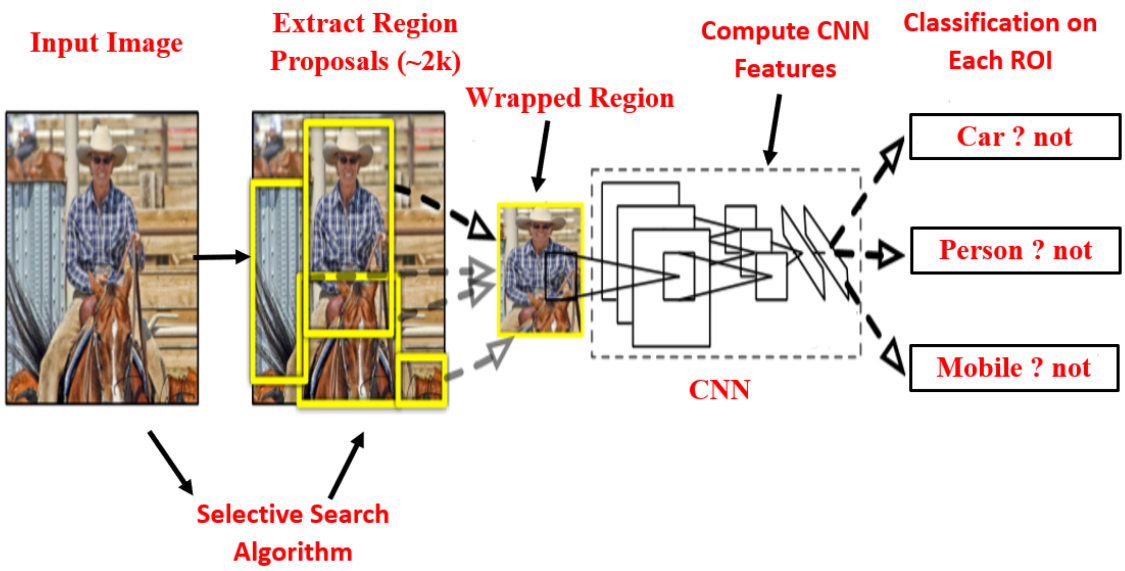



figure 2.11: RCNN architecture [86]

region proposal steps for better performance.

2. **Segmentation:** It is interesting in the development of CAD systems, significantly affecting diagnostic accuracy and the efficacy of medical image analysis. This process involves precisely isolating regions of interest, such as tumors or organs, from surrounding tissues in medical images. Accurate segmentation ensures that all subsequent operations, like feature extraction and analysis, rely on correct information, which leads to precise diagnoses. Moreover, segmentation supports treatment planning and monitoring by providing detailed outlines of disease extent and progression, critical for customizing patient-specific treatments. Thus, the quality of segmentation critically shapes the reliability and functionality of CAD systems in clinical applications [114]. This task can be summarized into three main types: manual segmentation, semi-automatic segmentation, and fully automatic segmentation [115].

   Firstly, the manual segmentation involves specialists and experts in the field in determining the region of interest (ROI) by marking each pixel that belongs to the outline of this region. While this method provides labeled images beneficial for algorithm testing and improvement, it is heavily based on the expertise and knowledge of experts.

   The semi-automatic segmentation allows user interaction for selecting an initial ROI approximation or manually modifying and verifying the region's contour to enhance segmentation accuracy.

In contrast, fully automatic segmentation does not require user interaction. In supervised learning approaches, only training data is needed, whereas unsupervised learning methods require labeled images obtained through manual segmentation for data validation.

In the area of lung cancer research, CT scan images encompass not only the lung area, but also other anatomical structures such as bone, heart, tissue, and portions of the liver. To streamline the detection of lung nodules, many studies opt to isolate the lung region from CT scan images as the initial step in the segmentation process. Subsequently, various segmentation techniques are employed to detect and segment lung nodules within this refined search space. In recent years, researchers have introduced numerous segmentation techniques aimed at enhancing image segmentation performance.

In this section, we present essential classical segmentation methods, each based on distinct criteria such as histogram, region, or contour analysis, as well as deep segmentation methods. These techniques are fundamental in lung cancer segmentation, known for their effectiveness and broad usage. We provide a concise overview of each technique, followed by an exploration of existing research using these methodologies.

- **Histogram-based segmentation**: Is a simple and widely used method for image segmentation, particularly in medical imaging. It partitions an image into different regions by analyzing the histogram of pixel intensity values [116]. Thresholding, a key aspect of this method, identifies a threshold value to separate pixel intensities into two segments: the foreground (pixels above the threshold) and the background (pixels below it) [117]. This approach is effective when the intensity characteristics of objects differ significantly from their surroundings. The method converts the image into a binary format, using various types of thresholding, such as binary, binary-inverse, truncate, to zero, and to zero-inverse. Table 2.2 explained all these types.

| Thresholding type | Equation |
|---|---|
| binary | $\text{dst(x,y)} = \begin{cases} maxval : & src(x,y) > thresh \\ 0 & : otherwise \end{cases}$ |
| Inverted binary | $\text{dst(x,y)} = \begin{cases} 0 : & src(x,y) > thresh \\ maxval & : otherwise \end{cases}$ |
| Truncated | $\text{dst(x,y)} = \begin{cases} threshold : & src(x,y) > thresh \\ src(x,y) & : otherwise \end{cases}$ |
| To Zero | $\text{dst(x,y)} = \begin{cases} src(x,y) : & src(x,y) > thresh \\ 0 & : otherwise \end{cases}$ |
| To Zero Inverted | $\text{dst(x,y)} = \begin{cases} 0 : & src(x,y) > thresh \\ src(x,y) & : otherwise \end{cases}$ |

Table 2.2: Thresholding types

Otsu's thresholding method plays a crucial role in medical image segmentation, especially for lung cancer detection. Developed by Nobuyuki Otsu [118], this technique automatically determines the optimal threshold for segmentation by analyzing the histogram of pixel intensities. Unlike manual methods, Otsu's algorithm dynamically calculates a threshold that minimizes intra-class variance between the foreground and background regions, ensuring effective separation. Its adaptive nature tailors the threshold to the specific image characteristics, making it highly effective in cases with varying contrast or intensity, which is essential for precise lung cancer diagnosis and treatment planning.

Clustering is a powerful technique categorized as histogram-based segmentation because it consists of partitioning a set of image data into many disjoint groups or clusters. This process replaces a set of data with clusters, which are collections of data points that are associated with them according to the same specific criterion (same color, same texture, etc.). In lung cancer detection, two methods are widely used: K-means clustering and Fuzzy C-Means clustering (FCM).
K-means clustering, also called flat clustering algorithm, "K" represents the number of clusters identified from the data and data points are attributed to a cluster in such a way that the sum of the squared distance between the data points and the center of gravity is minimal [119]. K-Means changes the points of each cluster until the sum can no more decrease. The result is a set of compact and clearly

separated clusters [**?**, 120, 121].

Unlike the k-means algorithm, Fuzzy C-means clustering (FCM), which is a soft clustering technique where each point is belonging to a centroid, in this algorithm, each point can be belonging to more than one cluster but with different quality.

- **Region-based segmentation**

  The region represents a set of pixels that have the same properties, which can be (texture, intensities, ...). Watershed segmentation is one of the classical segmentation algorithms that gave good results in lung cancer segmentation [122], processes the pixel values as a local topography using markers defined by the user, the algorithm floods the basins from the markers until the basins assigned to different markers meet on watershed lines.

  The watershed algorithm for image segmentation involves several key steps. First, the gradient magnitude of the input image is computed to highlight intensity changes, such as edges or object boundaries. Next, markers are selected to initiate the flooding process, either manually or automatically using methods like thresholding or detecting local extrema. The flooding process starts with these markers, gradually filling valleys until the basins of different markers meet, creating watershed lines that divide the image into segments. These segments correspond to distinct objects or regions of interest. Post-processing steps, such as merging or splitting regions, may be applied to refine segmentation results. Finally, the segmented regions are labeled and visualized for analysis [123, 124].

- **Contour-based segmentation**

  An edge is a border between two homogeneous regions with relatively distinct grayscale properties. Edge detection refers to the process of identification and localization of sharp discontinuities in an image, it is also used to detect isolated dots and fine lines [114]. Several techniques are used to detect edges such as the Canny filter, which is the most important operator that uses a multi-stage algorithm to detect a wide range of edges in images [125]. There is also the Robert edge detector which is rapid because the filter is small but it is also subject to noise interference, the filter will not tend to detect the edge if it is not sharpened [126]. Morphological operations are integral to medical imaging segmentation, offering significant value in this domain. By applying a structuring element to an input image, these operations produce an output image with enhanced features. They serve to extract various components of an image while preserving its shape and

structure, thereby effectively eliminating imperfections and enhancing overall image quality. The most common morphological operations are:

- *Dilation*: enlarges bright areas and reduces dark ones in an image, making objects more visible and filling in small holes within those objects.
- *Erosion* :shrinks light regions in an image by removing pixels from the boundaries of these regions and enlarges dark areas. It wears away the edges of objects, producing the opposite effect of dilation.
- *Opening*: first erodes an image and then dilates the eroded version, using the same structuring element for both operations. This process helps remove small bright spots and disconnect slight dark gaps.
- *Closing*: first dilates an image and then erodes the dilated version, also using the same structuring element. This sequence helps fill in small dark gaps and smooth out slight bright interruptions.

These operations have a wide variety of uses, which include noise suppression, isolating individual elements, joining disparate elements in an image and searching for holes of intensity in an image.

Contour-based segmentation methods are sensitive to noise and intensity variations, which can lead to inaccurate boundary detection and require complex pre-processing. They struggle with irregular shapes and are computationally intensive, particularly for high-resolution images, while also relying heavily on the initial contour placement, which can cause failures if done incorrectly. Region-based segmentation, while offering detailed results, also faces challenges due to its high computational demand and sensitivity to noise and small intensity variations, leading to potential over-segmentation. These methods are heavily dependent on parameter selection, and poor initial seeds can result in suboptimal outcomes, especially with complex structures that have varying intensities. Histogram-based segmentation, on the other hand, suffers from sensitivity to noise and relies on global histogram information, often missing local intensity variations. The arbitrary choice of threshold and the assumption of uniform illumination further reduce its effectiveness in complex or unevenly lit images. Overall, each method has specific strengths and weaknesses, necessitating careful consideration based on the imaging context.

- **Deep learning based segmentation**: Recent studies have leveraged deep learning, a core technique of artificial intelligence, not just for classifying images but

also for their segmentation. In particular, in the field of lung cancer detection, deep learning methods are employed to segment computed tomography (CT) images to precisely identify regions of interest (ROI).

Deep learning segmentation methods have demonstrated remarkable success in the realm of image segmentation. When juxtaposed with conventional machine learning and computer vision techniques, deep learning offers distinct advantages in terms of segmentation precision and efficiency. Consequently, leveraging deep learning for medical image segmentation can significantly aid physicians in ascertaining the size of diseased tumors and quantitatively evaluating treatment outcomes. This, in turn, leads to a substantial reduction in the workload of medical professionals [127].

In general, Convolutional Neural Networks (CNNs) facilitate image classification, taking an image as input and producing a corresponding label as output. However, in medical imaging, simply identifying abnormalities isn't enough; precise localization of these abnormalities is crucial. To address this need, various deep learning-based methods have been developed specifically for image segmentation, allowing detailed analysis and accurate identification of affected areas within medical images.

In medical imaging, The U-Net [128], a convolutional neural network renowned for its success in biomedical imaging segmentation, derives its name from its symmetric architecture, which resembles the letter "U". It consists of two primary components: the contracting path and the expansive path. This network design has garnered widespread recognition in numerous studies for its efficacy in image segmentation tasks. This method is well-suited for tasks requiring accurate delineation of object boundaries and segmentation of structures with complex shapes, such as organs and lesions in medical images. For instance, Niranjan Kumar S et al. [129] demonstrated its effectiveness in their study, where they utilized it to segment lung nodules. Its symmetrical design and skip connections enable effective feature learning and preservation of spatial context, making it a popular choice in the field of medical image analysis.

Figure 2.12 illustrates the architecture of U-net. The encoder or contracting path [130] is responsible for capturing context and extracting features from the input image. It consists of multiple convolutional layers followed by max-pooling layers, which gradually reduce the spatial dimensions of the input image while

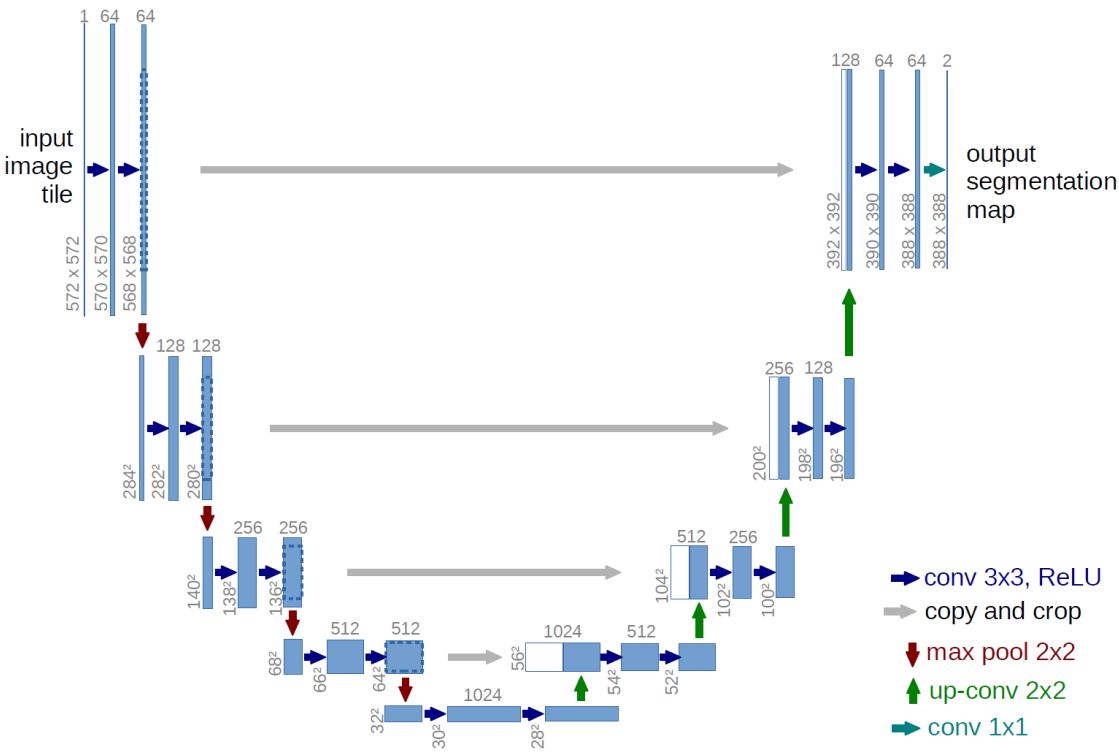



figure 2.12: U-net architecture [128]

increasing the number of feature channels.

These feature maps are then upsampled by the decoder, or the expansive path to the original input image size. The decoder is composed of a series of upsampling layers followed by convolutional layers, which gradually increase the spatial dimensions while reducing the number of feature channels.

The bridge between the contracting and expansive paths is called the bottleneck, which contains the deepest convolutional layers and retains high-level semantic information. Crucially, skip connections link corresponding encoder and decoder layers, ensuring the retention of vital spatial and detail information throughout the network. This setup culminates in an output layer, usually featuring a convolutional layer with a softmax activation for precise pixel-wise classification.

While U-Net excels in medical imaging segmentation tasks, particularly in cases requiring pixel-wise classification and boundary delineation, there are other approaches better suited where individual objects need to be distinguished.

### 2.4.3 Computer Aided Diagnosis (CADx) system for lung cancer

CADx systems aim to provide diagnostic interpretations or predictions based on the analysis of imaging data. In lung cancer field, CADx analyzes the detected nodules or lesions in lung cancer imaging data using sophisticated algorithms and computational techniques. These systems aim to provide diagnostic information and decision support to healthcare professionals by characterizing detected nodules based on various features extracted from medical images. CADx evaluates factors such as nodule size, shape, texture, and enhancement patterns to differentiate between benign and malignant nodules by using different technologies of machine learning or deep learning.

#### Classification using machine learning

In lung cancer classification using machine learning, feature extraction is a crucial step that typically follows the segmentation process, especially in medical image analysis for lung cancer diagnosis. This step entails extracting meaningful characteristics from segmented regions or nodules within lung CT scans, which may include descriptors related to shape, texture, intensity, and size of the nodules. By extracting relevant features from the segmented lung nodules, researchers and clinicians can effectively analyze and characterize the nodules for tasks such as classification (e.g., distinguishing between benign and malignant nodules), prognosis, treatment planning, and monitoring disease progression. This process plays a pivotal role in the use of image analysis techniques to assist in the diagnosis and management of lung cancer.

These features are then used to train machine learning models like:

- **Support Vector Machines (SVM)**: Supervised learning algorithms, including Support Vector Machines (SVM), are widely applied across domains such as healthcare, natural language processing, and image recognition. In lung cancer diagnosis, SVMs are frequently used to classify lung nodules as benign or malignant [131, 132].
  One of their key advantages, as noted by Bernhard Schölkopf, is their strong theoretical foundation in computational learning theory, alongside their proven performance in real-world applications [133].. In lung cancer diagnosis, SVMs help analyze complex medical data by effectively distinguishing between malignant and benign nodules, detecting subtle variations in imaging features from CT scans and X-rays.
- **K-Nearest Neighbors (KNN)**: The k-Nearest Neighbors (k-NN) algorithm is com-

monly used in lung cancer diagnosis [134]. It operates by selecting a predefined number of nearest neighbors (k) and calculating the distance between a query point and all other points in the dataset using metrics like Euclidean, Manhattan, or Hamming distance. After sorting the distances, KNN identifies the k-nearest points and, for classification tasks, assigns the query point to the most common class among its neighbors (majority voting). For regression tasks, it predicts a value based on the average of the neighbors' values [135].

- **Random Forests**: The random forest algorithm uses ensemble learning by building a collection of decision trees to collectively produce a more accurate prediction or outcome [136] that is used for both classification and regression tasks.
  In lung cancer diagnosis, it is used to classify lung nodules as malignant or non-malignant [137]. The process begins by randomly selecting subsets of the training data with replacement to build multiple decision trees. At each node of each tree, a random subset of features is considered for splitting, adding diversity and reducing correlation among the trees. Once the trees have been constructed, they independently predict the target variable for each input sample. For classification, the final prediction is determined by majority voting among all the trees, while for regression, it is typically the mean of the individual tree predictions.

### Classification with deep learning algorithm

Deep learning has achieved significant success across various fields, including computer vision, natural language processing, speech recognition, and medical image analysis. Unlike traditional machine learning, which requires manual feature extraction, deep learning automatically learns hierarchical features directly from raw data. Through multiple layers in a neural network, it captures increasingly complex patterns, making it highly effective for tasks like image classification and object detection. In lung cancer diagnosis, deep learning has advanced nodule detection, tumor classification, and patient outcome prediction with high precision, as demonstrated in numerous studies like [138,139]. Among the most common and informative imaging techniques for this purpose, we cite:

- **Convolutional Neural Networks (CNNs)**: Have achieved remarkable success in various computer vision tasks, including image recognition, classification, and medical image analysis. Their multi-layered structure transforms input images into output labels, enabling automatic learning and extraction of relevant features without manual

engineering. This capability is crucial in lung cancer diagnosis, where subtle nodule characteristics can indicate malignancy.

CNNs excel at identifying critical features such as edges, shapes, and textures, which are essential for distinguishing between benign and malignant nodules. Their robustness in handling high-dimensional image data allows them to learn hierarchical feature representations through multiple convolutional layers, enhancing the understanding of underlying patterns in lung images.

Additionally, CNNs improve diagnostic accuracy by generalizing from training data to unseen images. After being trained on a substantial dataset of labeled lung images, they can effectively apply learned features to new cases, increasing the efficiency and reliability of lung cancer diagnosis despite the variability in tumor appearance and the challenges of human image interpretation.

- **Transfer learning and pre-trained models**: Transfer learning and pre-trained models play a crucial role in analyzing medical imaging data for lung cancer using deep learning techniques [139]. By utilizing convolutional neural networks (CNNs) pre-trained on large datasets like ImageNet, essential visual patterns relevant to lung cancer diagnosis are extracted from lung CT scans. Fine-tuning these models on smaller, labeled datasets specific to lung cancer enhances their performance.

  Domain adaptation techniques help address discrepancies between the source domain of the pre-trained models and the target domain of lung CT scans, facilitating effective feature transfer. Data augmentation methods, including synthetic data generation, diversify the training dataset and help prevent overfitting. Additionally, compressed pre-trained models allow for deployment in resource-constrained settings, enabling real-time lung cancer diagnosis directly within medical imaging devices or healthcare systems.

## 2.5 Conclusion

In this chapter, we explored the role of Artificial Intelligence (AI) in healthcare, detailing fundamental concepts initially. Following this, we delved into the specifics of the Computer-Aided Detection and Diagnosis(CAD) system for lung cancer, which marks a significant advancement in medical imaging, enhancing the detection and diagnosis accuracy by analyzing scans like CTs and X-rays. These systems enable earlier detection of cancerous nodules, support consistent image interpretation, and act as second-opinion tools to aid radiologists.

However, challenges such as integrating these systems into medical workflows and ensuring they complement rather than replace human expertise need addressing. Overall, CAD systems hold the promise of improving outcomes in lung cancer treatment through earlier and more accurate detection

# Chapter 3

# A new approach based on deep learning for the detection and classification of lung cancer

## 3.1 Introduction

The emergence of diagnostic assistance systems for lung cancer has catalyzed a surge of research activity in the field. In this chapter, we explore the relevant literature and explore the various studies and developments related to this research domain. Following this comprehensive review, we conducted an in-depth analytical study to elucidate the advantages and drawbacks of existing approaches. By meticulously analyzing the limitations of previous research efforts, we identify key areas for improvement. Subsequently, we propose a customized solution aimed at optimizing the accuracy and reliability of lung cancer diagnosis. This proposed solution is customized to address the specific challenges and shortcomings identified through our thorough analysis, with the overarching goal of enhancing the effectiveness of lung cancer diagnostic procedures.

## 3.2 Related works

In the preceding chapter, we discussed lung nodule localization, highlighting its implementation through object detection and segmentation methods. These approaches emphasize the identification and precise delineation of nodules, utilizing techniques ranging from traditional methods to advanced deep learning frameworks. Here, we will provide a comprehensive overview of different studies in the field, evaluating their respective strengths and disadvantages.

In the advancement of CAD systems for lung cancer, many studies suggest the extraction of lung area from CT scan images as an initial step in the process. This crucial step, as proposed by Swati et al. [140] in their study, serves as a fundamental groundwork for subsequent analysis. They employed thresholding to differentiate between body and non-body pixels through an iterative process. Following this, morphological operations like erosion and dilation were applied to remove the body and other organs from CT scan images. The connected component method was then used to segment lung nodules. For nodule classification, the authors utilized a support vector machine (SVM), testing their methodology on 15 diseased lung images and achieving an accuracy of 92.5%.

N.A. Memon et al. [141] emphasize that accurate lung area segmentation is a critical step in developing CAD systems for lung cancer diagnosis. To address this, the authors proposed a segmentation technique designed to extract the lung region from CT scan images. Initially, they applied an optimal threshold to each image, followed by connectivity analysis of the thresholded regions. Then they used a region-growing method to further segment the lungs.

Their algorithm was tested on 25 datasets from patients obtained from Ackron University, USA, and Aga Khan Medical University, Karachi, Pakistan.

An automated CAD system is proposed by D. Sharma and G. Jindal [142] to identify lung cancer. Firstly, the authors have preprocessed images by the use of simple box blur and wiener filter. Since the CT scan image contains other substances than the lung organ, the authors have proposed the segmentation of the lung region before proceeding to the nodule segmentation. For this purpose, they have chosen edge detection method using sobel edge detection, then they have analyzed segmented lung area through feature extraction task to find the abnormality existed in the lung and detect which are cancerous. Their approach was tested on the LIDC dataset, achieving an accuracy rate of 80%.

In the same context of lung segmentation,Y. Itai et al. [143] introduced an automated technique to segment lung area. Initially, they employed thresholding, then, they refined the segmentation using a snakes or active contour model to achieve a final delineation of the lung area.

In a separate investigation, S. Makaju et al [144]. proposed a model aimed at identifying lung cancer through the analysis of CT scan images. Their approach started with preprocessing the images to eliminate noise, employing both median and gaussian filters. For segmentation, they opted for watershed segmentation due to its capability to accurately separate objects even when they overlap, a crucial feature for precisely delineating cancerous nodules, especially when they intersect with other structures. Thereafter, the authors computed various features from the segmented images, including area, perimeter, centroid, diameter, eccentricity, and mean intensity. These features were then used to train a support vector machine (SVM) classifier to differentiate between benign and malignant nodules. The authors tested their methodology using 16 DICOM images from the LIDC dataset for training the classifier, and validated the results with 5 additional images, comprising a total of 15 nodules, achieving an accuracy of 86.6%.

M. Javaid et al. [145] integrate several techniques to enhance lung nodule detection in early-stage lung cancer diagnosis. They begin with thresholding and histogram analysis for segment lung area accurately, followed by morphological closing. K-means clustering is then employed for initial nodule detection, refined using morphological opening method. Finally large nodules are classified using a Support Vector Machine (SVM) classifier.

In [146], A. Bhandary et al. have converted CT scan images from RGB scale to grayscale and resizing them into (227,227,1) pixels as the first step in their process. After data preprocessing, they divided the segmentation operation into two steps (lung extraction and nodule

segmentation). For lung extraction, the authors have applied threshold value to separate the image into two levels of contrast (high contrast and low and medium contrast), where high contrast sections represent bone and heart, and low and medium contrast represents tumor and other sections. For nodule detection, they utilized morphological segmentation which gave better results than watershed segmentation. However, the watershed method performed good results in the comparative study proposed by T. Heeneman and M. Hoogendoorn in [147].

P. Tripathi et al. [148] have presented a comparative study between several segmentation methods of lung cancer detection. At the beginning, they have used the median filter for preprocessing task to enhance the quality of input image. Then, the authors compared otsu thresholding, edge detection, and marker controlled watershed segmentation. The authors have calculated some features like (area, perimeter, mean intensity, and eccentricity) for each segmentation technique used in their study. They have found that marker-controlled watershed segmentation provides the best results than other methods.

S. Uzelaltinbulat and B. Ugur [149] have developed an algorithm to segment lung tumor. They started by converting images from DICOM format to jpeg format and resized them to (256*256) to improve their quality. In the proposed algorithm, the authors have chosen morphological operation (erosion) and median filter to pre-process images. After this, they have applied a thresholding method (otsu's method) to segment lung nodules. They have also used another morphological operation (opening) to eliminate the unnecessary segments in an image. The authors utilized a set of 70 images from LIDC-IDRI dataset, 50 of which contained tumors and 20 without. Their model achieved an accuracy of 97.14%.

A computer-aided system for the automatic diagnosis of lung cancer has been proposed by M. Gomathi and P. Thangaraj [131]. Firstly, the authors have used morphological operations to segment lung area from CT scan images (erosion to reduce noise and dilation and median filter to enhance CT images). Then, they applied the Fuzzy Possibility C-Mean algorithm (FPCM) to detect cancer nodules existing in the segmented lung region. To classify the nodules, the authors have used support vector machine. Their approach was tested on a dataset of 1000 images sourced from a reputable hospital.

Upon reviewing these studies, it becomes evident that the majority advocate for lung segmentation as an initial step in the process of segmenting lung nodules. This approach involves isolating the lung regions from the surrounding anatomical structures in CT images. By accurately delineating the lung boundaries, subsequent nodule segmentation algorithms can

focus specifically on the lung area, improving the precision and efficiency of nodule detection and characterization. Although, segmenting the lung from CT scan images before segmenting lung nodules can pose several drawbacks, including increased complexity in the segmentation pipeline, potential propagation of errors from lung segmentation to nodule detection, loss of contextual information vital for accurate nodule identification, heightened processing time due to additional computational steps, and challenges in handling lung pathologies that can affect segmentation accuracy since these pathological changes can distort the normal structure of the lungs, making it harder for automated systems to accurately segment or isolate the lungs, leading to potential errors in subsequent analyses, such as nodule detection. While this approach may offer some computational benefits, particularly in terms of reducing processing load, it must be carefully weighed against its potential negative impacts on accuracy and efficiency, especially in clinical settings where timely and precise nodule detection is crucial for patient care. Integrated segmentation methods that simultaneously address lung and nodule segmentation may present a more effective alternative, ensuring comprehensive analysis while mitigating the risks associated with segmented approaches.
More importantly, Segmenting the lung in the presence of juxtapleural nodules poses specific risks due to challenges such as partial volume effects, pleural attachment, artifacts, and shadowing. Juxtapleural nodules often exhibit blurred boundaries and can be attached to the pleural surface, making it difficult to accurately separate them during lung segmentation. This can result in underestimation or overestimation of nodule size and increase the likelihood of false-positive findings or inaccurate characterization. Given the clinical significance of juxtapleural nodules, which have a higher probability of malignancy, precise segmentation is essential for appropriate management decisions. Addressing these risks requires specialized segmentation algorithms tailored to handle juxtapleural nodules' unique characteristics and close collaboration between radiologists and computer scientists to ensure the development of reliable segmentation methods for lung cancer detection.

In addition, these researchers focus on the use of classical methods of segmentation that are characterized by their simplicity, efficiency, and interpretability, making them accessible and understandable for a wide range of users. These methods can provide reasonably accurate results with low computational overhead, particularly for simple segmentation tasks or when dealing with small datasets. However, the use of classical methods like morphological operations and edge detection for lung nodule segmentation face significant challenges due to the need for precise parameter selection, which often relies on trial-and-error and can lead to false detections. Moreover, these methods are highly sensitive to noise inherent in CT

scan images, which can introduce false edges and distort lung structures, ultimately compromising segmentation accuracy. The presence of noise not only increases the risk of false positives but also complicates the delineation of nodule boundaries, potentially resulting in under-segmentation or over-segmentation errors. Despite efforts to mitigate these challenges through preprocessing techniques and parameter optimization, classical methods may still fall short compared to more advanced approaches like deep learning-based segmentation in achieving robust and accurate segmentation of lung nodules.

With the rapid advancement of artificial intelligence, there's a growing emphasis on incorporating deep learning techniques not just for classification tasks but also for segmentation processes. This necessity has been underscored by the remarkable successes witnessed with models like U-Net in medical imaging [128].

A. Chon et al. [150] have presented their conducted research titled 'Deep Convolutional Neural Networks for Lung Cancer Detection', where they have started by trying to use the 3D segmented lung directly as an entry in the malignancy classifier but they have got bad results, which may be due to the large search space, so they entered small areas containing the top cancerous nodule. They have used U-net which takes a 2d CT slice with shape 256*256 as input and labels (256*256 mask nodule where pixel value=1 and the rest=0). Although U-net produces a strong signal for the real nodule, it also generates a large number of false positives.

Ying S. et al. [151] proposed a lung nodule detection method using the Faster R-CNN algorithm, which demonstrated strong performance. Their research highlighted the critical role of parameter optimization in enhancing the network structure and improving detection accuracy.

A new algorithm based on YOLOv3 for detecting lung nodules have been proposed by Xu, Kejia [152]. However, the Yolov5 is also used by Ewaidat h et al. [153], and Yan C. et al. [154] to detect lung nodules. Their process began with image preprocessing steps, which included resampling and normalization. They then applied an adaptive thresholding method along with morphological operations to effectively segment the lung area. Following this segmentation, they employed an enhanced version of YOLOv5 for the detection of lung nodules. Their experiments were conducted on the LUNA16 dataset, yielding an Average Precision (AP) of 94.8% and a sensitivity of 78.1% for the improved model.

Each method has its own set of advantages and disadvantages, and the selection of a

particular method depends on specific requirements and objectives. For instance, traditional techniques relying on contours, regions, and histograms may offer simplicity and faster processing times but might lack the precision and adaptability needed for complex tasks. On the other hand, deep learning approaches, while potentially providing higher accuracy and the ability to learn from large datasets, often require substantial computational resources and extensive training data. The decision on which method to employ should be based on factors such as the complexity of the task, the availability of data, computational resources, and the desired level of accuracy and robustness. Therefore, a careful evaluation of the strengths and limitations of each approach is crucial to selecting the most appropriate one for the given context and goals.

## 3.3 Proposed Method

To compare the precedent approaches, we have proposed certain criteria:
Do preprocessing techniques influence the quality of an image?
Does the use of certain types of filtering, especially with small kernels, fail to eliminate small nodules, particularly those between (3mm-30mm)?
Does lung segmentation not impact the accuracy of nodule segmentation? Is it reliable to proceed directly to nodule segmentation?

To address these questions, we have opted to experiment with object detection techniques that delineate a bounding box around lung nodules for localization. This approach enables us to monitor the evolution of the nodule in multiple CT scans, as the nodules may span multiple slices rather than appearing only in a single slice or location. In addition, lung nodules are small, round or oval-shaped growths in the lungs that are often detected through medical imaging like CT scans. They can vary in size, with micro-nodules being typically less than 10 mm in diameter, while larger nodules range between 10 mm and 30 mm. These nodules can be indicative of various conditions, with the detection of lung nodules serving as a potential early warning sign for lung cancer [155, 156].
The size of the nodules is important in assessing the risk to the patient. Smaller nodules are less likely to be cancerous, while larger ones raise more concern and may require further diagnostic procedures such as biopsy to determine their nature accurately [157]. Early detection and monitoring of these nodules are vital for timely intervention and effective management of potential health risks, especially in cases where malignancy is suspected.

For this reason, we have proposed a method for detecting and classifying lung nodules, particularly those between (3mm-30mm), which can be challenging for radiologists. This method relies on deep learning technology, specifically leveraging YOLOv7, and incorporating transfer learning for accurate nodule detection and classification.

Figure 3.1 illustrates the methodology adopted in our study. Firstly, we initiated the process by thoroughly preparing the dataset, converting DICOM images to PNG format and organizing the data to ensure compatibility with various deep learning algorithms. This step was crucial in streamlined the data loading process and making it easier to manipulate the images using common image processing tools. Next, we focused on detecting lung nodules using YOLOv7 transfer learning, employing three different types of input: whole images, preprocessed images using median and adaptive median filters, and segmented lung images. This multi-faceted approach allowed us to assess the impact of different preprocessing techniques on detection accuracy. Finally, we classified the detected lung nodules into three categories: benign, suspect or undefined, and malignant, using transfer learning and fine-tuning techniques to enhance the accuracy and reliability of the classification process. This comprehensive approach aimed to improve detection and classification performance, facilitating a more precise and early diagnosis of lung cancer.

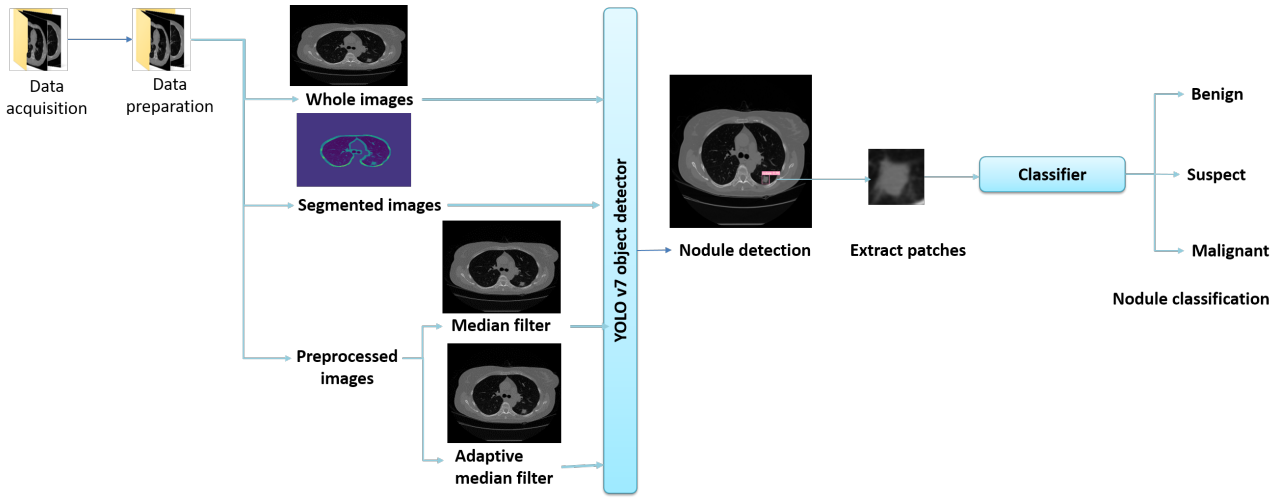



figure 3.1: The overall architecture of the proposed approach [158]

### 3.3.1 Data preparation

We began by collecting data from the Cancer Imaging Archive, using the LIDC-IDRI dataset. This dataset is one of the most widely employed datasets in lung cancer research, comprising

1018 patient cases with 244527 images.

A CT scan of the lungs provides a detailed visualization of not only the lungs themselves but also surrounding anatomical structures and tissues within the thoracic cavity. This includes vital organs such as the heart, major blood vessels, and portions of the liver, as well as bony structures like the ribs and sternum. Additionally, the scan captures air within the lungs, adipose tissue (fat), muscle, and portions of other organs that may be adjacent to the thoracic cavity. This comprehensive imaging modality offers valuable diagnostic information, allowing clinicians to assess lung health, detect abnormalities or lesions, evaluate bone integrity, and examine the overall condition of surrounding tissues, Figure 3.2 presents an example of the visualization of a CT scan image stored in DICOM format.

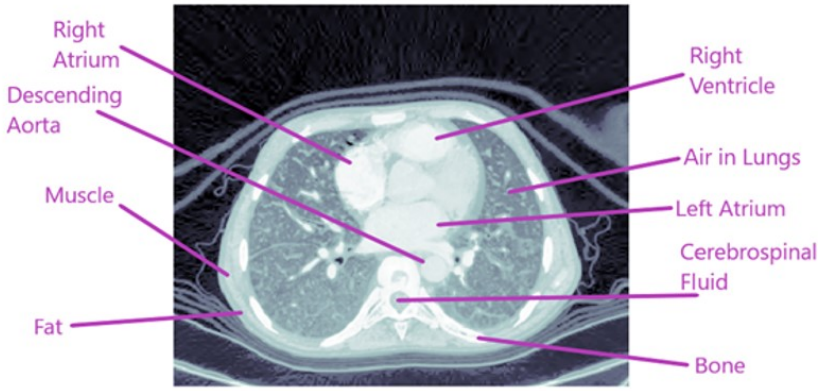



figure 3.2: Example of a CT scan image in DICOM format [159].

These CT scan images typically produce a series of images stored in the DICOM format. Each image represents a cross-sectional slice of the scanned body part, providing detailed information for medical diagnosis and analysis.

When discussing CT scans, the Hounsfield Unit (HU) scale is a crucial concept. It measures the radiodensity of tissues based on their attenuation of X-rays. Figure 3.3 shows this scale that assigns specific numerical values to different tissue types, with water having a HU value of 0, air having a negative value, and denser tissues such as bone having positive values [89]. Understanding the HU scale allows radiologists to distinguish between various tissues and structures in CT images, aiding in diagnosis and treatment planning. Additionally, changes in HU values can indicate pathological conditions or abnormalities within the body, providing valuable diagnostic insights.

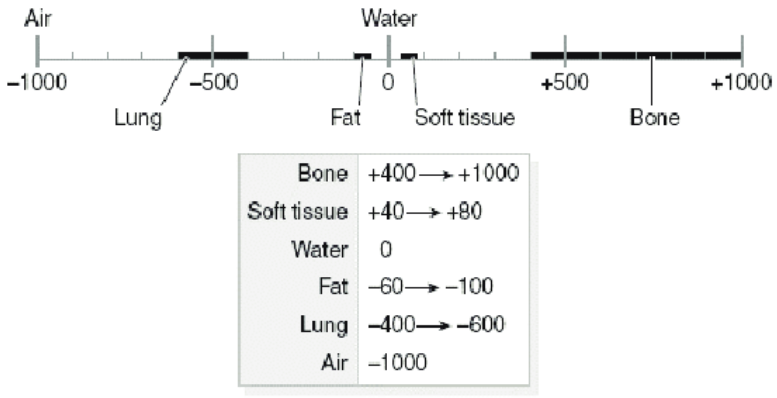



figure 3.3: The Hounsfield scale of CT numbers [160]

In preparing our dataset for lung cancer analysis, we followed a detailed workflow to sort, extract, and annotate DICOM images, ensuring the data is both accurately ordered and enriched with essential diagnostic details.

- Sorting of DICOM Images: The imaging dataset utilized in this study consists of 1018 patient folders, each containing a series of images stored in DICOM format. However, these images are not arranged in the same sequence as displayed in a DICOM viewer, which can lead to discrepancies during analysis. This inconsistency occurs because DICOM viewers organize slices based on the 'instance number' field in each image's metadata, ensuring they reflect the anatomical order of the scan series.
  To prepare the images for further processing, it is crucial to sort them according to their 'instance number' to maintain the original anatomical sequence. Manual sorting is time-intensive and impractical, especially in online environments where file handling is slower. To automate and streamline this process, we employed the DICOM SORT application [161]. This tool allows sorting by specific fields such as 'instance number' or other metadata as needed. By organizing the images in each patient folder, the application ensures that slices are properly ordered, providing a consistent and structured dataset for subsequent analysis.

- Extraction of Slices: After sorting the images, the next step is to extract only the slices containing nodules, as identified by radiologists. For this, we reference the LIDC Nodule Size Report [162], which provides detailed information about each detected nodule, including:

  – Slice Numbers with Nodules: The report indicates the exact slice numbers where

each nodule is visible, allowing us to directly locate and extract the relevant slices.

  - Coordinates (x, y): Representing the center of mass for each nodule, these coordinates help pinpoint the nodule's location within each slice, ensuring precision in ROI extraction.

- Image Format Conversion: This step involves converting the images to PNG format. This conversion simplifies the integration of medical imaging data into deep learning frameworks, allowing us to leverage diverse datasets for training and evaluation purposes. By converting DICOM images to this format, the dataset becomes more accessible and easier to work with across different deep learning technologies. This enables the exploration and implementation of advanced deep learning techniques for both tasks: lung nodules detection and classification. To do this, we have used the process explained as follow:

  - *Convert DICOM image to float*: Initially, we converted the DICOM images to float format to prevent overflow or underflow losses. This conversion provides a wider dynamic range and greater precision for representing pixel values. The float format accommodates both integer and fractional values, preserving fine details and minimizing quantization errors that may arise during conversion. Additionally, its compatibility with deep learning algorithms ensures optimal performance and enables comprehensive image analysis without the loss of clinically relevant information.
  - *Rescaling the grayscale values of an image between 0 and 255*: This involves adjusting the pixel intensities so that the darkest pixel becomes 0 (black) and the brightest pixel becomes 255 (white), with all other intensities linearly interpolated between these two extremes. This process enhances the contrast and visibility of the image while maintaining its relative proportions. It is a common preprocessing step in image analysis and visualization, making images more visually appealing and suitable for display on standard monitors or printing.
  - *Converting grayscale values to uint (unsigned integer) format*: It involves mapping the rescaled pixel intensities from the range [0, 255] to the integer range [0, 255]. This conversion ensures that the pixel values are represented as whole numbers without any fractional or decimal components.

- Lung Nodule Localization: To localize lung nodules effectively, we utilize the Nodule Size Report [162] that encodes the nodules' x and y coordinates, as well as their

boundary data, enabling precise identification of regions of interest (ROIs).

After identifying and localizing the nodules on the relevant slices, the resulting dataset includes paired information of lung slices and their corresponding localized nodule coordinates. This localized dataset plays a critical role in training and validating detection algorithms for lung nodule analysis.

- Lung Nodule classification: To make the dataset suitable for both segmentation and classification tasks in CAD systems for lung cancer, we enrich the dataset by incorporating malignancy classifications. Each radiologist provides a malignancy score for the nodules they identified, with scores typically ranging from benign to highly malignant.

  By parsing the XML file associated with each patient's scan series, we extract detailed annotations provided by four independent radiologists, each conducting separate reading sessions. These annotations offer comprehensive information, including the malignancy degree assigned to each nodule. The XML structure allows us to retrieve and analyze each radiologist's malignancy assessment for every nodule across the different reading sessions, ensuring a thorough evaluation of interobserver variability and consensus. Based on these scores, we categorize each nodule as:

  - Benign: Scores indicating low likelihood of malignancy.
  - Indeterminate: Scores representing borderline or uncertain malignancy.
  - Malignant: Scores indicating a high likelihood of malignancy.

After converting the images, the dataset was prepared for use in various artificial intelligence applications, resulting in images with a resolution of $512 \times 512$ pixels. The dataset was then split into three subsets: 70% for training (799 images), 10% for validation (115 images), and 20% for testing (228 images).
This preparation leads directly to one of the core challenges of this work, which is detecting lung nodules from CT scan images. The process typically involves essential preprocessing steps, such as image enhancement and lung segmentation, which are necessary before specifically identifying the nodules. These steps, as demonstrated in previous approaches, are crucial for improving the accuracy and reliability of nodule detection. However, the specific methods used for preprocessing and lung segmentation can vary, impacting the overall performance of the nodule detection system. Therefore, our proposal suggests comparing the efficacy of three distinct input types for lung nodule detection from CT scan images which are: whole images, preprocessed images and lung segmented images.

By comparing the performance of lung nodule detection using these three different input types, we can evaluate the impact of each one on the accuracy, of nodule detection algorithms. This comparative analysis can help identify the most effective approach for detecting lung nodules in CT scan images.

**The first input type: Whole images**

We utilized the images that were directly converted to png format without applying any preprocessing techniques, such as noise reduction or contrast enhancement, nor performing lung segmentation. This approach was taken to observe how well the model could perform without the benefit of refined image preparation or isolating the lung regions for more focused analysis. It allowed us to establish a baseline for comparison with more sophisticated preprocessing methods.

**The second input type: Preprocessed images**

The LIDC-IDRI dataset contains CT images, which inherently suffer from noise due to factors like radiation dose and equipment variations, hindering radiologists' ability to discern fine details and impeding edge detection and segmentation processes. To address this, filtering methods are employed to mitigate image noise. In our study, we utilized the median and adaptive median filters to reduce salt-and-pepper noise common in CT scans. However, the decision to apply filters depends on specific application requirements and trade-offs between noise reduction and feature preservation.

The main challenge of this study is to accurately detect small lung nodules while preserving critical image information vital for a precise lung cancer diagnosis. To address this, we utilized a minimal filter size, specifically a 3x3 kernel, to ensure that essential features are retained during the preprocessing stage. This small window size helps maintain the integrity of the image details, which is crucial for accurate detection of nodules.

**The third input: Lung segmented images**

This input type is designed to segment the lung region from CT scan images while effectively removing neighboring organs such as the liver, tissue, and heart. To do this, we used the K-means algorithm to extract two centroid values representing the background and foreground, respectively, and calculated their mean value as a threshold.

Afterther, we applied morphological operations (erosion and dilation) which are standard techniques in image processing used to alter object shape and size, where erosion operation

removes pixels from the edges of objects, while dilation adds pixels to these edges. The extent of pixel manipulation during these operations is determined by the size and shape of the structuring element, typically represented by a matrix or template. In our study, we used a 3x3 kernel for erosion and a 10x10 kernel for dilation, which consists of effectively balancing the removal of unwanted details with the preservation of significant structures in the CT scan images. The smaller 3x3 kernel for erosion targets minor noise and shrinks irrelevant features while maintaining the finer details of the lung's anatomy. In contrast, the larger 10x10 kernel for dilation is designed to expand key regions and fill gaps, thus restoring essential lung structures after erosion, as illustrated in Figure 3.4 that presents the result of lung segmentation.

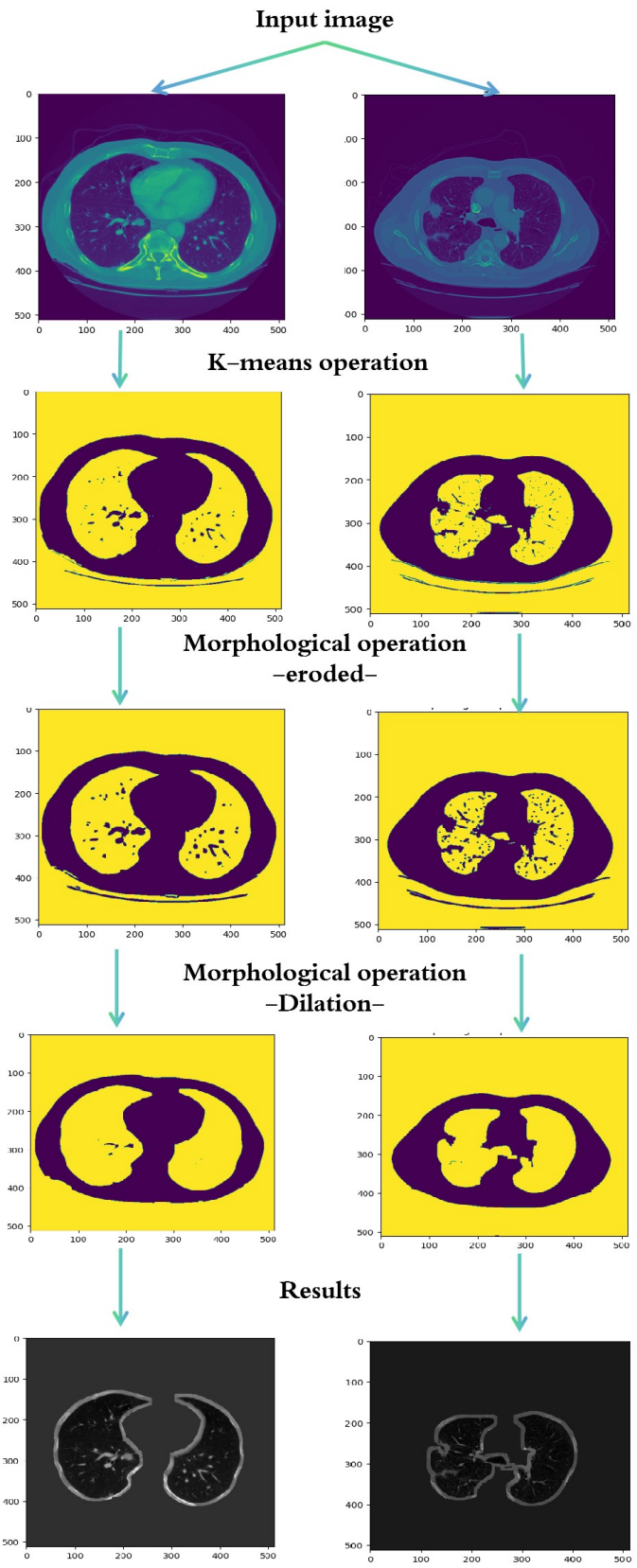



figure 3.4: The outcome after each step of lung segmentation process.

### 3.3.2 Lung nodule detection using transfer learning of YOLOv7

Object detection plays a pivotal role in lung cancer detection by automating the identification of suspicious nodules, which are potential indicators of malignancy. For this task, we utilized YOLOv7 [110], a state-of-the-art object detection model, renowned for its optimal balance between accuracy and speed. YOLOv7's advanced deep learning framework enables end-to-end training, allowing it to efficiently detect and localize lung nodules even amidst complex anatomical structures and varying nodule sizes.

A key strength of YOLOv7 lies in its transfer learning capability, which allows the adaptation of a pre-trained model to domain-specific datasets. By fine-tuning YOLOv7 on a specialized lung CT image dataset, we significantly enhanced its detection performance, even with limited training data. This approach not only improves accuracy but also ensures the model's effectiveness in handling real-world clinical scenarios.

YOLOv7's robust architecture, efficiency, and adaptability make it an excellent choice for the precise and efficient localization of lung nodules, contributing to early diagnosis and improved outcomes in lung cancer management.

step, typically achieving higher accuracy at the cost of increased computational complexity and slower processing. The schematic plot presented by the Figure 3.5illustrates these differences in their detection pipelines.

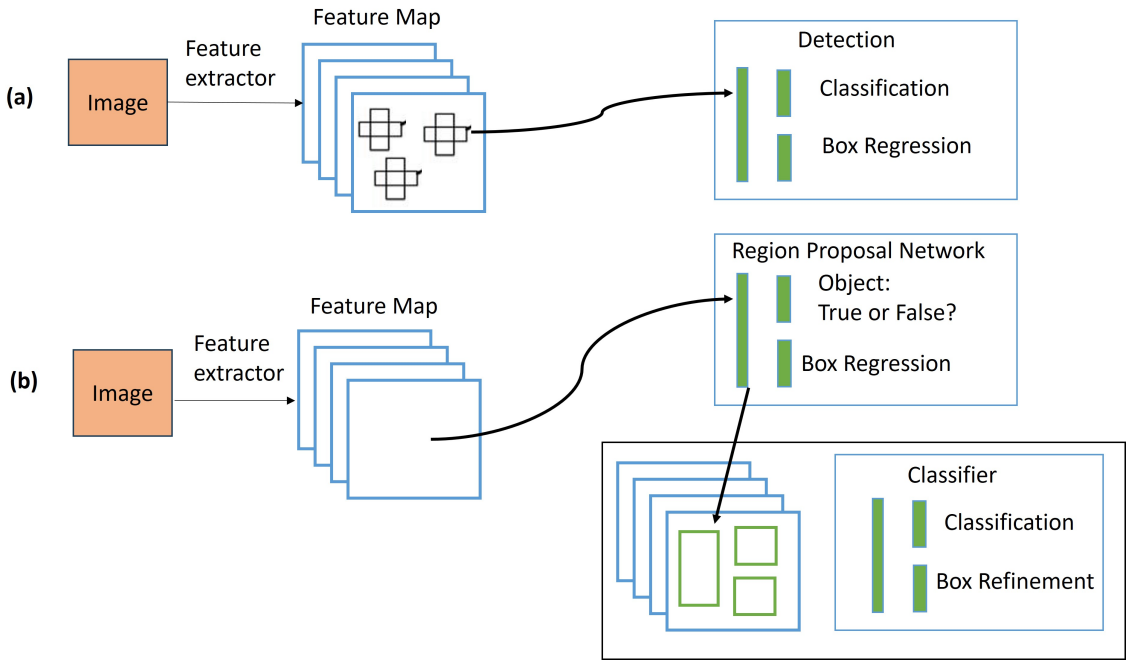



figure 3.5: Schematic plot for (a) one-stage detector and (b) two-stage detector [163]

### Training the YOLOv7 for nodule detection

The training process of the YOLOv7 model for nodule detection is illustrated in the Figure3.6 and explained as follow:

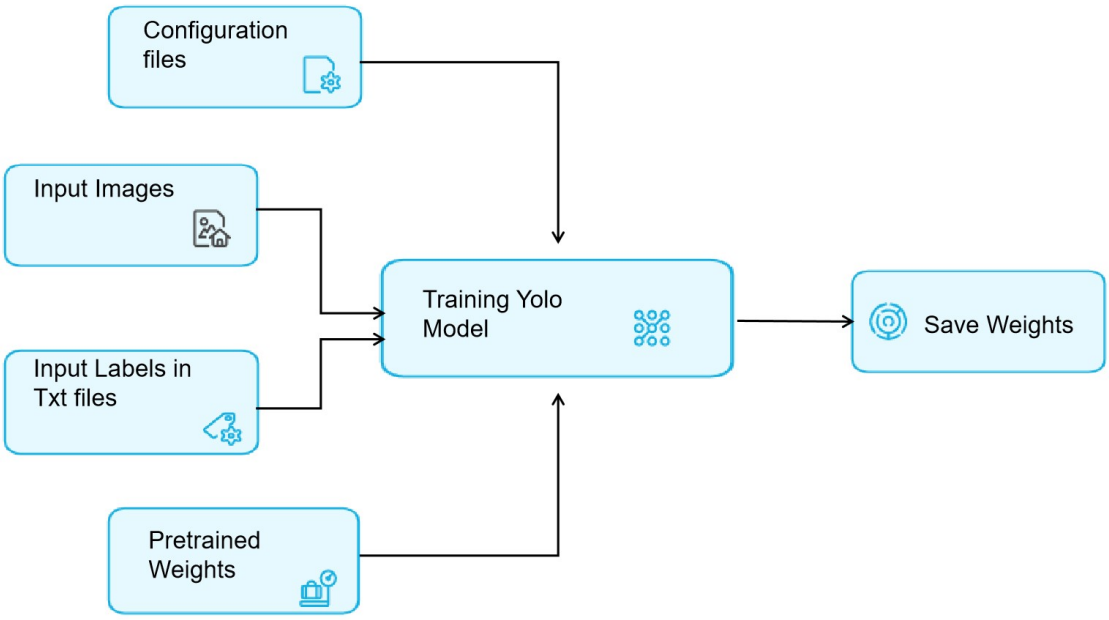



figure 3.6: Training YOLO process

- *Create a YOLOv7 dataset:* Firstly, we move on to transforming our inputs into the specific format required by YOLOv7. This process involves preprocessing the data, which includes organizing the images and their corresponding annotations in a way that aligns with YOLOv7's expectations, ensuring that the model can effectively utilize the dataset for training and detection tasks. For this purpose, we have extracted the necessary information to acquire bounding boxes with their coordinates. Then, we transformed the data into the YOLO-specific format, which involves creating a .txt file for each image.

  Each file contains a label corresponding to the image, with a line dedicated to each nodule occurring within the frame. Furthermore, YOLO requires several files to effectively initiate the training process these include the total count of classes, a text file enumerating the paths to all images earmarked for training, another text file listing the names of all classes, the directory path where trained weight files will be saved, and the pre-trained weights for the convolutional layers of the YOLO model, which are often initialized from weights trained on large-scale image datasets such as ImageNet.

- *Download pre-trained weights:* Obtain the weights of the YOLOv7 model pre-trained on a large dataset like COCO. These weights contain general features useful for object detection.

- *Adjust the model for specific task:* Modify the model to suit our task, which is detecting lung nodules. This may involve changing the number of output classes to match our dataset. For this task, we'll set the number of output classes to one, representing nodules.

- *Train the model:* Fine-tune the YOLOv7 model using the LIDC-IDRI dataset, which contains annotated lung nodules. During training, the model adapts its pre-trained weights to better detect nodules based on the characteristics of the LIDC-IDRI dataset.

- *Save weights:* Throughout the training process, data was collected, loss was analyzed, and model weights were captured at each epoch to save the best weights. After training, save two sets of weights:

  - Best.pt: This file contains the weights corresponding to the epoch with the best performance metrics, such as highest accuracy or lowest loss.
  - Last.pt: This file contains the weights saved at the completion of the last epoch.

  These saved weights can be utilized for inference in new data or for future fine-tuning tasks that allow us to leverage the general object detection capabilities learned from a large dataset and fine-tune the model to specialize in detecting lung nodules using the LIDC-IDRI dataset.

**Loss Function**

The losses are necessary for training YOLOv7 to accurately detect and localize objects in images, ensuring a balance between precision and recall. We have used two types of loss functions: Bounding box loss and objections loss.

1. Bounding box loss: Often called localization loss, quantifies the disparity between predicted bounding box coordinates and ground truth annotations. By minimizing bounding box loss during training, the model learns to precisely estimate objects' spatial extent and position within the image, leading to improved localization performance. Additionally, box loss contributes to the overall optimization process by guiding the model toward making more accurate predictions regarding object boundaries, thereby

enhancing the efficacy of object detection systems.
It measures the error in the predicted bounding box coordinates (x, y, width, height) compared to the ground truth. That means how accurately the predicted bounding boxes match the ground truth bounding boxes and it is given by equation3.1:

$$\text{Localization Loss} = \sum_{i=0}^{S^2} \sum_{j=0}^{B} 1_{ij}^{\text{obj}} \left[ (x_i - \hat{x}_i)^2 + (y_i - \hat{y}_i)^2 + (\sqrt{w_i} - \sqrt{\hat{w}_i})^2 + (\sqrt{h_i} - \sqrt{\hat{h}_i})^2 \right] \tag{3.1}$$

where:

- $S \times S$ is the size of the grid.
- $B$ is the number of bounding boxes per grid cell.
- $1_{ij}^{\text{obj}}$ is an indicator function that is 1 if the $j$- bounding box in cell $i$ contains an object, and 0 otherwise.
- $x_i, y_i$ are the center coordinates of the ground truth bounding box.
- $\hat{x}_i, \hat{y}_i$ are the center coordinates of the predicted bounding box.
- $w_i, h_i$ are the width and height of the ground truth bounding box.
- $\hat{w}_i, \hat{h}_i$ are the width and height of the predicted bounding box.

2. The objectness loss: Is a pivotal metric in object detection tasks, crucial for determining how effectively a model identifies objects within bounding boxes in an image. This loss function evaluates the model's capacity to distinguish between regions containing objects of interest and those representing background elements. It does so by assessing the confidence scores associated with predicted bounding boxes, helping estimate the likelihood that an object is within each box, thus facilitating precise object localization. Throughout the training process, minimizing objectness loss guides the model in refining its predictions and improving its ability to accurately identify objects in various contexts, it is given by the equation 3.2.

$$\text{Objectness Loss} = \sum_{i=0}^{S^2} \sum_{j=0}^{B} \left[ 1_{ij}^{\text{obj}} (C_{ij} - \hat{C}_{ij})^2 + \lambda_{\text{noobj}} 1_{ij}^{\text{noobj}} (C_{ij} - \hat{C}_{ij})^2 \right] \tag{3.2}$$

where:

- $S \times S$ is the size of the grid.

- $B$ is the number of bounding boxes per grid cell.
- $1_{ij}^{\text{obj}}$ is an indicator function that is 1 if the $j$-th bounding box in cell $i$ contains an object, and 0 otherwise.
- $1_{ij}^{\text{noobj}}$ is an indicator function that is 1 if the $j$-th bounding box in cell $i$ does not contain an object, and 0 otherwise.
- $C_{ij}$ is the ground truth confidence score for the $j$-th bounding box in cell $i$ (1 if object present, 0 if not).
- $\hat{C}_{ij}$ is the predicted confidence score for the $j$-th bounding box in cell $i$.
- $\lambda_{\text{noobj}}$ is a weight to balance the importance of the confidence loss for boxes that do not contain objects.

The overall loss function in YOLOv7 is a weighted sum of the box loss, objectness loss, and classification loss. In our work, We have not include the classification loss, instead, we focused solely on combining the two losses: the box loss and the objectness loss. This decision stems from our use of the YOLO model exclusively for detection rather than classification tasks. In our specific scenario, we are dealing with a single class labeled as 'nodule'.

This strategic choice was informed by our preliminary tests with YOLO, where we experimented with three classes: benign, suspect or undefined and malignant. During this testing phase, we observed that the mean Average Precision (mAP) significantly decreased when introducing multiple classes, suggesting that the model's performance was adversely affected. Consequently, we streamlined our approach to focus on nodule detection alone, allowing for a more accurate and efficient detection process.

### 3.3.3 Lung nodule classification with transfer learning of vgg16

To determine the potential malignancy of lung nodules, we have proposed the transfer learning of VGG16 that was trained on the ImageNet dataset, to classify the detected nodules into three categories (benign, suspect, and malignant), we have chosen a multiclass classification because LIDC-IDRI dataset contains CT scans of the lungs that four experienced radiologists have annotated. Each radiologist provides a Malignancy Degree (MD) for any detected nodules on a scale ranging from 1 to 5 reflecting the likelihood of a nodule being malignant based on its appearance in imaging studies:

- Score 1 (Definitely Benign): Low risk of malignancy, often associated with clearly benign characteristics ( stable nodules, specific calcification patterns).
- Score 2 (Probably Benign): Slightly higher risk but still considered benign; requires monitoring rather than immediate intervention.
- Score 3 (Indeterminate): Uncertain nature, further imaging or biopsy may be required.
- Score 4 (Probably Malignant): High suspicion of malignancy, often associated with characteristics that indicate the potential presence of lung cancer.
- Score 5 (Definitely Malignant): Strong evidence of malignancy, typically leads to urgent intervention, including biopsies or surgical consideration.

In our work, we have grouped the nodules with (MD= 1 or MD=2) as benign, nodules with MD= 3 as suspect or undefined, and nodules with (MD=4 and MD=5) as malignant as detailed:

- Benign Group (MD= 1 or MD=2): Nodules with malignancy degree of 1 or 2 are typically categorized as benign due to their low risk of malignancy. These scores represent nodules that exhibit features commonly associated with non-cancerous conditions, such as smooth edges, the presence of calcifications, or a lack of significant growth over time. In some cases, these lower scores may correlate with low-grade tumors, such as low-grade adenocarcinomas, which present as small, well-circumscribed nodules. These nodules often present ambiguous characteristics, such as mixed solid and ground-glass densities or irregular borders, which make it difficult to classify them as benign or malignant. These malignancy degrees would be unlikely to represent SCLC or aggressive NSCLC subtypes. They may indicate benign nodules or very early-stage, slow-growing NSCLC, such as well-differentiated (low-grade) adenocarcinomas. Low-grade tumors are less aggressive, so they may be associated with lower malignancy scores even if cancerous [164].
- Indeterminate or Suspect Group (MD=3): Nodules with a malignancy degree of 3 fall into an indeterminate or suspect category, where the likelihood of malignancy is uncertain. These nodules may present ambiguous characteristics, such as partially irregular borders or mixed densities that could indicate either a benign process or early malignancy. The uncertainty in this category makes it challenging to definitively classify the nodule as benign or malignant. These nodules might reflect early-stage NSCLC

where the features are not clearly indicative of malignancy but suspicious enough to warrant further investigation. These nodules could develop into more aggressive cancers over time but are not yet definitive.

- Malignant Group (MD=4 or MD=5): On the other hand, nodules with malignancy degree of 4 or 5 are grouped as malignant due to their high likelihood of being cancerous. These nodules often exhibit concerning radiological features, such as spiculated or irregular margins, rapid growth, or dense solid components, which significantly raise the suspicion of malignancy. These nodules are more likely to represent SCLC or aggressive forms of NSCLC like advanced adenocarcinoma or squamous cell carcinoma. SCLC is especially associated with rapidly growing, high-malignancy nodules. NSCLC subtypes like squamous cell carcinoma or poorly differentiated adenocarcinoma can also present with high malignancy scores, indicating advanced or aggressive cancer [165, 166].

We have proposed three different architectures: All three approaches follow the same steps, with the exception of the fourth step, which differs between approaches.

1. **Step 1: Load VGG16 without the top layers:** load the VGG16 model with pre-trained weights from the ImageNet dataset, excluding the top layers by setting include_top=False.
2. **Step 2: Freeze layers except the last two**: Only the last two layers' weights are trainable.
3. **Step 3: Create the model and add the VGG convolutional base.**
4. **Step 4:** The approaches differ in step 4:
   - *First Approach*: Figure 3.7:

     Add a flatten layer followed by a dense layer with 512 units and ReLU activation function.
   - *Second Approach*: Figure 3.8:

     Add a flatten layer, followed by a series of dense layers with ReLU activations (512, 256, 128, 64, and 32 units respectively), and Dropout layers with (50% and 25%).
   - *Third Approach*: Figure 3.9:

     Add just a flatten layer.

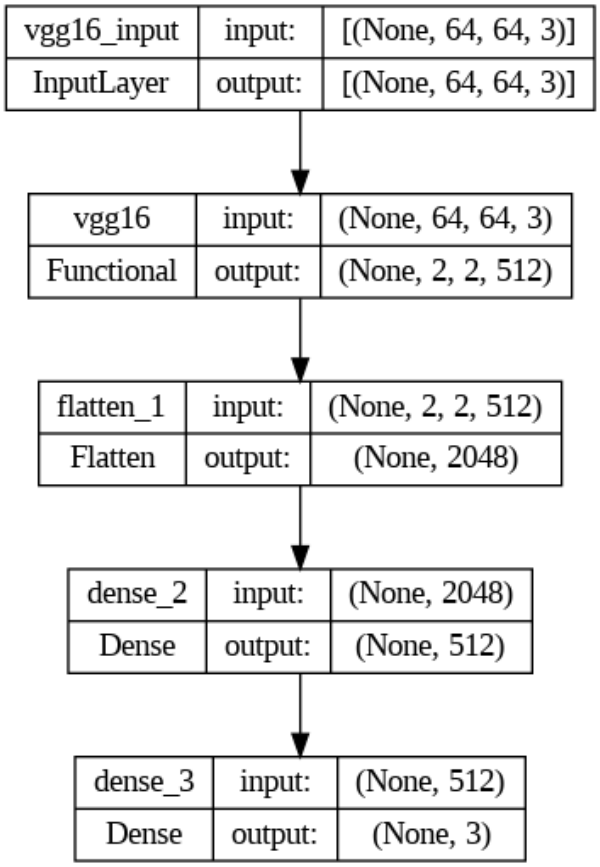



figure 3.7: First approach architecture

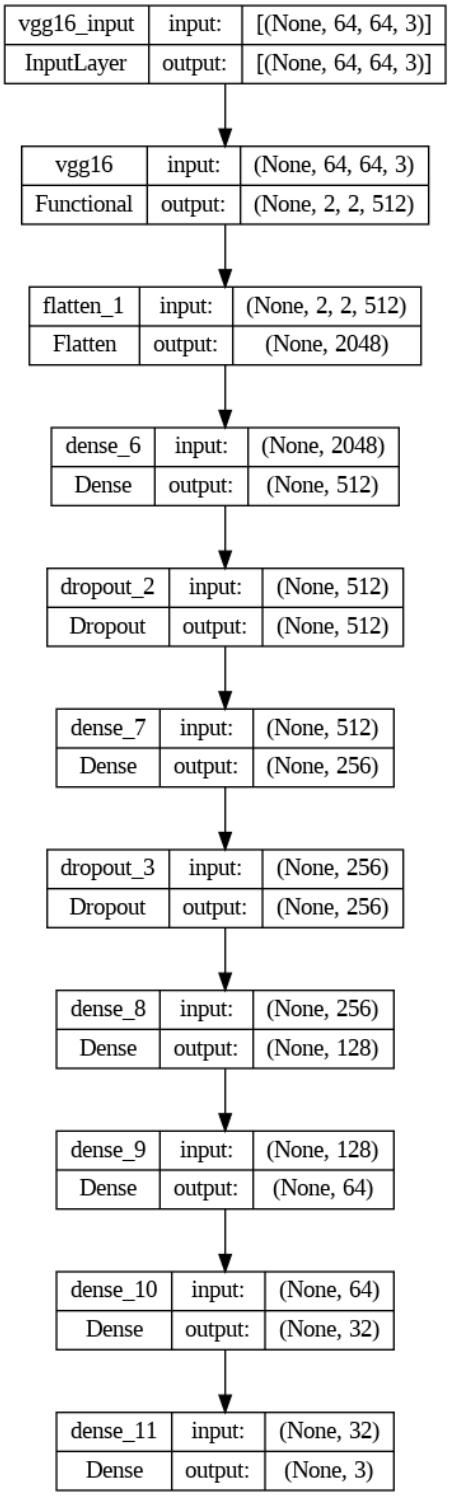



figure 3.8: Second approach architecture

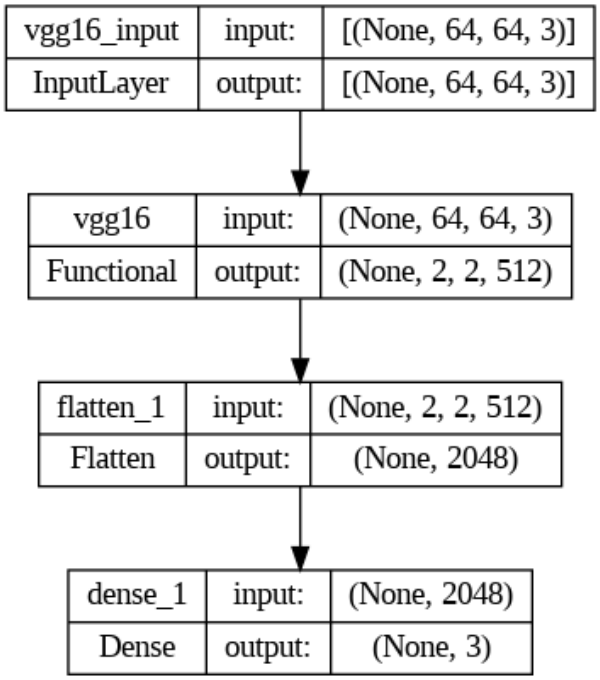



figure 3.9: Third approach architecture

5. **Step 5**: Finally, for all approaches:

   Final Layer: Add an output layer with 3 units and Softmax activation.

## 3.4 Conclusion

In this chapter, we have explored the state-of-the-art techniques for lung cancer detection and classification, highlighting their respective advantages and disadvantages. Following this overview, we have detailed the various methods employed in our study. Initially, we utilized YOLOv7 for lung cancer detection and subsequently applied VGG16 for lung cancer classification, leveraging the principle of transfer learning in both stages.

Our proposed approach has demonstrated promising results in both detection and classification tasks, which will be further detailed in the next chapter.

# Chapter 4

# Results and Discussion

## 4.1 Introduction

To validate the proposed approach, it is essential to conduct thorough evaluations. In this chapter, we will introduce the tools and programming languages employed in the implementation of the proposed models, along with the database utilized. Following this, we will provide a detailed analysis of the obtained results. This analysis used a comparative study with previous solutions to highlight the improvements and differences. Finally, we will conclude this chapter by summarizing and synthesizing the findings from our evaluations.

## 4.2 Software and Hardware

The proposed solution is implemented in Python, utilizing various libraries to ensure optimal functionality. For image processing tasks, we use libraries like NumPy and Pillow to store, preprocess, and manipulate image data. Keras is chosen for its modular design and support for multiple backends, while TensorFlow is favored for its scalability and performance. Finally, scikit-learn offers straightforward and efficient tools for predictive data analysis.

The implementation was carried out on a machine with the following specifications: Intel(R) Core(TM) i5-8265U CPU @ 1.60GHz (up to 1.80GHz), 8GB RAM, running Windows 10

## 4.3 Results

To evaluate the experimental results and facilitate transparency and reproducibility in research, enabling comparisons with state-of-the-art methods, we use various object localization and classification metrics.

Before talking about the different metrics used in this study, let's explain some important keys used in this context:

- True Positives (TP): These are the instances where the model correctly predicts the positive class.
- False Negatives (FN): These are the instances where the model fails to identify the positive class.
- True Negative (TN): These are the instances where the model correctly predicted the negative class.

- False Positive (FP): These are the instances where the model incorrectly predicted the positive class.

The different metrics used to evaluate our work are described below:

- *Mean Average Precision mAP:* The mean Average Precision (mAP) is a commonly used metric for evaluating object detection because it integrates both precision and recall, accounting for False Positives (FP) and False Negatives (FN). The mAP is calculated as the average of the Average Precision (AP) across several Intersections over Union (IoU) thresholds. However, the Average Precision (AP) represents the area under the precision-recall curve evaluated at a specific Intersection over Union (IoU) threshold, focusing on the relationship between precision and recall rather than simply averaging precision values [167]. The mean Average Precision (mAP) can be calculated as the mean of the Average Precision (AP) over several intersections over Union (IoU) thresholds. The following equation represents it:

$$\text{mAP} = \frac{1}{N} \sum_{i=1}^{N} \text{AP}_i \tag{4.1}$$

  where:

  - $N$ is the number of different IoU thresholds.
  - $\text{AP}_i$ is the Average Precision at the $i$-th IoU threshold.

- *Recall:* is an important performance metric in the context of classification and object detection tasks. Measures the ability of a model to identify all relevant instances within a data set correctly. In other words, recall is the ratio of correctly predicted positive observations to all the actual positives [168]. Mathematically, recall is defined by equation 4.2:

$$\text{Recall} = \frac{\text{True Positives (TP)}}{\text{True Positives (TP)} + \text{False Negatives (FN)}} \tag{4.2}$$

- *Precision:* is a performance metric used to evaluate the accuracy of a classification or object detection model. It measures the ratio of correctly predicted positive observations to the total predicted positives, indicating how many of the predicted positive instances are actually relevant [168].

$$\text{Precision} = \frac{\text{True Positives (TP)}}{\text{True Positives (TP)} + \text{False Positives (FP)}} \tag{4.3}$$

### 4.3.1 Lung nodules detection

Before training the model, we proposed three input types (whole images, preprocessed images, and segmented images) and conducted transfer learning using YOLOv7. Table 4.1 presents the outcomes of the nodule detection task, summarizing the model's performance across the various input types. These results will be analyzed and discussed in the following discussion

| Models | Input | Epoch | mAP | Precision | Recall |
|---|---|---|---|---|---|
| Model 1 | whole images | 89 | 81.28% | 82.68% | 74.72% |
| Model 2 | preprocessed images using median filter | 67 | 77.15% | 90.4% | 65.2% |
| Model 3 | preprocessed images using adaptive median filter | 93 | 75.91% | 70.4% | 76.5% |
| Model 4 | lung segmented images | 167 | 73.89% | 74.25% | 70.43% |

Table 4.1: Results of fine-tuned YOLOv7 for lung nodule detection [158]

- The first scenario: The images were utilized in their entirety after being converted from DICOM to PNG format, with no additional preprocessing steps such as noise reduction or enhancement, and without performing any lung segmentation to isolate the lung region. This allowed us to evaluate the model's performance on raw images, maintaining all original features and surrounding structures.
  Upon analyzing Figure 4.1, which illustrates the curves for box loss, mean Average Precision (mAP), precision, and recall, we observed that transfer learning with YOLOv7 applied to whole images demonstrates impressive performance.

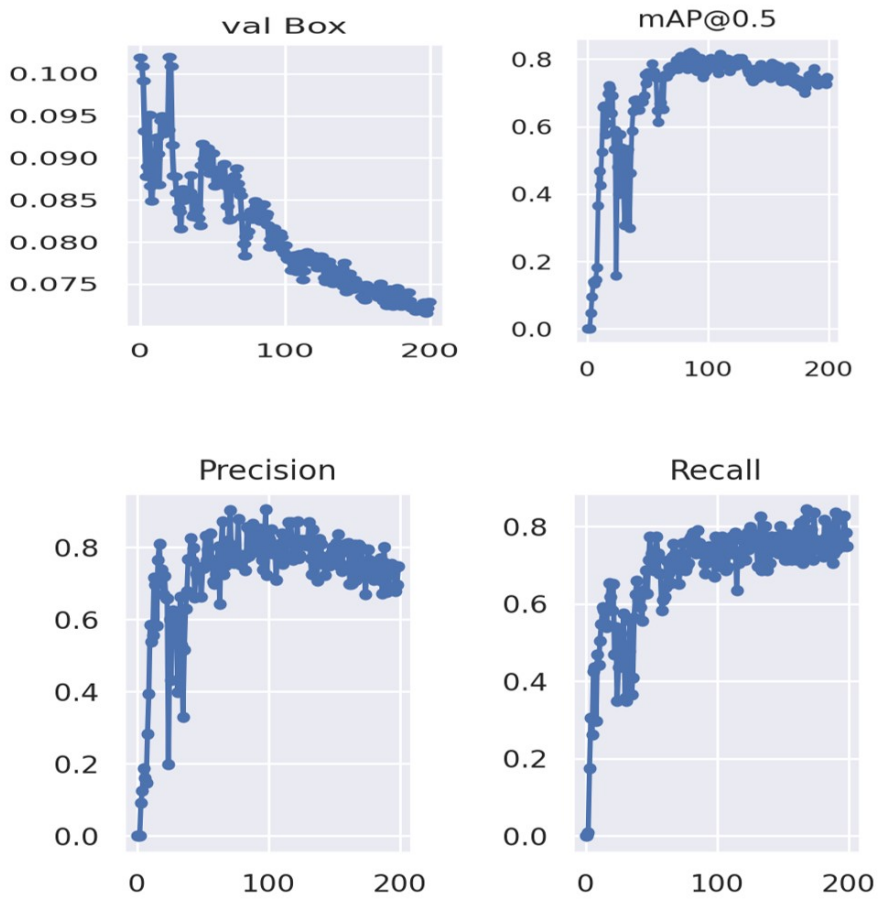



figure 4.1: Box loss, mAP, Precision and Recall curves of the first senario using whole images [158]

The model achieved a mean Average Precision (mAP) of 81.28%, indicating a high level of accuracy in detecting nodules across various Intersection over Union (IoU) thresholds. This result underscores the model's capability to accurately predict the locations of lung nodules within the images.

The precision score of 82.68% shows that significant majority of the model's positive predictions are correct. This means that when the model identifies a nodule, it is likely to be correct more than 82% of the time.

The recall score of 74.72% reflects the model's ability to detect most of the actual nodules present in the images. This means that the model is able to identify around 74% of all true nodules.

- The second scenario: we employed image filtering techniques to enhance the quality of the converted PNG images and reduce noise. Specifically, we applied two types of

filters: median and adaptive median filters to reduce salt and pepper noise from images and enhance their quality. By implementing both filtering methods, we aimed to determine which one more effectively improves the mean Average Precision (mAP) rate in lung nodule detection.

Figures 4.2 and 4.3 present the box loss, mAP, precision, and recall curves for both cases of input: preprocessed images with a median filter and preprocessed images with an adaptive median filter.

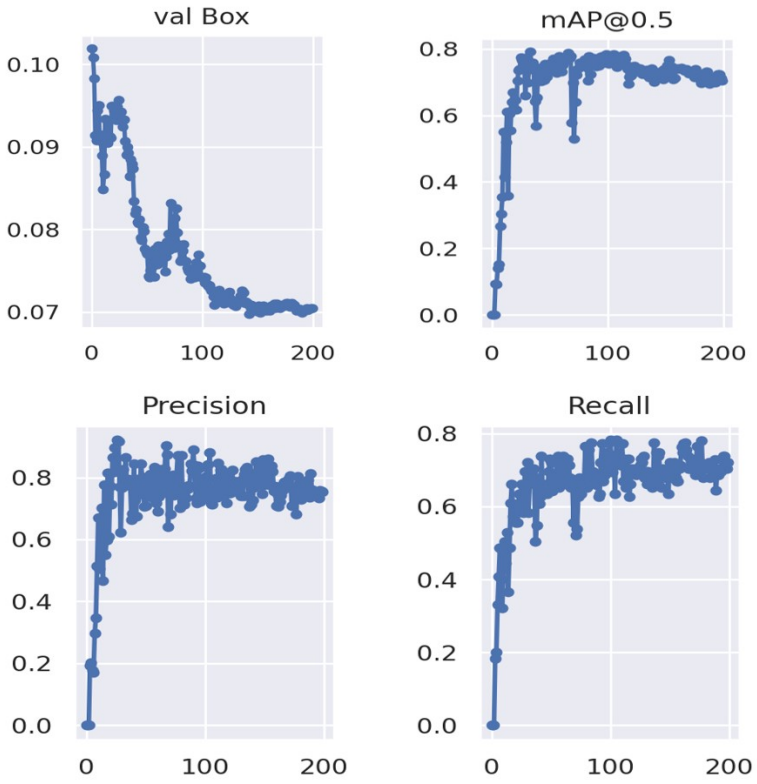



figure 4.2: Box loss, mAP, Precision and Recall curve using preprocessed images with median filter [158]

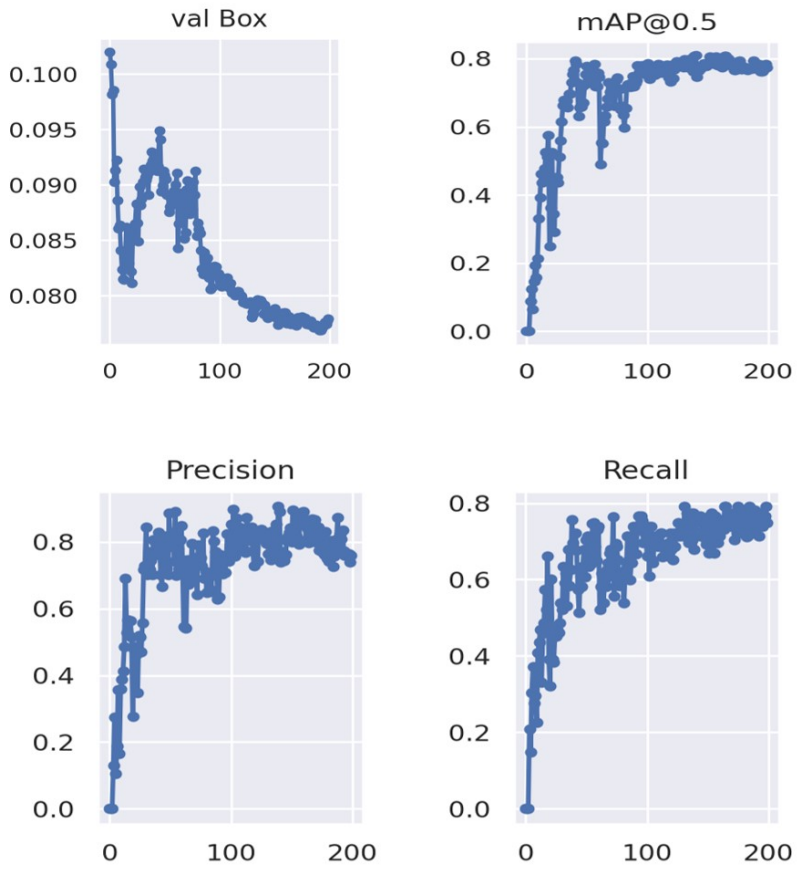



figure 4.3: Box loss, mAP, Precision and Recall curve using preprocessed images with adaptive median filter [158]

The mAP with the median filter is 77.15%, which is higher than the 75.91% mAP with the adaptive median filter. This suggests that the overall performance in terms of both precision and recall is slightly better when using the median filter.

The precision is significantly higher with the median filter at 90.4% compared to 70.4% with the adaptive median filter. High precision indicates that the model is very accurate in its positive predictions when using the median filter, meaning that most of the detected nodules are indeed correct detections.

The lower precision with the adaptive median filter suggests an increase in false positives, meaning the model incorrectly identifies more instances as nodule.

The recall is higher with the adaptive median filter at 76.5% compared to 65.2% with the median filter. This indicates that the model is better at detecting actual nodule present in the images when using the adaptive median filter. However, the lower recall with the median filter suggests that the model misses more actual nodule (false nega-

tives).

The median filter results in higher precision but lower recall, indicating the model is more conservative in its detections, preferring fewer false positives but missing some true positives. Conversely, the adaptive median filter increases recall but at the cost of precision, meaning the model is more liberal in its detections, capturing more true positives but generating more false positives.

- The third scenario involves using images that isolate the lungs by excluding surrounding organs, achieved through various lung segmentation techniques. By segmenting the lungs, structures such as the liver, tissue, bones, and heart are removed from CT scan images, allowing for a more focused analysis. This scenario is employed to assess how lung extraction affects the accuracy and effectiveness of nodule detection.

  Figure 4.4 presents the box loss, mAP, precision, and recall curve, demonstrating that transfer learning with YOLOv7 using lung-segmented images yields lower performance, achieving a mean Average Precision (mAP) of 73.89% that indicates moderate overall performance in terms of both precision and recall.

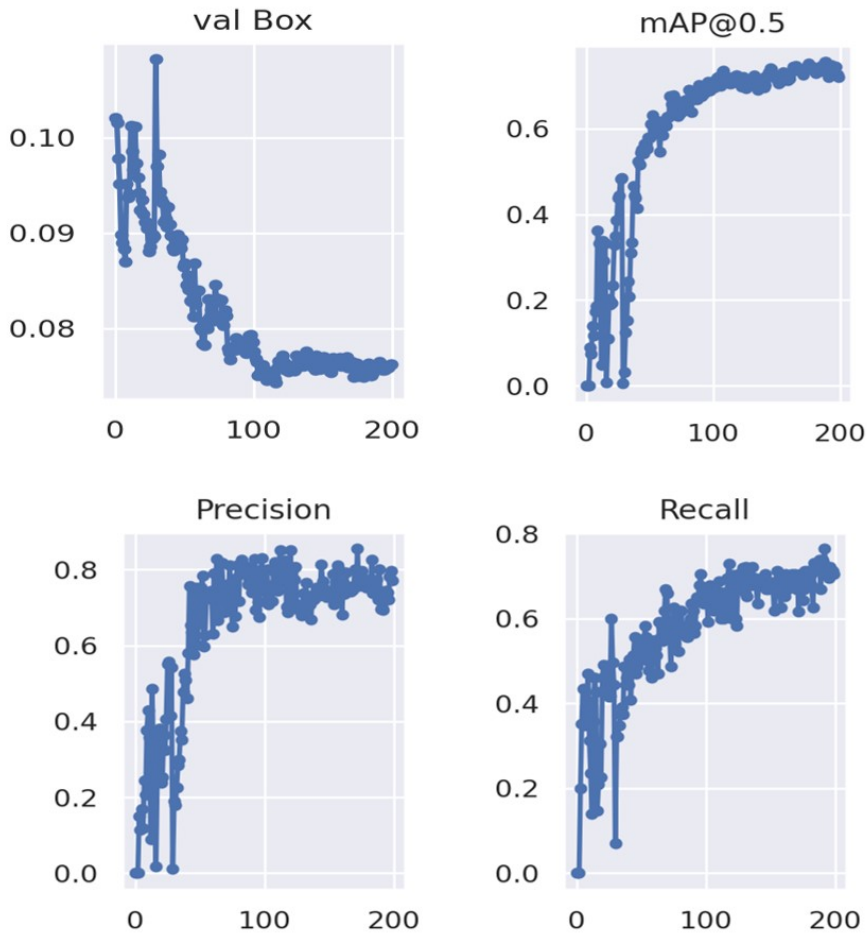



figure 4.4: Box loss, mAP, Precision and Recall curves using segmented images [158]

A precision of 74.25% suggests that when the model predicts a nodule, it is correct about 74% of the time. This indicates that there are a fair number of false positives, where the model incorrectly identifies background or irrelevant parts of the image as lung nodules.

A recall of 70.43% indicates that the model successfully detects around 70% of the actual lung nodules. This suggests that the model is missing about 30% of the true positive instances, resulting in false negatives.

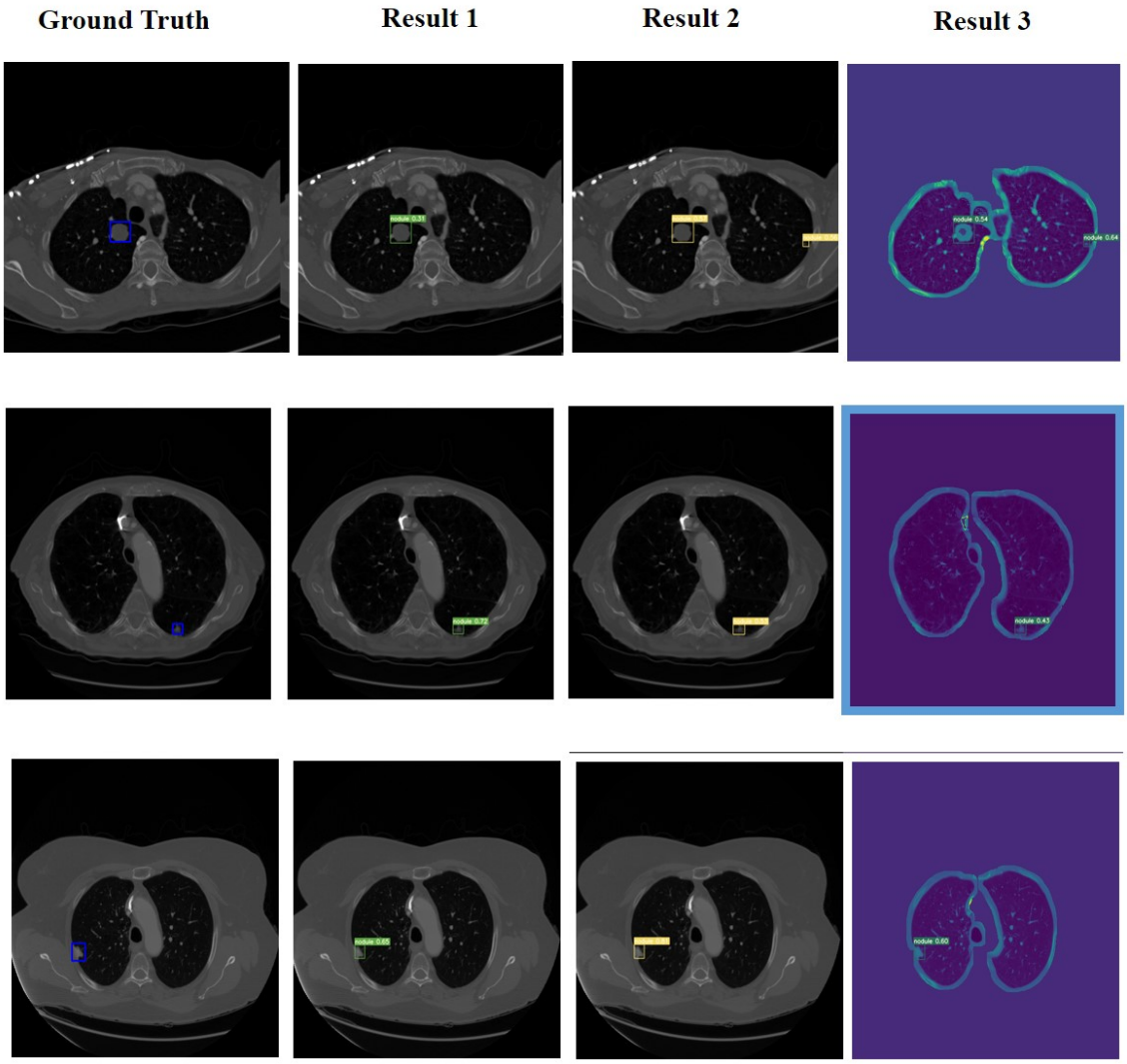



figure 4.5: Some samples of lung nodule detection using three different inputs (result 1: for whole image, result 2: for preprocessed images, result 3: for lung segmented images [158])

### 4.3.2 Lung nodules classification

Following the detection of lung nodules, the subsequent step involves their classification. In this study, we introduced a multiclass classification approach to categorize these nodules into three distinct classes: Benign, Suspect, and Malignant. The detected nodules were passed through a classifier for classification into these three categories. To accomplish this, we resized images into 64*64 pixels, then several experiments were conducted on our work based on the pre-trained Vgg16 model.

- The first experiment involves freezing all layers of the Vgg16 architecture except the

last two, then adding the Flatten layer followed by two Dense layers. The result is presented in the confusion metric that presented only 4 nodules benign are missclassify as malignant and 3 malignant nodules are missclassify as benign as presented in the confusion matrix (Figure 4.6).

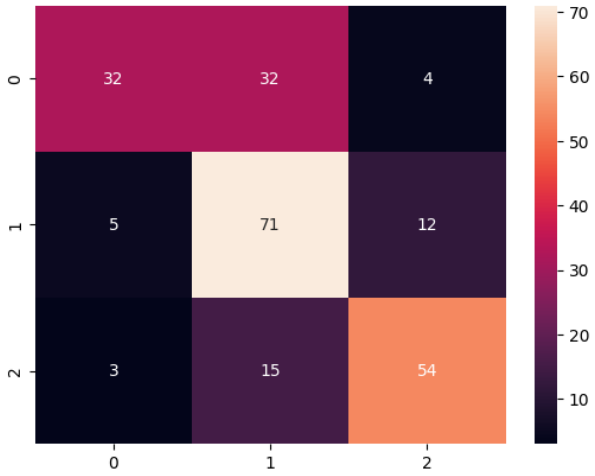



figure 4.6: Confusion matrix of the first model [158]

- The second experiment involves freezing all layers of the vgg16 architecture expect the last two, then adding flatten layer ,followed by a series of Dense layers with ReLU activations (512, 256, 128, 64, and 32 units respectively), and Dropout layers (50% and 25%). The results show that 7 nodules benign as classified malignant and 2 nodules malignant are classified as benign. Figure 4.7 presentes the confusion matrix of this model.

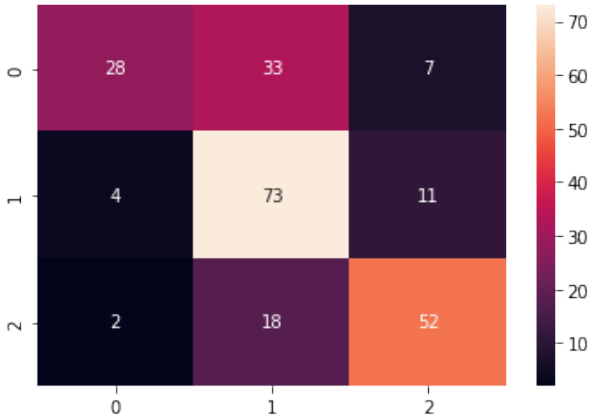



figure 4.7: Confusion matrix of the second model [158]

- The third experiment involves freezing all layers of the vgg16 architecture expect the last two, then add only flatten layer followed by one Dense layer of output. The results presented in the confusion matrix4.8 show that 4 nodules malignant are classified as benign and 6 malignant nodules are classified as benign.

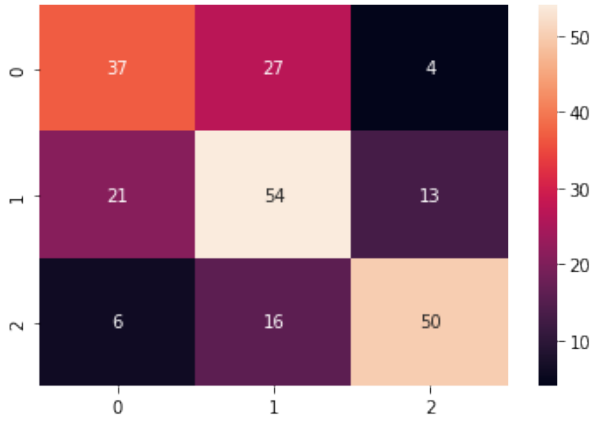



figure 4.8: Confusion matrix of the third model

## 4.4 Dicsussion

In this study, we proposed a process for the detection and classification of lung nodules using object detection techniques to identify lung nodules and transfer learning with fine-tuning for the classification of detected nodules.

During this process, we evaluated three distinct scenarios to demonstrate the influence of input images on lung nodule detection results. when we analyze the results presented in the precedent section, we found that the first scenario that uses the whole images as input to train the YOLOv7 gives the combination of mAP, precision and recall metrics which suggests that the model trained using transfer learning of YOLOv7 on whole images is quite effective as presented by the Figures 4.9 and 4.10 because it has:

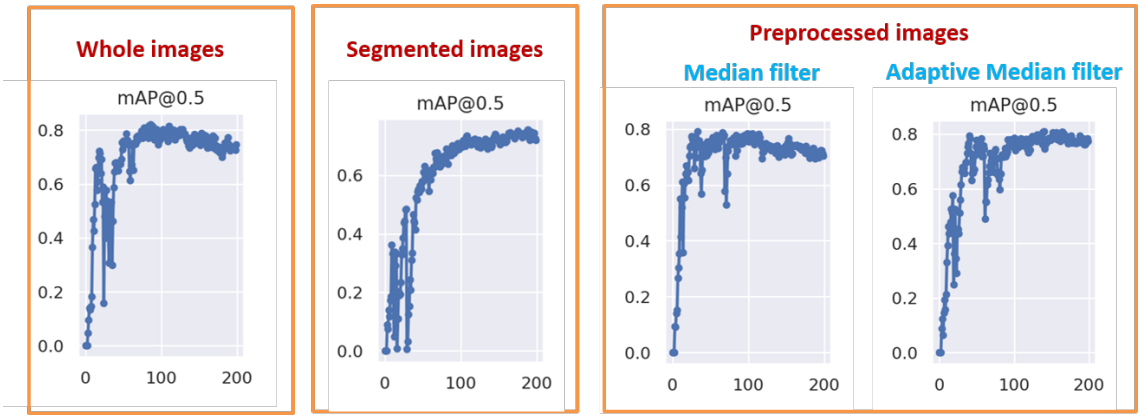



figure 4.9: mAP metric of different presented models

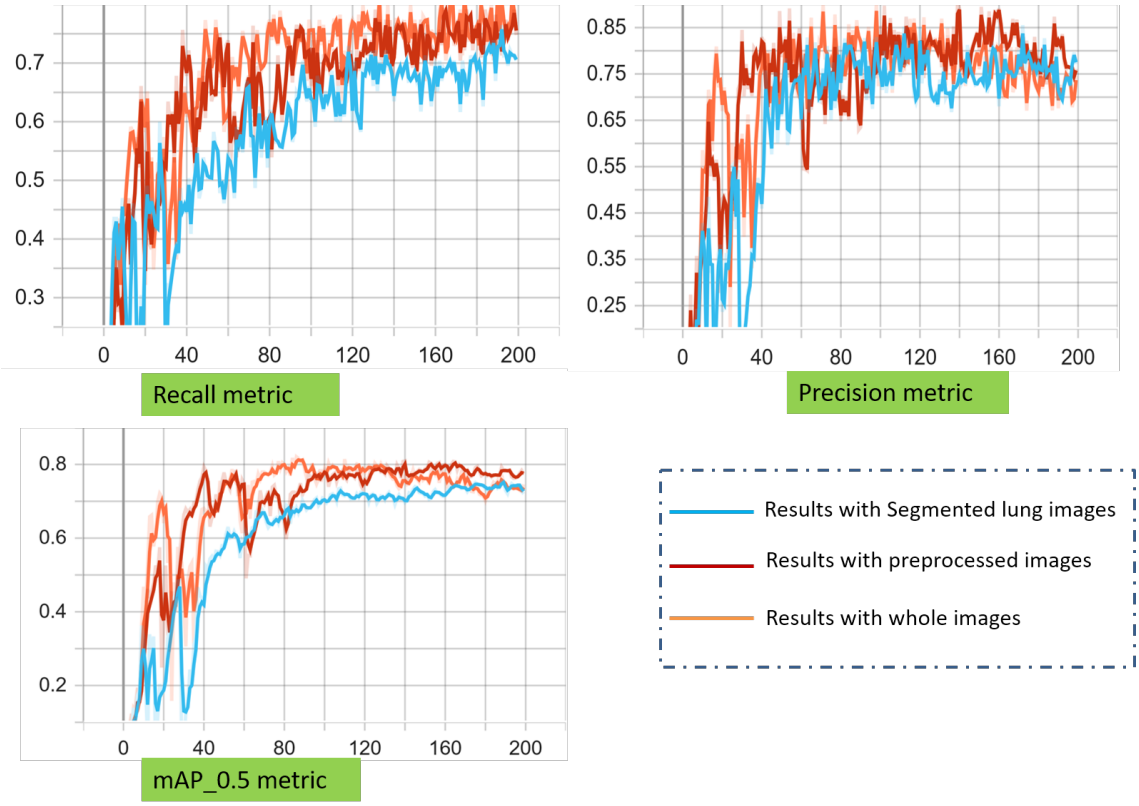



figure 4.10: Comparison of three different models

- High mAP that indicates the overall good performance of the model in object detection tasks.
- High Precision implies that the model is accurate and reliable in its predictions, with few false alarms

- Moderate to High Recall shows that while the model successfully identifies a substantial portion of the objects, there is still room for improvement in capturing more of the objects that are present.

These results indicate whole images retain all contextual information from the original DICOM scans, ensuring data consistency and completeness, which are crucial for accurately detecting and localizing lung nodules. By converting DICOM images to PNG format without additional preprocessing, the integrity of the input data is preserved, maintaining it in its most authentic form. This allows the model to learn more effectively from the training data, capturing a wider range of features including subtle contextual cues from surrounding anatomical structures. In contrast, filtering processes such as median and adaptive median filtering, modify images by smoothing out noise, which can obscure important details and introduce artifacts, leading to imbalances in precision and recall. For example, median filters can blur small nodules, while adaptive median filters might over-enhance certain features, leading to inconsistencies. Lung segmentation process focuses solely on lung regions itself might remove contextual information that could help in accurately detecting nodules, and can miss out on valuable contextual clues from surrounding tissues and structures, potentially resulting in incomplete or inaccurate detection as shown in Figure 4.11 errors can occur when using segmented lung images, particularly in missing the detection of juxtapleural nodules as it presented in Figure 4.11 (a). In addition, the accuracy of the lung segmentation process could impact the performance where poor segmentation could lead to incomplete or imprecise nodule detection.

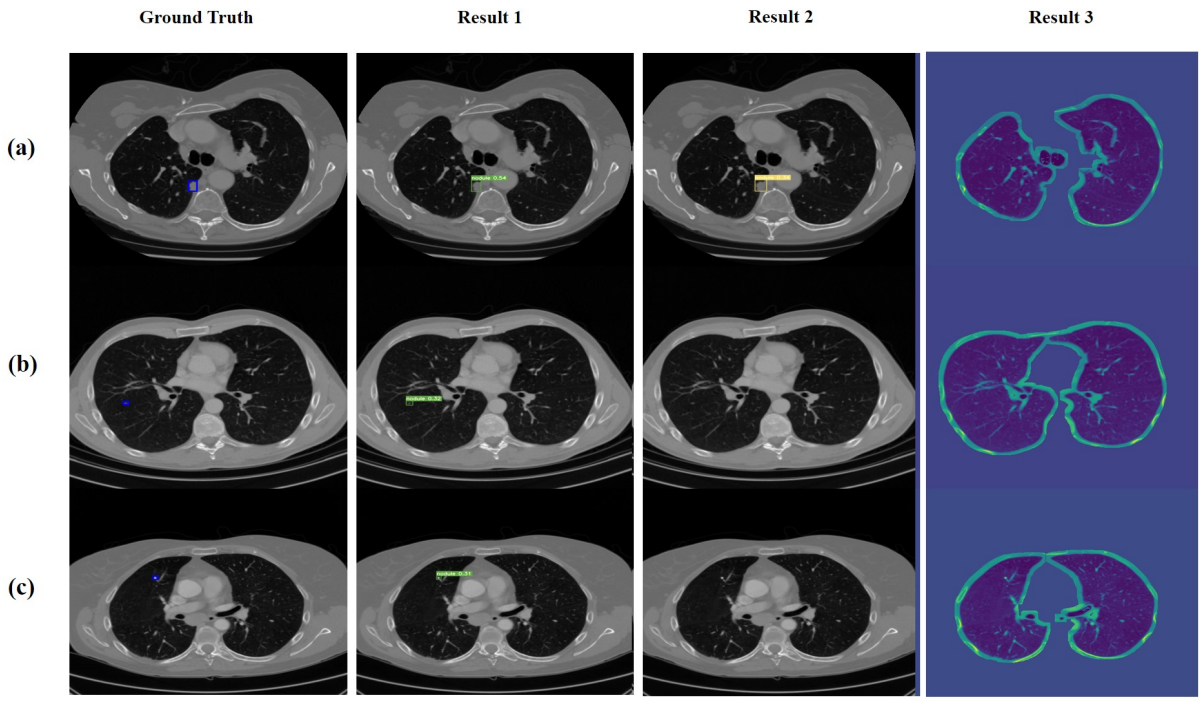



figure 4.11: Some samples that show the ability of the model to detect lung nodules when using whole images as input in training.

In the other hand, YOLOv7 is instrumental in achieving superior results in lung nodule detection due to its advanced neural network architecture, it's improved localization, confidence loss functions ensure precise bounding box predictions and reliable object presence probabilities. Its transfer learning capabilities, utilizing pre-trained weights, facilitate rapid adaptation to medical imaging tasks, enhancing performance even with smaller datasets. Furthermore, YOLOv7's real-time detection efficiency and ability to handle whole images, preserving all contextual information, lead to a balanced high mean Average Precision (mAP), precision, and recall. This comprehensive feature set makes YOLOv7 highly effective for medical imaging where maintaining high accuracy and minimizing both false positives and false negatives are critical.

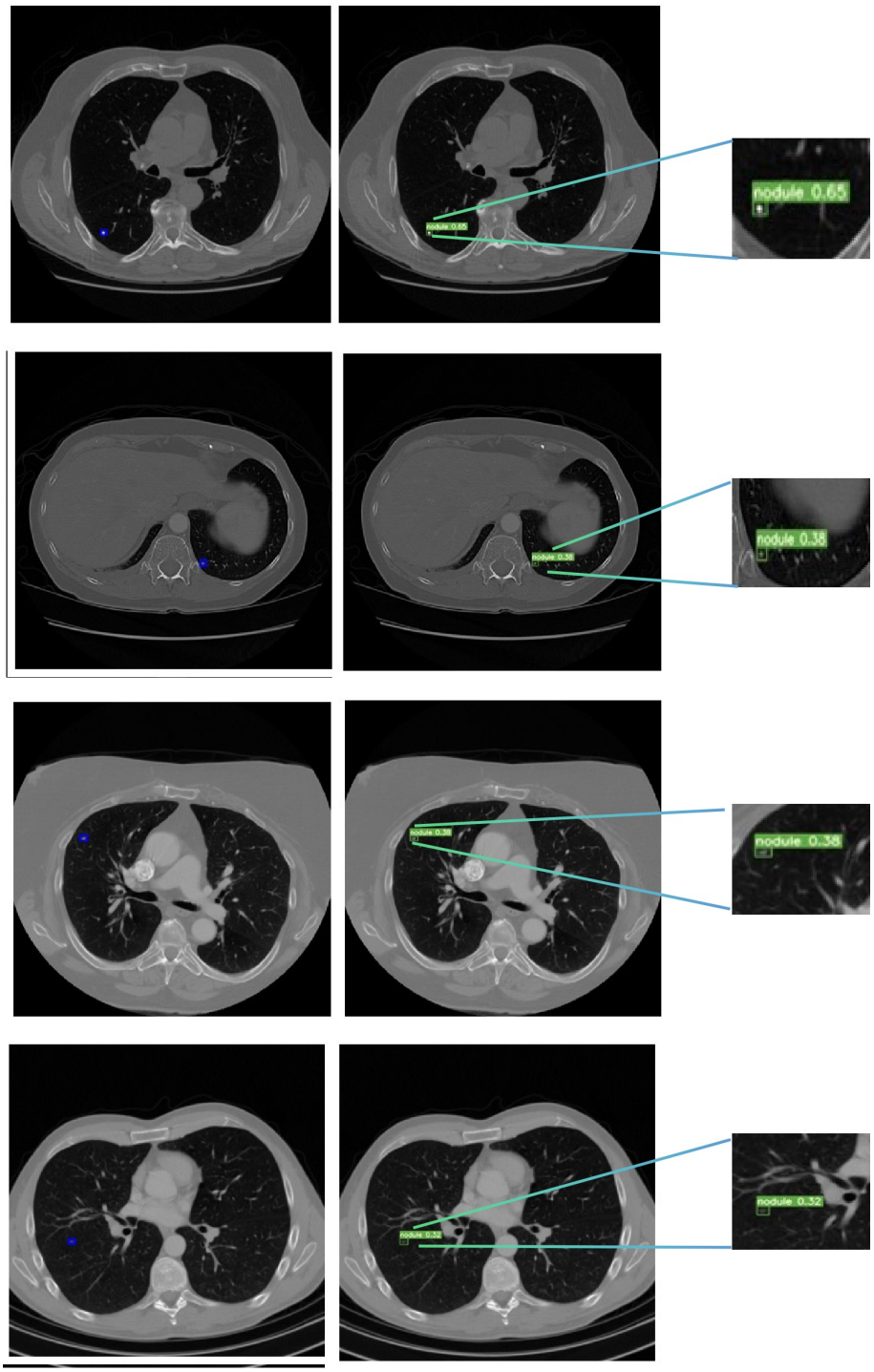



figure 4.12: The model's ability to detect small nodules

Figure 4.12 shows samples that demonstrate the model's ability to detect different lung nodules type like juxtraleural, solid, and also the smaller ones, which can assist radiologists in monitoring their evolution.

For lung cancer classification, three distinct models were evaluated each producing unique results in terms of simplicity, and effectiveness. For this task, it's essential to identify a model that not only minimizes misclassification rates but also aligns closely with radiologists' interpretations.

Model 1 emerges as the most suitable choice, it achieves strong performance by minimizing critical misclassifications, particularly between benign and malignant cases, which is essential in clinical contexts where misdiagnosing a malignant nodule as benign could delay necessary treatment. Model 1's simplicity, featuring only a single dense layer, reduces the risk of overfitting and enables more efficient optimization during training. This streamlined structure may be particularly advantageous when dealing with datasets that have limited samples or complex feature distributions. The combination of feature reusability, model simplicity, and optimization efficiency contributes to its superior performance in accurately classifying lung nodules. Consequently, Model 1 demonstrates robust potential for supporting radiologists in identifying high-risk cases with confidence, providing another reliable viewpoint in the decision-making process.

In terms of architecture, this model effectively leverages pre-trained features from VGG16 by incorporating frozen layers followed by a single dense layer. This structure allows it to extract a wide range of pre-trained features while maintaining simplicity, which enhances generalization for lung nodule classification. By freezing more layers, the model retains valuable knowledge from the pre-trained network, improving its feature extraction capabilities for this specific task.

Model 2 excels in handling suspect (indeterminate) cases, making it particularly valuable for cases that fall between benign and malignant. However, since its strength lies in managing these borderline cases rather than providing high accuracy in differentiating benign from malignant, it may be less suitable as the primary model in lung cancer diagnosis.

Model 3, on the other hand, shows the highest accuracy for benign cases, reducing the risk of benign cases being classified as malignant. This feature may be valuable in minimizing unnecessary treatment. However, Model 3's performance is less consistent for suspect and malignant cases, which are crucial categories in cancer diagnosis.

In terms of classification accuracy, each model achieves a low error rate, indicating strong alignment between the model predictions and radiologists' assessments. A key challenge arises when differentiating nodules in the benign and suspect categories due to the variability in malignancy scores assigned by radiologists. Each radiologist may interpret nodule features differently, leading to significant inter-observer variability. Training a deep learning model

on a dataset that reflects this range of assessments enables the algorithm to establish a more standardized and accurate classification method. This approach reduces individual biases and strengthens the model's overall accuracy, aligning it more closely with a consensus view that incorporates diverse expert opinions.

In our research, we have used Model 1, which is the optimal choice for lung cancer classification due to its balance of simplicity, efficiency, and strong performance in malignant case identification, aligning with clinical priorities. Model 2's nuanced handling of suspect cases makes it a valuable secondary option, while Model 3's ability to correctly classify benign cases could further support clinical decision-making in specific scenarios where benign classification is a priority.

To evaluate the performance of our proposed method, we compared it with other research studies. Table 4.2 shows the comparison results between our method and several lung nodule detection methods.

| Method | Data set | Algorithm | Metric | Result |
|---|---|---|---|---|
| Ref. [152] | Luna 16 | YOLOv3 | Average Precision | 83.5% |
| Ref. [154] | Luna 16 | YOLOV5 | Average Precision | 94.8% |
| Ref. [169] | Luna 16 | Faster RCNN | Sensitivity | 86.42% |
| Ref. [153] | LIDC-IDRI | YOLOv5 | Median accuracy Performance | 92.27% |
| Our method | LIDC-IDRI | YOLOv7 | mAP | 81.28% |

Table 4.2: Comparison results between the proposed method and some lung nodule detection methods.

The variations in results presented in the comparison table arise from differences in databases, the number of CT scan images, and the metrics used for performance evaluation. For a precise comparison with other research, it is essential to use an identical image database, as well as consistent training, validation, and test sets. Additionally, the configurations for the classifiers, including architecture, hyperparameters, and weight initialization, should be standardized.

Despite this, the results we obtained are considered good, especially in terms of the accuracy of detecting lung nodules, particularly those ranging between 3-30 mm. We observed this when conducting a test on a sample of images, as shown in Figure 1, which demonstrates the strength of the proposed method in the early detection of these nodules, allowing doctors to monitor them accurately.

## 4.5 Perspective

The proposed method offers several distinct advantages over existing approaches in lung nodule detection. Firstly, it eliminates the dependency on selecting optimal parameters, such as the size and shape of the structuring element, which can vary significantly between cases and impact detection accuracy. Secondly, unlike many traditional methods, it does not require the preliminary step of segmenting the lung area before detecting nodules. This simplification reduces preprocessing time and potential segmentation-related errors.

Additionally, by leveraging object detection algorithms, this method enables radiologists to effectively track nodules across adjacent slices in CT scans, improving the continuity and accuracy of nodule monitoring.

As future work, we aim to enhance our approach by incorporating 3D image analysis, which could provide richer spatial context and improve the accuracy of nodule localization and characterization. Moreover, we plan to apply our model to a broader range of datasets collected from different hospitals and imaging sources. This will allow us to evaluate its generalizability, compare classification performance across different datasets, and further refine the methodology for real-world clinical applications.

## 4.6 Conclusion

This chapter presented the tools used in implementing the proposed method. We then discussed the results obtained from the evaluation of our approach. Finally, a comparative study between our approach and related work demonstrated that the proposed models for detecting and classifying lung nodules, using object detection techniques and transfer learning based on deep learning technologies, are better suited to assist radiologists in the early detection of lung cancer which can save patient's life.

# General Conclusion

Lung cancer is one of the deadliest diseases due to its high mortality rate and challenges in treatment. It often evades early detection, leading to diagnoses at advanced stages when treatment options are limited and less effective. This late detection significantly reduces survival rates, as the cancer may have already metastasized.

Early detection is crucial as it greatly improves treatment outcomes by enabling timely interventions such as surgery, radiation therapy, or targeted treatments before the cancer spreads.

This research focuses on enhancing early detection methods for pulmonary nodules, particularly those between 3mm and 30mm, which pose a significant challenge for radiologists. Our approach consists of three main components. First, we curated a comprehensive database from the LIDC-IDRI dataset to support artificial intelligence applications. Second, we integrated advanced object detection algorithms into a computer-aided diagnosis (CAD) system tailored for lung cancer detection. This system improves the identification and tracking of lung nodules within CT scans, addressing variations in size, shape, and location that challenge traditional methods. By detecting nodules across multiple adjacent slices, our CAD system enhances diagnostic accuracy and aids healthcare professionals in early detection and treatment planning.

A key advantage of our method is the omission of traditional preprocessing and lung segmentation steps, significantly reducing processing time and computational costs while improving overall performance. This efficiency is validated by our evaluation of different input types for training the YOLOv7 object detector, where using entire images achieved an impressive mAP score of 81.28%.

Additionally, we propose a three-category classification for detected nodules, moving beyond the conventional benign-malignant binary system. This intermediate category helps identify nodules with malignancy-associated features that are not conclusively benign or malignant. By providing more nuanced guidance for follow-up protocols, this classification strategy enhances the accuracy of nodule assessment, ultimately contributing to better pa-

tient outcomes.

Overall, our approach improves early lung cancer detection by increasing diagnostic accuracy, reducing computational complexity, and providing a more informative classification system, thereby offering a valuable tool to assist radiologists in making more precise clinical decisions.

# Scientific Contributions

1. Mammeri Selma, Amroune Mohamed, Haouam Mohamed-Yassine, Bendib Issam, and Benkhelifa Elhadj. (2025). A Cascade Model to Detect and Segment Lung Nodule Using YOLOv8 and Resnet50U-Net. International Journal of Imaging Systems and Technology, 35(1), e70023.

2. Mammeri Selma, Amroune Mohamed, Haouam Mohamed-Yassine, Bendib Issam, and Corrêa Silva Aristofanes. (2024). "Early detection and diagnosis of lung cancer using YOLO v7, and transfer learning". Multimedia Tools and Applications, 83(10), 30965-30980.

3. Mammeri Selma, Amroune Mohamed, Haouam Mohamed-Yassine, Bendib Issam. (2021, October). "How to have a structured database for lung cancer segmentation using deep learning technologies". In 2021 International Conference on Networking and Advanced Systems (ICNAS) (pp. 1-5). IEEE.

# Bibliography


[1] cancer. https://www.who.int/news-room/fact-sheets/detail/cancer, 07 2023.

[2] Freddie Bray, Mathieu Laversanne, Hyuna Sung, Jacques Ferlay, Rebecca L Siegel, Isabelle Soerjomataram, and Ahmedin Jemal. Global cancer statistics 2022: Globocan estimates of incidence and mortality worldwide for 36 cancers in 185 countries. *CA: a cancer journal for clinicians*, 74(3):229–263, 2024.

[3] Johns Hopkins Medicine. Early detection of lung cancer. https://www.hopkinsmedicine.org/news/articles/2021/10/early-detection-of-lung-cancer, 2021. Accessed: October 5, 2023.

[4] Lung cancer. https://www.mayoclinic.org/diseases-conditions/lung-cancer/doctors-departments/ddc-20374629, 07 2024.

[5] Lung cancer. https://www.who.int/news-room/fact-sheets/detail/lung-cancer, 06 2023.

[6] Julie Marks. Lung cancer diagnosis: Procedures, results and accuracy. https://www.verywellhealth.com/lung-cancer-accurate-diagnosis-5219764, 08 2022. Accessed=july, 2024.

[7] Celine Mascaux, Nir Peled, Kavita Garg, Yasufumi Kato, Murry W Wynes, and Fred R Hirsch. Early detection and screening of lung cancer. *Expert review of molecular diagnostics*, 10(6):799–815, 2010.

[8] Beatriz Ocaña-Tienda, Alba Eroles-Simó, Julián Pérez-Beteta, Estanislao Arana, and Víctor M Pérez-García. Growth dynamics of lung nodules: implications for classification in lung cancer screening. *Cancer Imaging*, 24(1):113, 2024.

[9] Arthur CMD Guyton. *Text book of medical physiology*. China, 2006.

[10] Kimberly D Miller, Miranda Fidler-Benaoudia, Theresa H Keegan, Heather S Hipp, Ahmedin Jemal, and Rebecca L Siegel. Cancer statistics for adolescents and young adults, 2020. *CA: a cancer journal for clinicians*, 70(6):443–459, 2020.

[11] Andre Esteva, Alexandre Robicquet, Bharath Ramsundar, Volodymyr Kuleshov, Mark DePristo, Katherine Chou, Claire Cui, Greg Corrado, Sebastian Thrun, and Jeff Dean. A guide to deep learning in healthcare. *Nature medicine*, 25(1):24–29, 2019.

[12] Diego Ardila, Atilla P Kiraly, Sujeeth Bharadwaj, Bokyung Choi, Joshua J Reicher, Lily Peng, Daniel Tse, Mozziyar Etemadi, Wenxing Ye, Greg Corrado, et al. End-to-end lung cancer screening with three-dimensional deep learning on low-dose chest computed tomography. *Nature medicine*, 25(6):954–961, 2019.

[13] The respiratory system. https://www.teachpe.com/anatomy-physiology/the-respiratory-system, 02 2024.

[14] The respiratory system. https://my.clevelandclinic.org/health/diseases/4375-lung-cancer, 2022.

[15] How the lungs work. https://www.nhlbi.nih.gov/health/lungs, 03 2024.

[16] lung function. https://www.eea.europa.eu/help/glossary/eea-glossary/lung-function, 2006.

[17] The patient guide to heart, lung, and esophageal surgery. https://ctsurgerypatients.org/lung-esophageal-and-other-chest-diseases/lung-cancer, 2018.

[18] Ignacio I Wistuba and Adi F Gazdar. Lung cancer preneoplasia. *Annu. Rev. Pathol. Mech. Dis.*, 1:331–348, 2006.

[19] S. Srakocic. healthline. https://www.healthline.com/health/lung-cancer/types-of-non-small-cell-lung-cancer, 05 2022. Accessed=july, 2024.

[20] Lung american association. https://www.lung.org/lung-health-diseases/lung-disease-lookup/lung-cancer/symptoms-diagnosis/lung-cancer-staging, 2024.

[21] Lung cancer helpline. https://www.lungevity.org/for-patients-caregivers/navigating-your-diagnosis/lung-cancer-staging, 2 2021. Accessed: july, 25, 2023.

[22] Lung cancer. https://www.parkwaycancercentre.com/in/learn-about-cancer/types-of-cancer/cancer-details/lung-cancer#FAQ, 2 2024.

[23] Meng-Hua Tao. Epidemiology of lung cancer. *Lung Cancer and Imaging*, pages 4–1, 2019.

[24] Hyuna Sung, Jacques Ferlay, Rebecca L Siegel, Mathieu Laversanne, Isabelle Soerjomataram, Ahmedin Jemal, and Freddie Bray. Global cancer statistics 2020: Globocan estimates of incidence and mortality worldwide for 36 cancers in 185 countries. *CA: a cancer journal for clinicians*, 71(3):209–249, 2021.

[25] Freddie Bray, Jacques Ferlay, Isabelle Soerjomataram, Rebecca L Siegel, Lindsey A Torre, and Ahmedin Jemal. Global cancer statistics 2018: Globocan estimates of incidence and mortality worldwide for 36 cancers in 185 countries. *CA: a cancer journal for clinicians*, 68(6):394–424, 2018.

[26] International Agency for Research on Cancer. Cancer fact sheet: Algeria. = https://gco.iarc.who.int/media/globocan/factsheets/populations/12-algeria-fact-sheet.pdf, note = Accessed: 21-Oct-2024, 2024.

[27] Myrna CB Godoy and David P Naidich. Subsolid pulmonary nodules and the spectrum of peripheral adenocarcinomas of the lung: recommended interim guidelines for assessment and management. *Radiology*, 253(3):606–622, 2009.

[28] David R Baldwin and Matthew EJ Callister. The british thoracic society guidelines on the investigation and management of pulmonary nodules. *Thorax*, 70(8):794–798, 2015.

[29] Peter J Mazzone and Louis Lam. Evaluating the patient with a pulmonary nodule: a review. *Jama*, 327(3):264–273, 2022.

[30] Ivana Kulhánová, Ariana Znaor, Kevin D Shield, Melina Arnold, Jérôme Vignat, Maya Charafeddine, Ibtihal Fadhil, Heba Fouad, Amal Al-Omari, Ali Saeed Al-Zahrani, et al. Proportion of cancers attributable to major lifestyle and environmental risk factors in the eastern mediterranean region. *International journal of cancer*, 146(3):646–656, 2020.

[31] JSEM Ferlay, I Soerjomataram, M Ervik, R Dikshit, S Eser, C Mathers, M Rebelo, DM Parkin, D Forman, and F Bray. Cancer incidence and mortality worldwide: Iarc cancerbase. *Globocan*, 2013(1):11, 2012.

[32] Boris D Lushniak, Jonathan M Samet, Terry F Pechacek, Leslie A Norman, and Peter A Taylor. The health consequences of smoking—50 years of progress: A report of the surgeon general. 2014.

[33] Jonathan M Samet. Radon and lung cancer. *JNCI: Journal of the National Cancer Institute*, 81(10):745–758, 1989.

[34] Mariona Riudavets, Marta Garcia de Herreros, Benjamin Besse, and Laura Mezquita. Radon and lung cancer: current trends and future perspectives. *Cancers*, 14(13):3142, 2022.

[35] DF Xing, CD Xu, XY Liao, TY Xing, SP Cheng, MG Hu, and JX Wang. Spatial association between outdoor air pollution and lung cancer incidence in china. *BMC public health*, 19:1–11, 2019.

[36] Mohammad Zamiri Bidary, Mehrdad Sahranavard, Arash Akhavan Rezayat, Alireza Omranzadeh, Seyyed Hasan Hoseiny, Ali Kabirian, and Amirhossein Sahebkar. Opium as a carcinogen: A systematic review and meta-analysis. *EClinicalMedicine*, 33, 2021.

[37] Agence nationale de sécurité sanitaire de l'alimentation, de l'environnement et du travail. Asbestos and occupational lung cancer risks, 2023. Retrieved from https://www.anses.fr.

[38] Institut National de Recherche et de Sécurité. Lung cancer and professional exposure risks, 2023. Retrieved from https://www.inrs.fr.

[39] International agency for research on cancer. https://www.iarc.who.int/. Accessed=july, 2024.

[40] N Hollings and P Shaw. Diagnostic imaging of lung cancer. *European Respiratory Journal*, 19(4):722–742, 2002.

[41] Lungevity transforming lung cancer. https://www.mayoclinic.org/diseases-conditions/lung-cancer/diagnosis-treatment/drc-20374627, 04 2024.

[42] Pranav Modi and Abhay Uppe. Lung biopsy techniques and clinical significance. 2020.

[43] Lungevity transforming lung cancer. https://www.lungevity.org/for-patients-caregivers/lung-cancer-101/diagnosing-lung-cancer/tissue-biopsies, 09 2024.

[44] Ahmed Hosny, Chintan Parmar, John Quackenbush, Lawrence H Schwartz, and Hugo JWL Aerts. Artificial intelligence in radiology. *Nature Reviews Cancer*, 18(8):500–510, 2018.

[45] Eric J Topol. High-performance medicine: the convergence of human and artificial intelligence. *Nature medicine*, 25(1):44–56, 2019.

[46] Shigao Huang, Jie Yang, Simon Fong, and Qi Zhao. Artificial intelligence in cancer diagnosis and prognosis: Opportunities and challenges. *Cancer letters*, 471:61–71, 2020.

[47] Colton Ladbury, Arya Amini, Ameish Govindarajan, Isa Mambetsariev, Dan J Raz, Erminia Massarelli, Terence Williams, Andrei Rodin, and Ravi Salgia. Integration of artificial intelligence in lung cancer: Rise of the machine. *Cell Reports Medicine*, 2023.

[48] Kevin B Johnson, Wei-Qi Wei, Dilhan Weeraratne, Mark E Frisse, Karl Misulis, Kyu Rhee, Juan Zhao, and Jane L Snowdon. Precision medicine, ai, and the future of personalized health care. *Clinical and translational science*, 14(1):86–93, 2021.

[49] Alan Alexander, Adam Jiang, Cara Ferreira, and Delphine Zurkiya. An intelligent future for medical imaging: a market outlook on artificial intelligence for medical imaging. *Journal of the American College of Radiology*, 17(1):165–170, 2020.

[50] How ai-powered medical imaging is transforming healthcare. https://www.onixnet.com/blog/how-ai-powered-medical-imaging-is-transforming-healthcare/, 2024.

[51] Xiaoli Tang. The role of artificial intelligence in medical imaging research. *BJR| Open*, 2(1):20190031, 2019.

[52] National library of medicine. https://medlineplus.gov/genetics/understanding/precisionmedicine/definition/, 05 2022.

[53] Nicholas J Schork. Artificial intelligence and personalized medicine. *Precision medicine in Cancer therapy*, pages 265–283, 2019.

[54] Hugo JWL Aerts. The potential of radiomic-based phenotyping in precision medicine: a review. *JAMA oncology*, 2(12):1636–1642, 2016.

[55] Simon A Keek, Ralph Th Leijenaar, Arthur Jochems, and Henry C Woodruff. A review on radiomics and the future of theranostics for patient selection in precision medicine. *The British journal of radiology*, 91(1091):20170926, 2018.

[56] Ayman El-Baz, Garth M Beache, Georgy Gimel'farb, Kenji Suzuki, Kazunori Okada, Ahmed Elnakib, Ahmed Soliman, Behnoush Abdollahi, et al. Computer-aided diagnosis systems for lung cancer: challenges and methodologies. *International journal of biomedical imaging*, 2013, 2013.

[57] Sung Eun Song, Bo Kyoung Seo, Kyu Ran Cho, Ok Hee Woo, Gil Soo Son, Chulhan Kim, Sung Bum Cho, and Soon-Sun Kwon. Computer-aided detection (cad) system for breast mri in assessment of local tumor extent, nodal status, and multifocality of invasive breast cancers: preliminary study. *Cancer Imaging*, 15(1):1–9, 2015.

[58] U Raghavendra, U Rajendra Acharya, and Hojjat Adeli. Artificial intelligence techniques for automated diagnosis of neurological disorders. *European neurology*, 82(1-3):41–64, 2020.

[59] Reed T Sutton, David Pincock, Daniel C Baumgart, Daniel C Sadowski, Richard N Fedorak, and Karen I Kroeker. An overview of clinical decision support systems: benefits, risks, and strategies for success. *NPJ digital medicine*, 3(1):17, 2020.

[60] John McCarthy, Marvin L Minsky, Nathaniel Rochester, and Claude E Shannon. A proposal for the dartmouth summer research project on artificial intelligence, august 31, 1955. *AI magazine*, 27(4):12–12, 2006.

[61] Stuart J Russell and Peter Norvig. *Artificial intelligence a modern approach*. London, 2010.

[62] Zhi-Hua Zhou. *Machine learning*. Springer Nature, 2021.

[63] Dwi Ana Ratna Wati and Dika Abadianto. Design of face detection and recognition system for smart home security application. In *2017 2nd International conferences on Information Technology, Information Systems and Electrical Engineering (ICITISEE)*, pages 342–347. IEEE, 2017.

[64] Jay Nanduri, Yuting Jia, Anand Oka, John Beaver, and Yung-Wen Liu. Microsoft uses machine learning and optimization to reduce e-commerce fraud. *INFORMS Journal on Applied Analytics*, 50(1):64–79, 2020.

[65] Jovani Dalzochio, Rafael Kunst, Edison Pignaton, Alecio Binotto, Srijnan Sanyal, Jose Favilla, and Jorge Barbosa. Machine learning and reasoning for predictive maintenance in industry 4.0: Current status and challenges. *Computers in Industry*, 123:103298, 2020.

[66] Divya Gangwani and Pranav Gangwani. Applications of machine learning and artificial intelligence in intelligent transportation system: A review. *Applications of Artificial Intelligence and Machine Learning: Select Proceedings of ICAAAIML 2020*, pages 203–216, 2021.

[67] Andrew L Beam and Isaac S Kohane. Big data and machine learning in health care. *Jama*, 319(13):1317–1318, 2018.

[68] Danton S Char, Nigam H Shah, and David Magnus. Implementing machine learning in health care—addressing ethical challenges. *The New England journal of medicine*, 378(11):981, 2018.

[69] Friederike Mey, Jim Clauwaert, Kirsten Van Huffel, Willem Waegeman, and Marjan De Mey. Improving the performance of machine learning models for biotechnology: The quest for deus ex machina. *Biotechnology advances*, 53:107858, 2021.

[70] What is supervised learning? https://www.ibm.com/topics/supervised-learning, 2024.

[71] javatpoint. https://www.javatpoint.com/supervised-machine-learning, 2024.

[72] Brennan Whitfield. Regression in machine learning: What it is and examples of different models. https://builtin.com/data-science/regression-machine-learning, 08 2024.

[73] Introduction à l'apprentissage automatique. https://projeduc.github.io/intro_apprentissage_automatique/regression.html, 2023.

[74] By Mayank Banoula. Classification in machine learning: What it is classification models. https://www.simplilearn.com/tutorials/machine-learning-tutorial/classification-in-machine-learning, 05 2023.

[75] Zoumana Keita. Classification in machine learning: An introduction. https://www.datacamp.com/blog/classification-machine-learning, 08 2024.

[76] M Emre Celebi and Kemal Aydin. *Unsupervised learning algorithms*, volume 9. Springer, 2016.

[77] Mark Scapicchio Jim Holdsworth. Random forest: A complete guide for machine learning. https://www.ibm.com/topics/deep-learning/, 06 2024.

[78] ARTZAI Picon Ruiz, AITOR Alvarez Gila, Unai Irusta, JONE Echazarra Huguet, et al. Why deep learning performs better than classical machine learning? *Dyna Ingenieria E Industria*, 2020.

[79] Asmaa Halbouni, Teddy Surya Gunawan, Mohamed Hadi Habaebi, Murad Halbouni, Mira Kartiwi, and Robiah Ahmad. Machine learning and deep learning approaches for cybersecurity: A review. *IEEE Access*, 10:19572–19585, 2022.

[80] Chris M Bishop. Neural networks and their applications. *Review of scientific instruments*, 65(6):1803–1832, 1994.

[81] Daniel Svozil, Vladimir Kvasnicka, and Jiri Pospichal. Introduction to multi-layer feed-forward neural networks. *Chemometrics and intelligent laboratory systems*, 39(1):43–62, 1997.

[82] Saleh Albelwi and Ausif Mahmood. A framework for designing the architectures of deep convolutional neural networks. *Entropy*, 19(6):242, 2017.

[83] Antonio Fernandez. Which activation function suits better to your deep learning scenario? https://datascience.aero/aviation-function-deep-learning/, 10 2020.

[84] Keiron O'shea and Ryan Nash. An introduction to convolutional neural networks. *arXiv preprint arXiv:1511.08458*, 2015.

[85] Saad Albawi, Tareq Abed Mohammed, and Saad Al-Zawi. Understanding of a convolutional neural network. In *2017 international conference on engineering and technology (ICET)*, pages 1–6. Ieee, 2017.

[86] Jens Smiatek, Christoph Clemens, Liliana Montano Herrera, Sabine Arnold, Bettina Knapp, Beate Presser, Alexander Jung, Thomas Wucherpfennig, and Erich Bluhmki. Generic and specific recurrent neural network models: Applications for large and small scale biopharmaceutical upstream processes. *Biotechnology Reports*, 31:e00640, 2021.

[87] Macedo Firmino, Giovani Angelo, Higor Morais, Marcel R Dantas, and Ricardo Valentim. Computer-aided detection (cade) and diagnosis (cadx) system for lung cancer with likelihood of malignancy. *Biomedical engineering online*, 15(1):1–17, 2016.

[88] Krishna Kant Singh and Akansha Singh. A study of image segmentation algorithms for different types of images. *International Journal of Computer Science Issues (IJCSI)*, 7(5):414, 2010.

[89] Converting ct data to hounsfield units. http://www.idlcoyote.com/fileio_tips/hounsfield.html, 10 2020.

[90] Lidc-idri lung nodule public data set dicom and xml annotation detailed. https://www.programmersought.com/article/795071672/, 10 2020.

[91] Samuel G Armato III, Geoffrey McLennan, Luc Bidaut, Michael F McNitt-Gray, Charles R Meyer, Anthony P Reeves, Binsheng Zhao, Denise R Aberle, Claudia I Henschke, Eric A Hoffman, et al. The lung image database consortium (lidc) and image database resource initiative (idri): a completed reference database of lung nodules on ct scans. *Medical physics*, 38(2):915–931, 2011.

[92] Samuel G Armato III, Karen Drukker, Feng Li, Lubomir Hadjiiski, Georgia D Tourassi, Roger M Engelmann, Maryellen L Giger, George Redmond, Keyvan Farahani, Justin S Kirby, et al. Lungx challenge for computerized lung nodule classification. *Journal of Medical Imaging*, 3(4):044506–044506, 2016.

[93] Arnaud Arindra Adiyoso Setio, Alberto Traverso, Thomas De Bel, Moira SN Berens, Cas Van Den Bogaard, Piergiorgio Cerello, Hao Chen, Qi Dou, Maria Evelina Fantacci, Bram Geurts, et al. Validation, comparison, and combination of algorithms for automatic detection of pulmonary nodules in computed tomography images: the luna16 challenge. *Medical image analysis*, 42:1–13, 2017.

[94] Martin Dolejsi, Jan Kybic, Michal Polovincák, and Stanislav Tuma. The lung time: Annotated lung nodule dataset and nodule detection framework. In *Medical Imaging 2009: Computer-Aided Diagnosis*, volume 7260, pages 538–545. SPIE, 2009.

[95] Lung time. http://cmp.felk.cvut.cz/LungTIME/, 06 2020.

[96] Shaimaa Bakr, Olivier Gevaert, Sebastian Echegaray, Kelsey Ayers, Mu Zhou, Majid Shafiq, Hong Zheng, Jalen Anthony Benson, Weiruo Zhang, Ann NC Leung, et al. A radiogenomic dataset of non-small cell lung cancer. *Scientific data*, 5(1):1–9, 2018.

[97] National Lung Screening Trial Research Team. The national lung screening trial: overview and study design. *Radiology*, 258(1):243–253, 2011.

[98] The iq-othnccd lung cancer dataset. https://data.mendeley.com/datasets/bhmdr45bh2/1, 09 2020.

[99] L. SaiRamesh G. Raghuraman S. Indira Priyadharsini, N. Mangayarkarasi. Lung nodule detection on ct images using image processing techniques. *International Journal of Pure and Applied Mathematics*, 119(7):479–487, 2018.

[100] S Ashwin, J Ramesh, S Aravind Kumar, and K Gunavathi. Efficient and reliable lung nodule detection using a neural network based computer aided diagnosis system. In *2012 International Conference on Emerging Trends in Electrical Engineering and Energy Management (ICETEEEM)*, pages 135–142. IEEE, 2012.

[101] Nidhi S Nadkarni and Sangam Borkar. Detection of lung cancer in ct images using image processing. In *2019 3rd International Conference on Trends in Electronics and Informatics (ICOEI)*, pages 863–866. IEEE, 2019.

[102] Charles Poynton. *Digital video and HD: Algorithms and Interfaces*. Elsevier, 2012.

[103] Joseph Redmon, Santosh Divvala, Ross Girshick, and Ali Farhadi. You only look once: Unified, real-time object detection. In *Proceedings of the IEEE conference on computer vision and pattern recognition*, pages 779–788, 2016.

[104] Youshan Zhang. Stall number detection of cow teats key frames. *arXiv preprint arXiv:2303.10444*, 2023.

[105] Joseph Redmon and Ali Farhadi. Yolo9000: better, faster, stronger. In *Proceedings of the IEEE conference on computer vision and pattern recognition*, pages 7263–7271, 2017.

[106] Joseph Redmon and Ali Farhadi. Yolov3: An incremental improvement. *arXiv preprint arXiv:1804.02767*, 2018.

[107] Alexey Bochkovskiy, Chien-Yao Wang, and Hong-Yuan Mark Liao. Yolov4: Optimal speed and accuracy of object detection. *arXiv preprint arXiv:2004.10934*, 2020.

[108] Jacob Solawetz Joseph Nelson. Yolov5 is here: State-of-the-art object detection at 140 fps. https://blog.roboflow.com/yolov5-is-here/, 06 2020.

[109] Chuyi Li, Lulu Li, Hongliang Jiang, Kaiheng Weng, Yifei Geng, Liang Li, Zaidan Ke, Qingyuan Li, Meng Cheng, Weiqiang Nie, et al. Yolov6: A single-stage object detection framework for industrial applications. *arXiv preprint arXiv:2209.02976*, 2022.

[110] Chien-Yao Wang, Alexey Bochkovskiy, and Hong-Yuan Mark Liao. Yolov7: Trainable bag-of-freebies sets new state-of-the-art for real-time object detectors. In *Proceedings of the IEEE/CVF conference on computer vision and pattern recognition*, pages 7464–7475, 2023.

[111] Ross Girshick, Jeff Donahue, Trevor Darrell, and Jitendra Malik. Rich feature hierarchies for accurate object detection and semantic segmentation. In *Proceedings of the IEEE conference on computer vision and pattern recognition*, pages 580–587, 2014.

[112] Ying Su, Dan Li, and Xiaodong Chen. Lung nodule detection based on faster r-cnn framework. *Computer Methods and Programs in Biomedicine*, 200:105866, 2021.

[113] Mohammad Omid Khairandish, R Gurta, and Meenakshi Sharma. A hybrid model of faster r-cnn and svm for tumor detection and classification of mri brain images. *Int. J. Mech. Prod. Eng. Res. Dev*, 10(3):6863–6876, 2020.

[114] Salem Saleh Al-Amri, NV Kalyankar, and SD Khamitkar. Image segmentation by using edge detection. *International journal on computer science and engineering*, 2(3):804–807, 2010.

[115] Intisar Rizwan I Haque and Jeremiah Neubert. Deep learning approaches to biomedical image segmentation. *Informatics in Medicine Unlocked*, 18:100297, 2020.

[116] Niblack Thresholding, PSNR Sauvola, and Jaccard. Image segmentation by using thresholding techniques for medical images. 2016.

[117] R Beaulah Jeyavathana, R Balasubramanian, and A Anbarasa Pandian. A survey: analysis on preprocessing and segmentation techniques for medical images. *International Journal of Research and Scientific Innovation (IJRSI)*, 3, 2016.

[118] Nobuyuki Otsu et al. A threshold selection method from gray-level histograms. *Automatica*, 11(285-296):23–27, 1975.

[119] Sandeep Kumar Dubey and Sandeep Vijay. A review of image segmentation using clustering methods. *International Journal of Applied Engineering Research*, 13(5):2484–2489, 2018.

[120] Younes Benzaki. Machine learning made easy. https://mrmint.fr/algorithme-k-means, 04 2018.

[121] Ml - clustering k-means algorithm. https://www.tutorialspoint.com/machine_learning_with_python/machine_learning_with_python_clustering_algorithms_k_means.htm, 11 2020.

[122] S Avinash, K Manjunath, and S Senthil Kumar. An improved image processing analysis for the detection of lung cancer using gabor filters and watershed segmentation technique. In *2016 International Conference on Inventive Computation Technologies (ICICT)*, volume 3, pages 1–6. IEEE, 2016.

[123] Kostas Haris, Serafim N Efstratiadis, Nikolaos Maglaveras, and Aggelos K Katsaggelos. Hybrid image segmentation using watersheds and fast region merging. *IEEE Transactions on image processing*, 7(12):1684–1699, 1998.

[124] Adrian Rosebrock. Watershed opencv. https://pyimagesearch.com/2015/11/02/watershed-opencv/, 11 2015.

[125] R Muthukrishnan and Miyilsamy Radha. Edge detection techniques for image segmentation. *International Journal of Computer Science & Information Technology*, 3(6):259, 2011.

[126] Roborealm vision for machine. http://www.roborealm.com/help/Roberts_Edge.php, 2020.

[127] Xiangbin Liu, Liping Song, Shuai Liu, and Yudong Zhang. A review of deep-learning-based medical image segmentation methods. *Sustainability*, 13(3):1224, 2021.

[128] Olaf Ronneberger, Philipp Fischer, and Thomas Brox. U-net: Convolutional networks for biomedical image segmentation. In *Medical image computing and computer-assisted intervention–MICCAI 2015: 18th international conference, Munich, Germany, October 5-9, 2015, proceedings, part III 18*, pages 234–241. Springer, 2015.

[129] S Niranjan Kumar, P Malin Bruntha, S Isaac Daniel, J Ajay Kirubakar, R Elaine Kiruba, Siril Sam, and S Immanuel Alex Pandian. Lung nodule segmentation using unet. In *2021 7th International conference on advanced computing and communication systems (ICACCS)*, volume 1, pages 420–424. IEEE, 2021.

[130] The iq-othnccd lung cancer dataset. https://medium.com/@saba99/unet-3aa28aa2aecf, 01 2021.

[131] M Gomathi and P Thangaraj. A computer aided diagnosis system for lung cancer detection using support vector machine. *American Journal of Applied Sciences*, 7(12):1532, 2010.

[132] A Asuntha, A Brindha, S Indirani, and Andy Srinivasan. Lung cancer detection using svm algorithm and optimization techniques. *J. Chem. Pharm. Sci*, 9(4):3198–3203, 2016.

[133] Marti A. Hearst, Susan T Dumais, Edgar Osuna, John Platt, and Bernhard Scholkopf. Support vector machines. *IEEE Intelligent Systems and their applications*, 13(4):18–28, 1998.

[134] Negar Maleki, Yasser Zeinali, and Seyed Taghi Akhavan Niaki. A k-nn method for lung cancer prognosis with the use of a genetic algorithm for feature selection. *Expert Systems with Applications*, 164:113981, 2021.

[135] P Bhuvaneswari and A Brintha Therese. Detection of cancer in lung with k-nn classification using genetic algorithm. *Procedia Materials Science*, 10:433–440, 2015.

[136] Niklas Donges. Random forest: A complete guide for machine learning. https://builtin.com/data-science/random-forest-algorithm/, 08 2024.

[137] Shu Ling Alycia Lee, Abbas Z Kouzani, and Eric J Hu. Random forest based lung nodule classification aided by clustering. *Computerized medical imaging and graphics*, 34(7):535–542, 2010.

[138] R Pandian, V Vedanarayanan, DNS Ravi Kumar, and R Rajakumar. Detection and classification of lung cancer using cnn and google net. *Measurement: Sensors*, 24:100588, 2022.

[139] Pranjal Sahu, Dantong Yu, Mallesham Dasari, Fei Hou, and Hong Qin. A lightweight multi-section cnn for lung nodule classification and malignancy estimation. *IEEE journal of biomedical and health informatics*, 23(3):960–968, 2018.

[140] P. Tidke Swati and Chakkarwar. Classification of lung tumor using svm 1 ms. 2012.

[141] Nisar Ahmed Memon, Anwar Majid Mirza, and SAM Gilani. Segmentation of lungs from CT scan images for early diagnosis of lung cancer. In *Proceedings of world academy of science, engineering and technology*, volume 14, pages 228–233, 2006.

[142] Disha Sharma and Gagandeep Jindal. Identifying lung cancer using image processing techniques. In *International Conference on Computational Techniques and Artificial Intelligence (ICCTAI)*, volume 17, pages 872–880. Citeseer, 2011.

[143] Yoshinori Itai, Hyoungseop Kim, Seiji Ishikawa, Shigehiko Katsuragawa, Takayuki Ishida, Katsumi Nakamura, and Akiyoshi Yamamoto. Automatic segmentation of lung areas based on snakes and extraction of abnormal areas. In *17th IEEE International Conference on Tools with Artificial Intelligence (ICTAI'05)*, pages 5–pp. IEEE, 2005.

[144] Suren Makaju, PWC Prasad, Abeer Alsadoon, AK Singh, and A Elchouemi. Lung cancer detection using ct scan images. *Procedia Computer Science*, 125:107–114, 2018.

[145] Muzzamil Javaid, Moazzam Javid, Muhammad Zia Ur Rehman, and Syed Irtiza Ali Shah. A novel approach to cad system for the detection of lung nodules in ct images. *Computer methods and programs in biomedicine*, 135:125–139, 2016.

[146] Abhir Bhandary, G Ananth Prabhu, V Rajinikanth, K Palani Thanaraj, Suresh Chandra Satapathy, David E Robbins, Charles Shasky, Yu-Dong Zhang, João Manuel RS Tavares, and N Sri Madhava Raja. Deep-learning framework to detect lung abnormality–a study with chest x-ray and lung ct scan images. *Pattern Recognition Letters*, 129:271–278, 2020.

[147] Thomas Heeneman and Mark Hoogendoorn. Lung nodule detection by using deep learning. *University of Amsterdam, Research Paper*, 2018.

[148] Priyanshu Tripathi, Shweta Tyagi, and Madhwendra Nath. A comparative analysis of segmentation techniques for lung cancer detection. *Pattern Recognition and Image Analysis*, 29(1):167–173, 2019.

[149] Selin Uzelaltinbulat and Buse Ugur. Lung tumor segmentation algorithm. *Procedia computer science*, 120:140–147, 2017.

[150] Albert Chon, Niranjan Balachandar, and Peter Lu. Deep convolutional neural networks for lung cancer detection. *Standford University*, 2017.

[151] Ying Su, Dan Li, and Xiaodong Chen. Lung nodule detection based on faster r-cnn framework. *Computer Methods and Programs in Biomedicine*, 200:105866, 2021.

[152] Kejia Xu, Hong Jiang, and Wenfang Tang. A new object detection algorithm based on yolov3 for lung nodules. In *Proceedings of the 2020 6th International Conference*

*on Computing and Artificial Intelligence*, New York, NY, USA, 2020. Association for Computing Machinery.

[153] Haytham Al Ewaidat and Youness El Brag. Identification of lung nodules ct scan using yolov5 based on convolution neural network. *arXiv preprint arXiv:2301.02166*, 2022.

[154] Chun-Man Yan and Cheng Wang. Automatic detection and localization of pulmonary nodules in ct images based on yolov5. *Journal of Computers*, 33(3):113–123, 2022.

[155] Pulmonary nodules. https://my.clevelandclinic.org/health/diseases/14799-pulmonary-nodules., 12 2020.

[156] What are lung nodules? https://www.lungevity.org/lung-cancer-basics/screening-early-detection/what-are-lung-nodules#:~:text=They%20may%20also%20be%20referred,detected%20by%20screening%20are%20cancerous., 09 2021.

[157] Daniel Yetman. What to know about the sizes of lung nodules. https://www.healthline.com/health/lung-cancer/lung-nodule-size-chart#next-steps., 09 2024.

[158] Selma Mammeri, Mohamed Amroune, Mohamed-Yassine Haouam, Issam Bendib, and Aristofanes Corrêa Silva. Early detection and diagnosis of lung cancer using yolo v7, and transfer learning. *Multimedia Tools and Applications*, 83(10):30965–30980, 2024.

[159] Javier García. Interpretation of ct scan images: Dicom format. https://www.sycaimedical.com/post/interpretation-of-ct-scan-images-dicom-format, 03 2021.

[160] Omnia Elsayed, Khaled Mahar, Mohamed Kholief, and Hatem A Khater. Automatic detection of the pulmonary nodules from ct images. In *2015 SAI Intelligent Systems Conference (IntelliSys)*, pages 742–746. IEEE, 2015.

[161] Dicom sort. https://dicomsort.com/documentation.html, 06 2020.

[162] A. P. Reeves and A. M. Biancardi. The lung image database consortium (lidc) nodule size report, October 27 2011. Release: 2011-10-27-2. Available at: /lidc/.

[163] Vanessa Ndonhong Kemajou, Anqi Bao, and Olivier Germain. Wellbore schematics to structured data using artificial intelligence tools. In *Offshore Technology Conference*, page D011S010R006. OTC, 2019.

[164] Adenocarcinoma. https://www.cancercenter.com/adenocarcinoma#:~:text=Typically%2C%20adenocarcinoma%20tumors%20are%20given,cells%20are%20poorly%20differentiated%20adenocarcinoma, 07 2022.

[165] William D Travis, Elisabeth Brambilla, Masayuki Noguchi, Andrew G Nicholson, Kim R Geisinger, Yasushi Yatabe, David G Beer, Charles A Powell, Gregory J Riely, Paul E Van Schil, et al. International association for the study of lung cancer/american thoracic society/european respiratory society international multidisciplinary classification of lung adenocarcinoma. *Journal of thoracic oncology*, 6(2):244–285, 2011.

[166] Adenocarcinoma cancers. https://my.clevelandclinic.org/health/diseases/21652-adenocarcinoma-cancers, 06 2024.

[167] Mian Muhammad Talha, Hikmat Ullah Khan, Saqib Iqbal, Mohammed Alghobiri, Tassawar Iqbal, and Muhammad Fayyaz. Deep learning in news recommender systems: A comprehensive survey, challenges and future trends. *Neurocomputing*, page 126881, 2023.

[168] Brendan Juba and Hai S Le. Precision-recall versus accuracy and the role of large data sets. In *Proceedings of the AAAI conference on artificial intelligence*, volume 33, pages 4039–4048, 2019.

[169] Automated pulmonary nodule detection in ct images using deep convolutional neural networks. *Pattern Recognition*, 85:109–119, 2019.